In vitro Characterisation of the Interactions between Fyn Tyrosine Kinase and Disabled-1

Diplomarbeit

Zur Erlangung des akademischen Grades

Diplomingenieur

eingereicht von

Romana Elisabeth Ranftl

Betreuerin: Peggy Stolt-Bergner, Ph.D.

Mitbetreuerin: Dipl. Ing. Barbara Nussbaumer

Matrikelnummer 0040098

Wien, 15.06.2011

Table of Contents

1 Abstract

Reelin, a glycoprotein secreted by specialised neurons, triggers a signalling cascade that regulates neuronal migration and laminar organisation in the developing brain and was also shown to have functions in the adult brain. Aberrant Reelin signalling is implicated in a number of severe mental disorders and degenerative diseases. A crucial step in this extensively studied pathway is the tyrosine-phosphorylation of the intracellular adaptor protein Disabled-1 (Dab1) by members of the Src family of kinases (SFKs), which is induced by clustering of Reelin receptors VLDLR and ApoER2. SFK-mediated tyrosyl-phosphorylation on four respective functional sites of Dab1 transmits the Reelin signal to downstream interaction partners. The mechanism of how SFKs target and discriminate the four Dab1 phosphorylation sites are not fully understood; structural studies might lead to a better understanding in this context. Therefore, in preparation for crystallisation experiments the specific interactions between Dab1 and Fyn tyrosine-kinase, the major enzyme involved in this process, have been investigated. Short variants of both proteins were recombinantly expressed in *E. coli* and purification strategies using different chromatographic steps to reach a high degree of purity were developed. The purified Fyn SH2-Kinase construct was used in Isothermal Titration Calibration (ITC) experiments to determine the binding affinity of the Src homology domain-2 to individually tyrosyl-phosphorylated synthetic Dab1 peptides. Further, a radioactivity-based kinase assay to determine the affinity of the enzyme towards the different phosphorylation sites was established. Additionally, a static light scattering based method was applied to test the stability of the Fyn construct in different buffer systems and in the presence of certain additives that might improve crystallisation. In conclusion, the Fyn SH2-kinase showed stronger binding affinities towards phosphotyrosines 185 and 198 compared to phosphorylated Y220 and Y232. Phosphorylation of Y185 and Y198 seems to serve as docking sites for SFKs.

2 Zusammenfassung

Reelin, ein Glycoprotein, steuert die Entwicklung bestimmter Gehirnregionen im Embryo durch Initiation einer intrazellulären Signalkaskade. Im ausgereiften Gehirn ist es außerdem an Prozessen beteiligt, die im Zusammenhang mit Lernfähigkeit und Gedächtnisbildung stehen. Ein elementarer Schritt im Reelin Signalweg ist die Anlagerung von Phosphatgruppen (Phosphorylierung) an das Adapterprotein Disabled-1 (Dab1) durch Enzyme der Src Kinase Familie (SFKs). Die wichtigste Tyrosin-Kinase in diesem Zusammenhang ist Fyn, die genauen Interaktionsmechanismen des Enzyms mit den vier potentiellen Dab1 Tyrosin-Phosphorylierungsstellen sind jedoch unklar. Die strukturbiologische Analyse von Komplexen aus beiden Proteinen, in Kombination mit biochemischen und zellbiologischen Versuchen, könnte die Bindungs- und Phosphorylierungsvorgänge aufklären, die der Weiterleitung des Reelin Signals zugrunde liegen.

Das Ziel dieser Arbeit war die biochemische Charakterisierung der Protein-Protein Interaktionen zwischen Fyn und Dab1 als Vorbereitung für die geplante Kristallisation und Röntgenstrukturanalyse. Zu diesem Zweck wurden gekürzte und teilweise mutierte Varianten der beiden Proteine in *E. coli* rekombinant exprimiert und Strategien zu deren Aufreinigung mit verschiedenen chromatographischen Methoden entwickelt und optimiert. Bindungsstudien mit Isothermaler Titrations Kalorimetrie (ITC) dienten dazu, die Affinität der Fyn SH2 Domäne (Src-homology 2) zu verschiedenen synthetischen Dab1-Phosphotyrosinpeptiden zu ermitteln. Zusätzlich wurde ein Enzymaktivitätstest zur Bestimmung der kinetischen Eigenschaften der Fyn SH2-Kinase etabliert.

Resultierend kann der Schluss gezogen werden, dass die SH2 Domäne der Tyrosin-Kinase Fyn unter den gegebenen experimentellen Bedingungen eine größere Bindungsaffinität zu den phosphorylierten Tyrosinen 185 und 198 in Dab1 zeigt. Diese Phosphotyrosine könnten als Ankerstellen für das Enzym dienen, um eine korrekte Phosphorylierung der beiden anderen Tyrosinreste (220 und 232) zu gewährleisten.

3 Introduction

Due to controlled migration during mammalian brain development, neurons are able to form defined “architectonic” patterns such as the typical inside-out lamination of the neocortex. (Lambert, Goffinet 2001; Cooper 2008) Generally, in multicellular organisms cell migration allows for conducted and specific positioning of cells, especially during embryonic development but also for maintenance purposes like wound healing or during immune response. Errors in migration processes commonly lead to severe symptoms. In the brain for example, mispositioning of neurons is linked to a number of degenerative diseases and human mental disorders (reviewed by Gressens, 2006; Fatemi et al., 2005).

Defects related to neuronal migration during embryonic brain development are prevalently caused by aberrant Reelin signalling; this biochemical pathway regulates the architectonic formation of different areas in the brain, such as the cortex, cerebellum or hippocampus but is also involved in a variety of processes in the adult brain. Reelin, a glycoprotein, signals migrating neurons to stop when they have reached their destination, and thus coordinates proper cell positioning. (D’Arcangelo 1995, D’Arcangelo 1997) Defects in this signalling pathway usually result in abnormal cyto-architecture of the respective brain areas, as it is observed for example in the Reeler mouse mutant (Lambert, Goffinet 2001, Katsuyama & Terashima 2009). The phenotype of this spontaneously occurring mutant mouse strain was first described more than fifty years ago, and is linked to lack of Reelin expression (D’Arcangelo 1995). The Reelin signalling cascade has been extensively investigated and described, however, many details remain unclear (reviewed by Förster et al. 2010, Frotscher et al. 2009 and 2010). In humans, defective Reelin signalling causes the Norman-Roberts-type lissencephaly (Hong et al., 2000)

This work particularly aims to biochemically characterise molecular interactions occurring within the Reelin pathway between the intracellular adapter protein disabled-1 and the non-receptor protein tyrosine-kinase Fyn. These interactions, which were demonstrated to be crucial for the cytosolic transduction of the Reelin induced signal, involve protein-protein binding and phosphorylation reactions (Howell et al., 1997 and 1999; Bock and Herz, 2003; Arnaud et al., 2003b). Investigation of the principles of these processes could provide insights in the specific role and function of Src family kinases in

Reelin signalling. It is not clear how the non-receptor tyrosine kinase interacts with the target protein; whether the kinase binds one site and further phosphorylation occurs “in cis” or “in trans”, which means whether the phosphorylation reaction is catalysed at the same molecule the kinase is bound to or at a Dab1 in close proximity, respectively. Transduction of the Reelin signal across the cell membrane requires clustering or dimerisation of lipoprotein receptors, but how the oligomerisation influences the function of SFKs is unclear.

3.1 The Reelin-signalling pathway

3.1.1 Anatomy of Reelin Signalling

In the developing mammalian brain, neurons are typically positioned in six cortical layers with respect to their birth date and are therefore organised in an “inside-outside” gradient, which means that the younger neurons migrate further than older neuronal cells. Neurons proliferate in the ventricular zone and the newly generated cells are then migrating towards the cortical plate along glial fibre cells that radially span the cortex (see figure 3.1, left panel). In early stages, the neurons settle horizontally to form the marginal zone (green) and the subplate (red). The early neurons of the marginal zone (e.g. Cajal-Retzius cells, CR) specialise to secrete Reelin, which binds to lipoprotein receptors VLDLR (very low density lipoprotein receptor) and ApoER2 (apolipoprotein E receptor 2) of motile neurons to prevent migration, which allows the formation of the defined architectonic patterns under the control of the Reelin signalling pathway. The signal stimulates the detachment from glial cells and the translocation of the cell soma to the top of the cortical plate. This continuously pushes the cells of the marginal zone outwards (reviewed by Rice & Curran, 2001 and Lambert, Goffinet; 2001).

Reelin additionally functions in postnatal and late stages of brain development in neuronal maturation, formation of correct synaptic circuits and promotion of the formation of dendritic spines; the latter has been shown in hippocampal neurons (Niu et al. 2008). Reelin further influences synaptic transmission and memory processes by enhancing the long-term potentiation (LTP), a form of synaptic plasticity associated with learning and memory (Frotscher M., 2010) In this context, alternative splicing of ApoER2

was found to be involved in modulating the activity of glutamate receptors of the NMDA and AMPA type (Beffert et al., 2005; Frotscher M., 2010). Therefore, in addition to the expression in CR cells in the marginal zone, Reelin is also expressed by GABAeric interneurons after birth and the adult brain (Förster et al.; 2010).

Furthermore, disruption of Reelin function in the adult hippocampus leads to repositioning of mature and differentiated neurons, suggesting a role in stabilising neuronal circuitry and plasticity (Frotscher M., 2010).

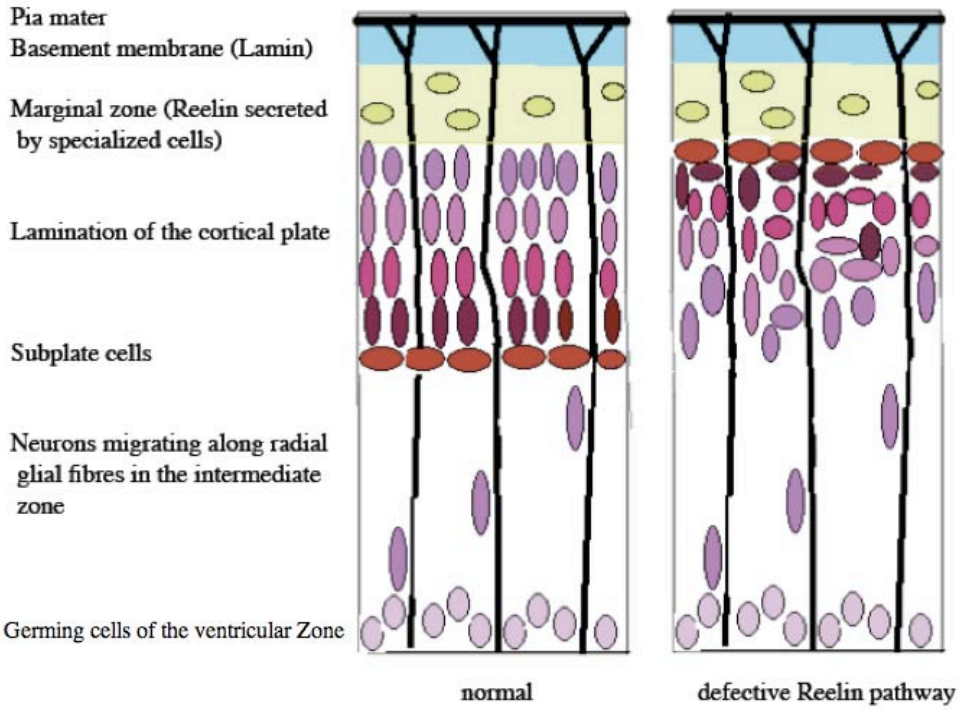

Fig. 3.1: Schematic representation of the normal "inside-out lamination" and disordered neuron-pattern in the cortex. Under the control of the Reelin signalling pathway, younger neurons are migrating further than older neurons. The age of cells is illustrated in a changing colour from light pink to bordeaux red, except for early neurons of the marginal zone (green) and the subplate (red).

The naturally occurring *reeler* mouse mutant is lacking Reelin, hence displays a variety of behavioural abnormalities (e.g. ataxia, tremor and a reeling gait) due to disordered brain architecture (see figure 3.2). The reeler mouse is extensively used as animal model in neuroscience (reviewed by Katsuyama & Terashima, 2009).

Linearity of the Reelin pathway was demonstrated in several genetic experiments in which the individual genes involved were knocked out in mice. The inactivation or naturally occurring mutation of either *reelin*, both *vldlr* and *apoer2*, or *dab1*, a gene coding for an intramolecular adaptor protein associated with the Reelin-receptors, leads to the

reeler-like phenotype (D'Arcangelo et al. 1997; Trommsdorff et al., 1999; Sheldon et al., 1997; Howell et al., 2000) in which the organisation of neuronal layers is disordered in the cortex, the cerebellum and the hippocampus due to aberrant Reelin signalling. The typical inside-out lamination of neurons is reversed, as illustrated in the right panel of figure 3.1 and in figure 3.2, because younger cells push the already settled cells further outwards (Cooper, 2008; Katsuyama & Terashima, 2009).

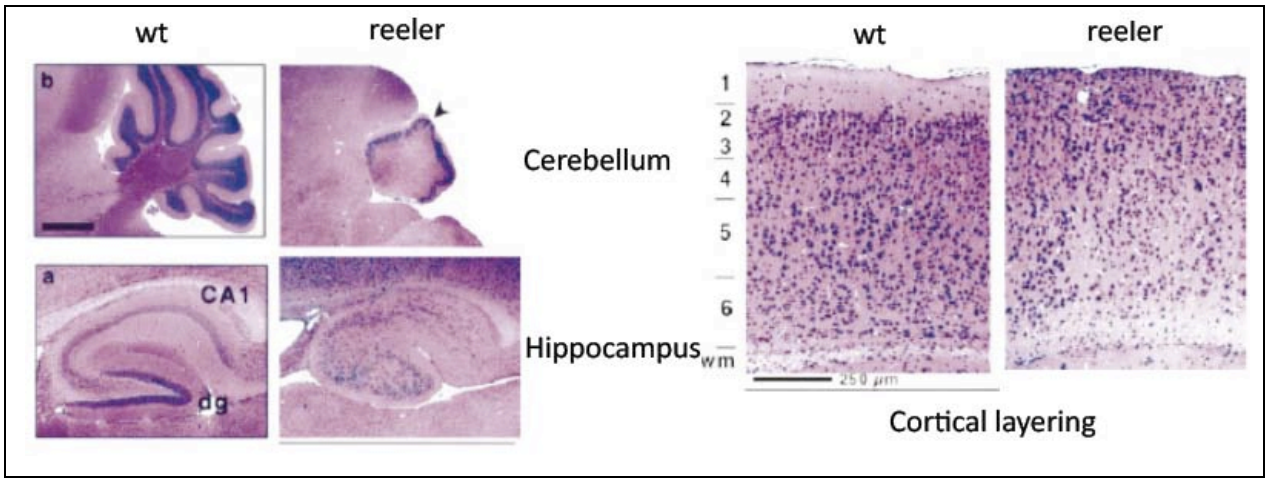

Fig. 3.2: Hisological comparison of wild-type and reeler mice brains. The typical reeler phenotype shows organisational defects in the cerebellum and the hippocampus and the classical layering in the cortex is disordered (Trommsdorff et al, 1999).

3.1.2 Molecular Mechanism of Reelin Signalling

Reelin is a large glycoprotein of about 400 kDa, which is secreted by Cajal-Retzius cells and other specialised neurons in the developing and mature brain (D'Arcangelo et al., 1995). Binding of the oligomeric Reelin protein to the extracellular domain of lipoprotein receptors **VLDLR** and **ApoER2** in target cells (Trommsdorff et al., 1999; D'Arcangelo et al. 1999) results in the clustering of these transmembrane receptors. The intracellular adaptor protein **disabled-1 (Dab1)** associates with the receptors by recognising the non-phosphorylated NPXY motif in their intracellular region with its phosphotyrosine binding domain (PTB domain) (Trommsdorff et al. 1998, Howell et al. 1997). Reelin-mediated clustering of lipoprotein receptors triggers the tyrosine phosphorylation of Dab1 predominantly by **Fyn**, but also other members of the Src Family of kinases (SFKs) (See figure 3.3). The interaction of Reelin with the receptors activates these non-receptor

tyrosine kinases (Howell et al., 2000; Arnaud et al., 2003b; Bock and Herz, 2003; Strasser et al. 2004; Jossin et al. 2004).

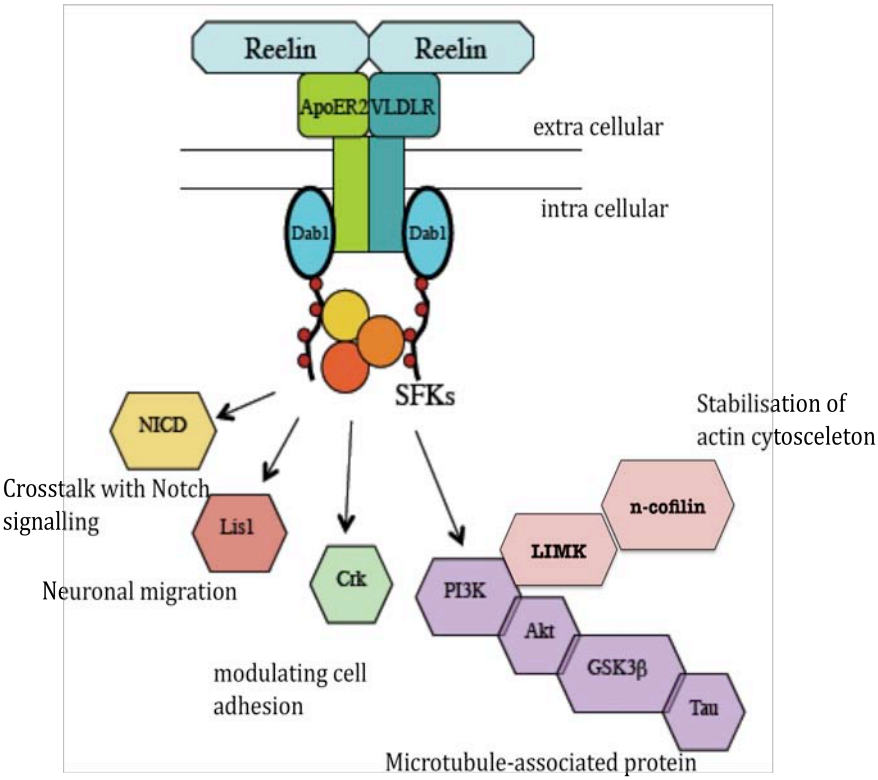

Fig. 3.3: Schematic model representing the Reelin signalling cascade. Lipoprotein receptor dimerisation upon extracellular binding of oligomerised Reelin results in tyrosine phosphorylation in the unstructured tail of Dab1 by members of the Src Kinase family. Dab1 phosphorylation transmits the Reelin signal by interactions of the intracellular adaptor protein with a variety of signalling molecules, which are involved in modulations of the cytoskeleton and neuronal migration.

The mouse protein Dab1 was first identified as Src SH2-domain interaction partner, and is predominantly expressed in the nervous system (Howell et al., 1997). It was shown to interact with the cytoplasmic tails of members of LDL receptor family or the amyloid precurser protein (APP). Tyrosine-phosphorylation of the scaffold protein promotes interaction with a number of non-receptor tyrosine kinases, including Abl in addition to SFKs. The *dab1* gene (2412 nucleotides) is expressed as a variety of Dab1 protein isoforms that differ in size and result from alternative splicing; the largest isoform is 555 residues long. A shorter isoform containing the first 250 amino acids has been shown to rescue the full-length dab1 gene (Howell et al. 1997).

The only structured domain of the Dab1 protein is a N-terminal **phosphotyrosine binding (PTB) domain** that is preferentially selective for a non-tyrosine-phosphorylated NPxY motif in binding partners such as VLDLR and ApoER2. The simultaneous interaction of the PTB with phosphoinositides (PI) such as phosphatidylinositol-4,5-bisphosphate (PI-4,5P2) allows the localisation and concentration of the protein at the inner leaflet of the plasma membrane, which may facilitate the recruitment of the adaptor protein to the Reelin receptors and hence Dab1 tyrosine phosphorylation (Stolt et al., 2003, 2005) (see figure 3.4 and 3.5).

A cluster of five tyrosine residues is located in close proximity to the Dab1 PTB domain in the **unstructured C-terminal tail**. Four of these tyrosine residues (Y185/Y198/Y220 and Y232; ere referred to as A/B/C and D respectively) have been shown to be essential for the functional role of Dab1 during embryonic development (Howell et al., 2000). The tyrosines function as docking sites for SH2 domains of SFKs in their phosphorylated state but also serve as substrates for the members of this non-receptor tyrosine kinase family (Songyang et al., 1995; Howell et al., 2000; Keshvara et al., 2001; Bock & Herz, 2003; Katyal et al., 2007; Feng & Cooper 2009). The sequence surrounding the tyrosine stretch shows characteristic hallmarks of typical substrates for SFKs and other tyrosine kinases such as acidic residues at position -3 or -4 relative to the tyrosine, an aliphatic residue at position -1 and hydrophobic amino acids or proline at position +3 (Howell et al., 2000).

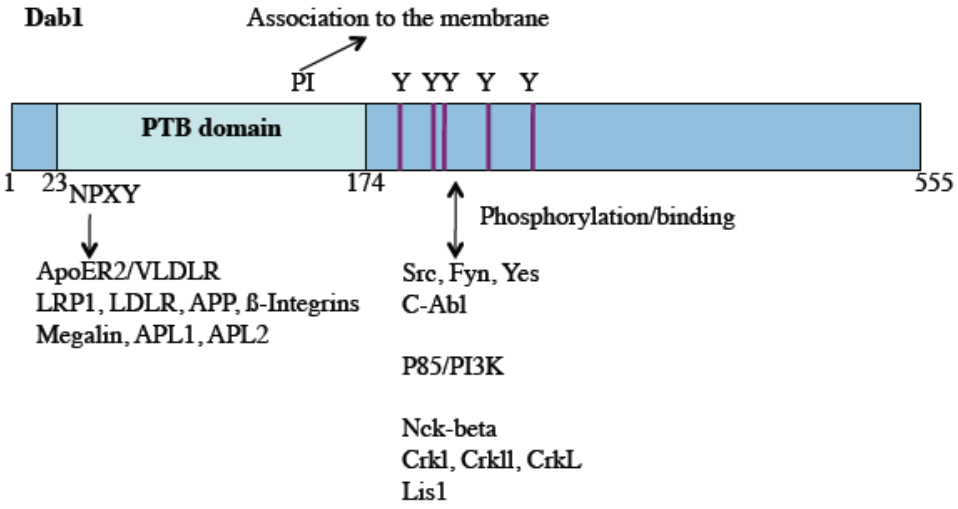

Fig. 3.4: Schematic representation of the domain-architecture of the 555 amino acid long isoform of Disabled-1. Indicated are also molecules that were shown to interact with the intracellular adaptor, either with an NPxY motif that is recognized by the PTB domain, or with the stretch of tyrosine residues that is located C-terminally to the PTB domain in the unstructured tail.

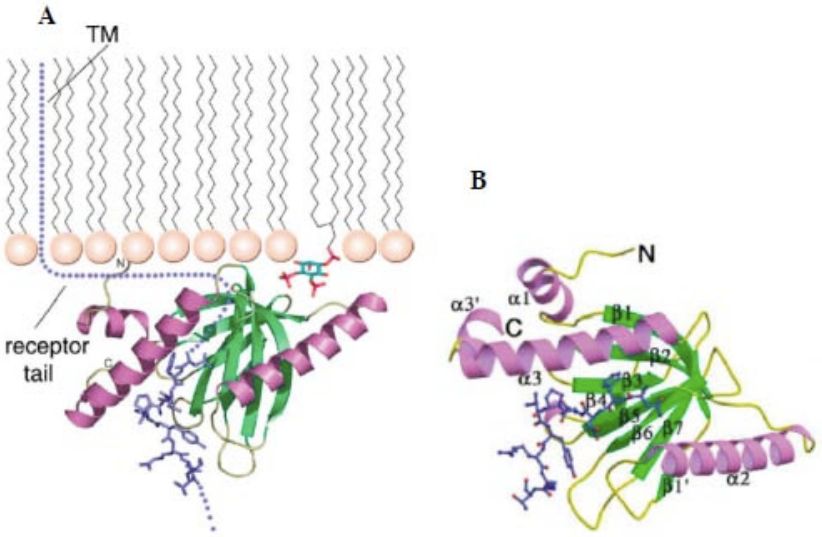

Fig. 3.5: A Model for the arrangement of the Dab1-ApoER2 complex at the membrane by interaction of the Dab1 PTB domain with phosphatidylinositol-4,5-bisphosphate . **B** Dab1 PTB domain in ribbon representation with the bound ApoER2 peptide in ball and stick form. β-strands are coloured green and α-helices pink. (Both figures reprinted from Stolt et al. 2003, Structure Vol. 11, 569-579).

Y198 and Y220 seem to be the major sites of Reelin-induced Dab1 phosphorylation in neurons during embryonic development (Keshvara et al., 2001). Both tyrosines have been demonstrated to mediate binding to the SH2-domain of Fyn, Src or Abl *in vitro* in the phosphorylated state, however, Fyn seems to be the major enzyme involved in phosphorylating Dab1 in Reelin signalling (Howell et al., 1997 and 2000; Arnaud et al., 2003b; Keshvara et al., 2001). By using knock-in mouse mutants it could be demonstrated that phenylalanine mutations at either the Y185 and Y198 or the Y220 and Y232 Dab1 phosphorylation sites disrupt the Reelin signal and prevent normal development of the brain. However, each mutant phenotype is complemented and rescued with the other mutant. Both, AB and CD, seem to have distinct functions, and assumingly, at least one tyrosine of each is necessary to stimulate the SFK- mediated phosphorylation upon Reelin stimulation (Feng & Cooper 2009). Additionally, it has been shown that Y185/Y198 fits a SFK consensus sequence, while Y220/Y232 resemble an Abl consensus sequence (Songyang et al., 1995). Further studies that used reconstitution of Dab1 mutational defects with other Dab1 mutants suggest that the function of phosphroylated Y185 is equivalent to Y198 and that phsophorylation of Y220 is functionally similar to Y232. It seems that the phosphorylation of one tyrosine of each of these sites (AB and CD) is sufficient for transmitting the Reelin signal (Morimura & Ogawa, 2009). By testing the effects of pharmacological inhibitors of SFKs and the Abl family on Reelin-mediated Dab1

phosphorylation in neuron cultures, it could be demonstrated that SFKs are involved in this process. In this context, Fyn tyrosine kinase is the main enzyme required *in vivo* for a correct Dab1 phosphorylation, however, in absence of fyn related members of the SFKs such as Src and Yes seem to complement its function (Arnaud et al., 2003b; Bock and Herz, 2003).

In neurons, Dab1 is both a binding partner and physiological substrate for SFKs, especially Fyn. Basal levels of phosphorylated Dab1 are present in the developing brain, which may provide initial binding sites for the SFK SH2 domain (Arnaud et al., 2003a and 2003b). Upon stimulation of cultured neurons with Reelin, SFKs become activated and Dab1 phosphorylation occurs at tyrosines 198 and 220 and is amplified (Keshvara et al., 2001). However, the precise molecular mechanism underlying SFK activation by receptor clustering is unclear.

Similar to knock-out mouse mutants of Reelin, ApoER2/VLDLR and Dab1, mice that are expressing a mutated variant of Dab1 with all tyrosine phosphorylation sites being substituted to phenylalanine, also exhibits a *reeler*-like phenotype (Howell et al., 2000). These findings suggest that the phosphorylation of the Dab1 adaptor molecule is a crucial step in the Reelin pathway. For SFKs, the knock-out of both Fyn and Src is required to yield the classical *reeler*-like layering defects (Kuo et al., 2005). When only Fyn is deficient in mice, the neuronal positioning defects are rather subtle, which is probably due to compensational effects by other SFKs. Unfortunately, mice with a multiple knock-out of Src family kinases are not viable. Similar to reeler mice, Fyn deficient mouse mutants show elevated levels of Dab1 protein in the brain (Arnaud et al., 2003; Bock & Herz, 2003).

3.1.3 Downstream signalling

Tyrosine-phosphorylated Dab1 provides a scaffold for several other molecules involved in processes downstream of Dab1 and is thought to initiate the formation of a multiprotein signalling complex that primarily links the Reelin signal with the actin cytoskeleton (May et al., 2005; Stolt & Bock 2006). Members of the Crk-family of adaptor proteins were detected among these interaction partners, and are involved in modulating cell adhesion and migration. Y220 and Y232 seem to be critically involved in Dab1-interactions with Crk-family proteins (Chen et al., 2004; Huang et al., 2004).

Dab1 phosphorylation further activates PI3 kinase by interacting with its regulatory p85α subunit, which leads to phosphorylation and activation of Akt, which inactivates GSK-3β. The latter has several interaction partners and modulates for example Tau phosphorylation, a microtubule-associated protein (Beffert et al., 2002). However, *tau*-deficient animals do not display any abnormal cellular organisation or migrational defects (Harada et al., 1994). Only very recently it was observed that the phosphorylation of the F-actin binding protein n-cofilin by LIM-kinase 1 also requires Reelin-induced activation of PI3 kinase (Bock et al. 2003; Chai et al, 2009).
Additionally, there seems to be a crosstalk between Reelin signalling and other signalling pathways involved in the regulation of neuronal positioning during brain development, such as the cdk5 (cyclin-dependent kinase 5) and Lis1. Cdk5 acts in parallel with Reelin in neuronal migration during brain development, thereby also influencing for example microtubeles (reviewed for example by Cooper, 2008). Lis1 is also one of the key players in neuronal migration. The defective *lis1* gene is involved in the human neuronal migration disorder type 1 lissencephaly (Assadi et al., 2003, Gupta et al., 2002). Recently, a cross talk with Notch signalling was reported. Dab1 is interacting with NICD (Notch intracellular domain) (Hashimoto-Torii et al., 2008).

Upon Reelin-induced tyrosine phosphorylation, phospho-Dab1 is polyubiqutinylated and subsequently degraded by the proteasome, which is probably required to terminate the signal and thus ensure a transient response to Reelin (Arnaud et al., 2003a). In mice lacking Reelin or the according receptors, however, Dab1 accumulates (Rice et al., 1998). Ubiquitination of Dab1 is assumed to result in the phosphorylation-dependent endocytosis of the entire reelin signalling complex. In contrast to the proteasome-degraded Dab1, Reelin is targeted do the lysosome. The lipoprotein receptors are recycled back to the plasma membrane (Bock et al., 2004).

3.1.4 Src Family Kinases

The reversible and dynamic phosphorylation of proteins is an essential regulatory feature in nearly every cell biological process. These reactions are mediated by two groups of enzymes, protein kinases and their counterparts the phosphoprotein phosphatases.

Protein kinases are enzymes that transfer terminal phosphoryl groups of ATP onto specific serine/threonine or tyrosine residues of their protein substrates. Such proteins are involved in a variety of important cellular and signalling processes, hence when defective, they are implicated in various diseases, especially cancers (Yeatman T. J., 2004). Therefore, this large group of enzymes (with more than 500 protein kinases encoded in the human genome) is an interesting and extensively studied target for the design and development of new drugs and therapeutic inhibitors (Roskoski R. Jr., 2004 and 2005; Boggon and Eck, 2004).

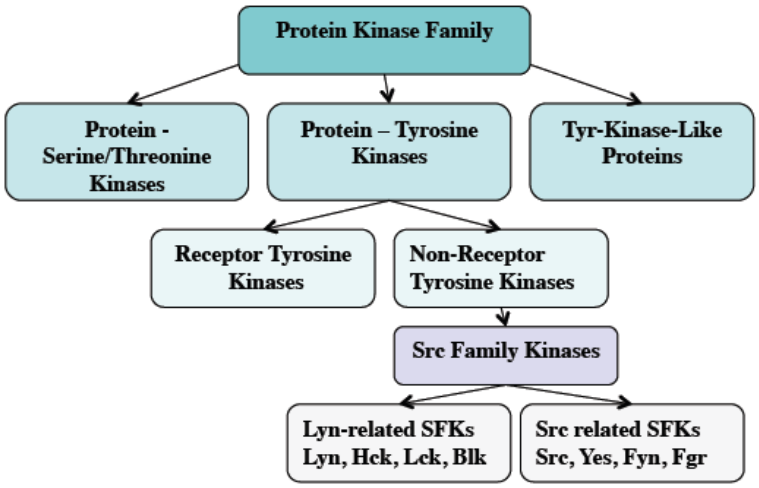

Protein Kinase: $MgATP^{1-} + Protein\text{-}OH \rightarrow Protein\text{-}OPO_3^{2-} + MgADP + H^+$

Phophoprotein Phosphatase: $Protein\text{-}OPO_3^{2-} + H_2O \rightarrow Protein\text{-}OH + HOPO_3^{2-}$

Fig. 3.6: Overview of protein kinases with special regard to the family of Src kinases, which belong to the non-receptor tyrosine kinases. Protein phosphorylation reactions catalysed by protein kinases and phosphoprotein kinases, which reverse the action of protein kinases.

Many transmembrane receptors involved in a variety of fundamental signal transduction processes lack an internal catalytic activity domain and require non-receptor kinases, such as the **Src family of tyrosine kinases (SFKs)**(Cooper and Qian, 2008). This family comprises 8 members (Lyn, Blk, Hck, Lck, and Src, Fgr, Fyn, Yes), which share a similar domain architecture and mode of regulation. SFKs are present in different tissues, but only Src, Fyn and Yes are expressed ubiquitously in all cell types. They are functionally involved in a number of signalling pathways and play important roles in cell proliferation and differentiation, cell adhesion, morphology and cellular motility, for example during embryonic development. The *src* gene was the first human proto-oncogene described; it is

a homolog of *v-src*, the avian Rouse sarcoma virus Src kinase encoding oncogene, which is involved in tumorgenesis (reviewed by Ingley E., 2008 and Roskoski R. Jr., 2004 and 2005). Due to its aberrant activity in many types of cancers and other pathophysiological processes the Src tyrosine kinase is one of the most extensively studied proteins, both in structure and function.

3.1.4.1 Domain arrangement of Src family kinases

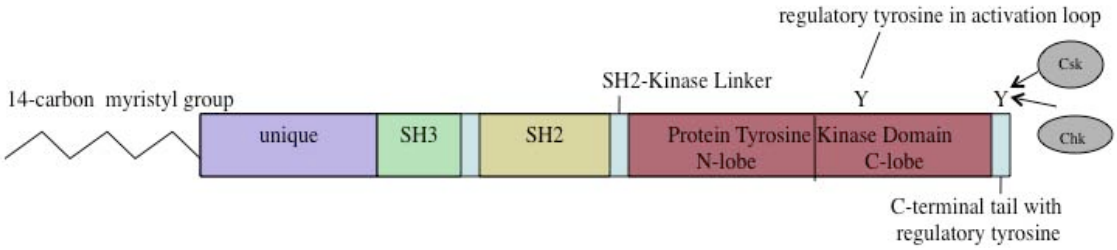

Fig. 3.7: Domain organization of Src as example for members of the family of Src kinases. An aliphatic myristoyl group is attached at the aminoterminal SH4 domain, which facilitates the attachment to membranes. The Src homology domains 2 and 3 are protein-protein interaction domains that allow for a precise targeting to the substrate. The two tyrosines shown in the figure are important for regulation of the kinase activity.

The highly variable **unique region** (50-70 residues) located at the N-terminus is the most divergent region within members of the Src kinase family and adds specificity and individuality. Yet, only little structural data is available for this part of SFKs (Ingley, 2008). In Src, an aliphatic myristoyl group of 14 carbon residues is attached to the unique region, which is thought to facilitate the targeting of the protein to the membrane, however, it is not sufficient to ensure membrane association (Brown and Cooper, 1996). For v-Src the myristoyl group was shown to be necessary to allow for the transformation of cells (Schulz et al.; 1985; Ingley, 2008).

The Src homology domains SH2 and SH3 function as protein-protein interaction domains that are commonly found in a variety of signalling proteins. Both domains are important for targeting the enzyme to protein substrates and for proper positioning of the kinase domain (SH1), which is responsible for the enzymatic activity. Additionally, these domains play a key role in regulation of SFKs by intramolecular interactions upon phosphorylation events (reviewed by Ingley E., 2008 and Roskoski R. Jr., 2004 and 2005).

The **SH3 domain** is about 60 amino acid residues long and usually binds to proline-rich motifs with the PxxP consensus sequence, which tends to adopt a left-handed helical conformation with low sequence specificity in the SH3 complexed form. The β-barrel architecture of SH3 domains consists of five antiparallel β-strands and two loops that are also involved in ligand binding (see figure 3.9) (reviewed by Brown and Cooper, 1996).

The **SH2 domain** consists of about 100 amino acids and interacts with specific sequence motifs that contain a phosphorylated tyrosine residue. For example, Fyn tyrosine kinase preferentially selects pYEEI compared to other consensus sequences. In addition to the phosphotyrosine, the isoleucine residue within this consensus binding sequence motif most influences binding selectivity (Songyang et al., 1995). In the SH2 domain fold typically two α-helices surround a conserved antiparallel β-sheet that is composed of four β-strands (see figure 3.8). The conserved positively charged binding pocket accommodates the bound phospho-tyrosine moiety perfectly by providing partners for the formation of hydrogen bonds, such as a highly invariable arginine residue located in strand βB. The binding pocket is surrounded by variable amino acid residues, which determine the specificity towards the respective binding motifs. For example, the Fyn SH2 domain provides an additional hydrophobic pocket for the isoleucine side chain of the pYEEI motif (Waksman et a., 1993;). Generally, SH2 domains function as protein-protein interaction units in a number of multidomain proteins including transcription factors, ubiquitin ligases, GTpase-activating proteins and of course tyrosine kinases and phosphatases (Boggon and Eck, 2004).

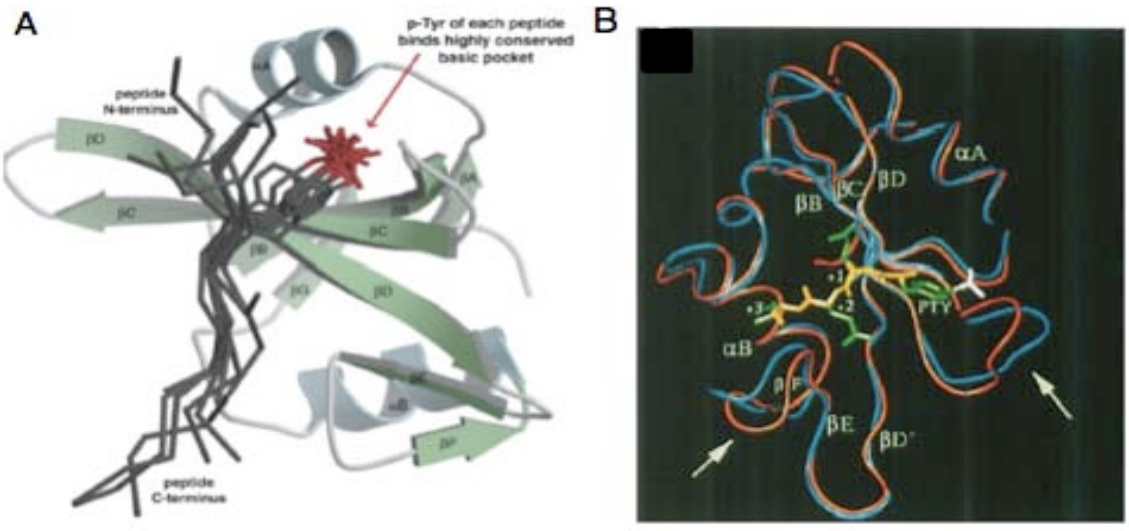

Fig. 3.8: A Src SH2 domain with eight different ligands superimposed (figure reprinted from *Schlessinger and Lemmon, 2003, Science's stke, 191, re12*). **B** Structural changes induced in the uncomplexed Src SH2 domain (blue) upon phosphotyroyl peptide binding (Reprinted from *Waksman et al., 1993, Cell 72, 779-790*).

The **Kinase domain (SH1)** shows the characteristic protein kinase architecture that consists of a small amino-terminal (N) and a large carboxyl-terminal (C) lobe (see figure 3.9). The N-lobe has a predominantly antiparallel β-sheet structure (5 β-strands and a single α-helix termed C helix) and is mainly required for anchoring and orienting ATP. In this context, the glycine-rich G-loop (also termed P-loop for phosphate binding) is important for coordinating the nucleotide phosphates. The C-helix is also important in the regulatory mechanism deployed by SFKs by changing its conformation upon activation of the enzyme. The C-lobe, which has a predominantly α-helical structure, is also involved in ATP binding but to a lesser extent than the N-lobe. It contains the activation loop with the regulatory tyrosine residue (Y416 in chicken Src), which stabilizes the active state when phosphorylated by autophosphorylation. The conformation of the A-loop differs in the active and inactive state of the kinase and forms a short helix in the dormant form, which buries the regulatory tyrosine. The catalytic site of SFKs lies within the cleft between the two lobes, which move relative to each other to open or close the cleft.
Three conserved amino acids (K/D/D) contribute to the catalytic core motif. In human Src for example, Lys295 forms ion pairs with α- and β-phosphates of ATP, Asp386 orients the substrate-tyrosine in a catalytically competent state and subtracts a proton to facilitate nucleophilic attack of the γ-phosphorus atom of MgATP. Finally, Asp404 binds Mg^{2+} (or Mn^{2+}) to coordinate the β- and γ-phosphate groups of ATP. In most non-receptor tyrosine kinases generally the catalytic loop consists of the sequence HRDLRAAN (Xu et al., 1997 and 1999, Ingley E., 2008). The active site conformations were found to be strikingly similar by comparing several tyrosine and serine/threonine kinases in their active and autoinhibited state (Huse and Kuriyan, 2002). The inactive states of miscellaneous protein kinases, however, can be structurally different due to individual regulatory mechanisms (Boggon and Eck, 2004).

Another important tyrosine is located in the **regulatory C-terminal tail** (Y527 in chicken Src). It is required for stabilisation of the dormant state of SFKs upon phosphorylation by specialised protein tyrosine kinases (reviewed by Ingley E., 2008 and Roskoski R. Jr., 2004 and 2005). SFKs are always phosphorylated at either one of the above-mentioned regulatory tyrosines or on both sites, depending on the activation state.

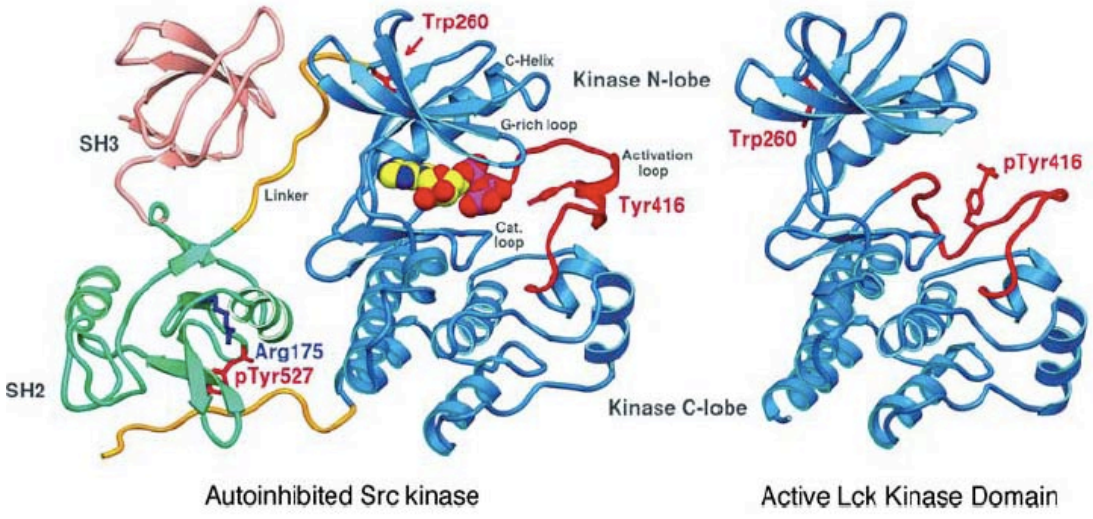

Fig. 3.9: Ribbon diagrams of the three-dimensional structure of Src family tyrosine kinases. On the left, inactive form of c-Src with a phosphorylated regulatory tyrosine 527 in the C-terminal tail. On the right, the kinase domain of Lck, a member of SFKs, in the active state with a phosphorylated tyrosine 416 in the activation loop of the C-lobe (reprinted from *Boggon and Eck, 2004, Oncogene 23, 7918-7927*).

3.1.4.2 Aspects of regulation for the family of Src kinases

SFKs are involved in numerous processes during the cell cycle and have important functions in cellular signalling; hence a tight regulation is necessary to maintain the physiological state of the cell. Deregulation and aberrant expression or increased activation of SFKs is characteristic for different types of cancers and other diseases (Yeatman T. J., 2004). Regulation of SFKs involves both extrinsic factors and intrinsic regulatory mechanisms (Ingley E., 2008).

Extrinsically, a range of receptors that are involved in various signal transduction pathways control SFKs. For example, ligand-induced receptor clustering (as in the Reelin pathway) triggers the activation of SFKs. Additionally, the levels of substrate molecules such as Dab1 and other protein adaptors influence SFKs activity (Roskoski R. Jr., 2004). In a self-regulatory cycle the elimination of phosphorylated Dab1 is triggered by a prolonged Reelin signal by inducing the ubiquitination and thus proteasomal degradation of Dab1 and internalisation of ApoER2. By keeping the phosphorylated Dab1 levels low the activity of SFKs is regulated, considering the dual role of Dab1 both as substrate and binding partner of SFKs (May, Herz and Bock, 2005). Ubiquitination and subsequent proteasomal degradation is also involved in regulating SFKs. Highly active SFKs are

marked for degradation with ubiquitin, so that the protein levels are decreased, as has been shown for Lyn (reviewed by Ingley E., 2008).

Tyrosine phophorylation is not only the main function of SFKs, it provides also an important feature for regulatory aspects. Members of the Src family of kinases contain several tyrosine and serine residues that have been demonstrated to alter activity upon phosphorylation. As mentioned above, two **regulatory tyrosine residues** are of utmost importance for controlling the activity of SFKs. One of them is located in the activation loop (Y416 in chicken c-Src) and the other in the C-terminal regulatory tail (Y527 in chicken c-Src) (Porter et al., 2000; Roskoski R. Jr., 2005, Engen et al., 2008). Under normal physiological conditions *in vivo*, 90-95% of Src is phosphorylated at the regulatory tail and hence in a dormant state (Zheng et al., 2000). The activity of Tyr527 phosphorylated Src has been shown to be decreased to only 0.2% to 20% of the unphosphorylated enzyme, depending on the applied experimental conditions. The controlled phosphorylation allows for only transient activation of Src kinases. Protein tyrosine kinases such as Csk (COOH-terminal Src kinase) or Chk (Csk homologous kinase have been shown to catalyse this regulatory phosphorylation reaction that leads to inactivation of the SFK (Okada & Nakagawa, 1989; Roskoski R. Jr., 2004). These enzymes are closely related to SFKs and show strong substrate specificity for the C-terminal SFK motif (reviewed by Chong et al., 2005). Cbp (Csk binding protein) recruits Csk/Chk to the membrane and increases the affinity towards SFKs compared to free Csk (Ingley, 2008).
SFKs have evolved an elegant and complex **autoinhibitory mechanism** for regulating kinase activity. The tyrosine phosphorylation in the C-terminal tail induces intramolecular binding by the SH2 domain, and the SH3 domain interacts with the proline-rich linker region that connects SH2 and the kinase domain. Hence the two protein-protein interaction modules turn inward and pack closely to the kinase domain (see figure 3.10). The intramolecular interactions result in a restrained conformation, in which none of the protein interaction domains of the enzyme are accessible and the catalytic domain is locked in the inactive state (See figure 3.9 and 3.10). The SH3 domain packs against the N-lobe and the SH2 domain against the C-lobe, leading to displacement of the C-helix, which further disrupts the interaction between Gly310 (C-loop) and Tyr382 (catalytic loop). These intramolecular interactions are strong enough to maintain the inactive conformation of SFKs, however, compared to interactions with more specific substrates the affinity is rather low in order to allow for the binding of exogenous ligands

(reviewed by Roskoski R. Jr., 2004; Ingley E., 2008). For example, the linker containing the SH3 domain-binding site includes proline residues, however, not in the typical PxxP consensus sequence of an SH3 domain interaction site, but it forms a left-handed polyproline type II helix in the bound state (Xu et al., 1999). The sequence surrounding pTyr527 is EPQYQPGEN (524-532), which is different from the preferred pYEEI binding site for the Src SH2 domain (Wang et al., 2001).

Displacement of intramolecular bound SH2 and SH3 hence occurs when substrate is available to compete for binding. Activation of SFKs further requires dephosphorylation of the regulatory tail tyrosine residue by corresponding phosphoprotein phosphatases. Unfortunately, it is unclear which precise phosphatases are involved in regulation, although several enzymes have been demonstrated to possibly be involved in these processes. Among other phosphatases, PEP (proline-enriched tyrosine phosphatase) seems most likely to be responsible for the dephosphorylation of the A-loop (Roskoski R. Jr.; 2004; Ingley, 2008).

Small perturbations in the crucial regulatory intermolecular interactions of SFKs can alter the kinase activity by stabilizing the active conformation. In the oncogenic v-Src protein, for example, the autoinhibitory phosphorylation site in the regulatory C-terminal tail is missing. Other mutations that block for example the binding of the SH2 domain to the tyrosyl-phosphorylated tail were found to keep Src in the activated state (reviewed by Boggon and Eck, 2004).

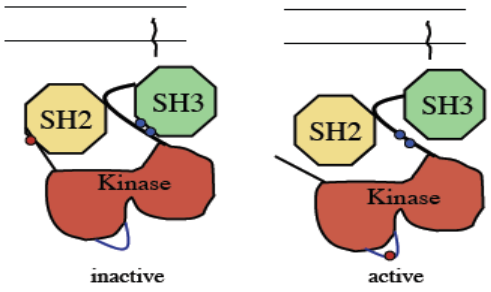

Fig. 3.10: General schematic illustration of the inactive and active configuration of SFK2. Left, the inactive form is represented, showing the intramolecular interactions between SH2 and the phosphorylated regulatory tyrosine residue in the C-terminal tail of the enzyme (red sphere). The SH3 domain binds to a proline-rich left-handed helix in linker region between SH2 and the kinase domain (blue spheres). Phosphorylation of the regulatory tyrosine in the C-terminal tail is catalysed by protein kinases such Csk or Chk. In the active configuration, shown at the right, the protein interaction domains are released from the intramolecular interactions, the C-terminal tyrosine is dephosphorylated, but the tyrosine residue in the activation loop of the kinase domain underwent autophosphorylation.

In order to gain full kinase activity upon activation in the presence of substrate or activating molecules, the enzyme undergoes **autophosphorylation at the A-loop site** (Sun et al., 1998). It is likely that other members of the SFK mediate the tyrosine phsophorylation in the A-loop in a trans-autophosphorylation mechanism. Tyrosyl-phosphorylation influences changes in the conformation of the A-loop, which is forming a short α-helix in the inactive state that makes the tyrosine unavailable for modification and has a stabilizing effect (see figure 3.11). However, in the active form the phospho-tyrosine can form a salt bridge with a conserved arginine residue, which is thought to have a stabilising function. Only activated Src with a dephosphorylated Tyr527 in the regulatory tail can undergo autophosphorylation (Sun et al., 1998, reviewed by Ingley E., 2008).

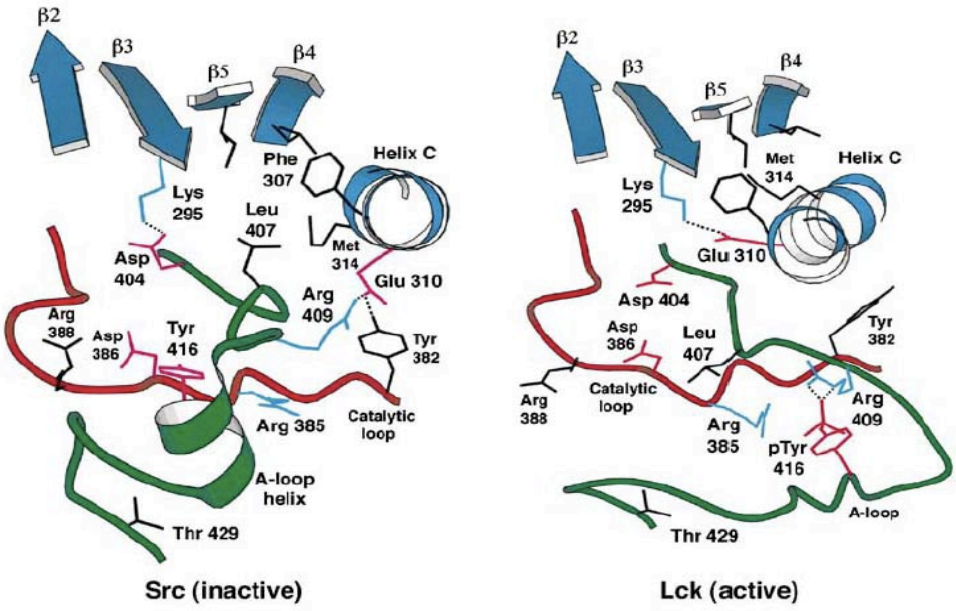

Fig. 3.11: Schematic representation of the active site of SFKs in the inactive and active state. Note the changes in conformation of the C-helix of the N-lobe (blue) that disturb the interaction between Gly310 and Tyr 382 (catalytic loop). Furthermore, the activation loop forms a short helix (making Tyr416 inaccessible for phosphorylation) in the active state, which is distorted in the inactive enzyme (figure reprinted from *Boggon and Eck, 2004, Oncogene 23: 7918-7927*).

3.1.5 Interaction mechanism of Fyn tyrosine kinase and Disabled-1

Reelin induces the phsophorylation of the Dab1 adaptor, which is bound to the receptors, upon the dimerisation by activating Fyn and other SFKs (Howell et al; 2000; Strasser et

al., 2004). However, a basal level of SFKs activity is assumed to be responsible for the small amount of constitutively phosphorylated Dab1 present in neurons. Tyrosine residues 198 and 220 were detected to be the major Reelin-induced phosphorylation sites in neurons during embryonic development (Keshvara et al., 2001). Both tyrosines in the phsoporylated state have been demonstrated to mediate binding to the SH2-domain of SFKs *in vitro* (Howell et al., 1997). They also resemble typical SFK binding consensus sequences (Songyang et al., 1995).

The structural and molecular mechanism regulating Reelin signal transduction by Fyn kinase activation and receptor clustering is not yet fully understood. Generally, the trans-phosphorylation of Dab1 by SFKs is likely, which means that the phosphorylation reaction is catalysed at an adjacent Dab1 molecule located in close proximity to the molecule the tyrosine kinase is bound to via its SH2 domain (see figure 3.12). This hypothesis also explains the need of receptor clustering, which brings the associated Dab1 molecules closer together (Feng and Cooper, 2008). Also the autophosphorylation of SFKs in the A-loop is thought to occur rather in trans than in cis; there is evidence that different SFKs can phosphorylate each other (Ingley E., 2008).
Targeting of Dab1 in a cis-position, which implicates that the phosphorylation happens on the same Dab1 molecule the Fyn is bound to (see figure 3.12), be another possibility to describe the phosphorylation mechanism (Mayer et al., 1995).

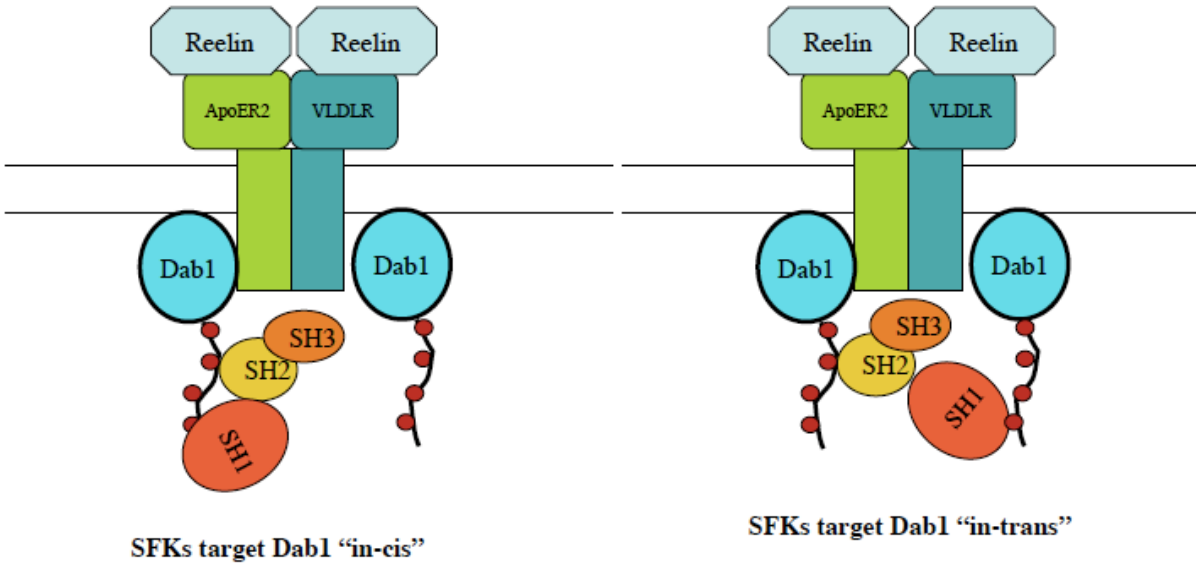

Fig. 3.12: It is unclear whether Fyn and other members of SFKs phosphorylate Dab1 "in cis" (at the same molecule the enzyme is attached to via the SH2 domain) or "in trans" (bound at one molecule but phosphorylating an adjacent Dab1).

3.2 Outline of the Diploma Project

Considering its essential functions in brain development, it is important to elucidate the details of Reelin signalling to understand how migrating neurons in the cortex and hippocampus are positioned in the typical laminated pattern, which is required for the formation of correct neuronal circuits. The phosphorylation of Dab1 is certainly a crucial step in this pathway, but the mechanisms by which SFKs target and discriminate the four Dab1 phosphorylation sites are not yet clear. From examining the sequence surrounding the tyrosine residues, it seems possible that the Dab1 phosphorylation sites have different functions in downstream signalling (Howell et al., 2000). Several experiments using knock-in mice expressing Dab1 isoforms with different patterns of tyrosine mutated to phenylalanine support this assumption (Feng & Cooper 2009; Morimura & Ogawa, 2009).

Structural studies in combination with biochemical data could provide a better understanding and insight in this context. Such combinatorial approaches might be helpful to determine whether the activated Fyn kinase phosphorylates Dab1 molecules “in cis” or “ in trans” position, as discussed above (see figure 3.12). Furthermore, such experiments could provide information about regulation and activation of SFKs. Clearly, the SH2 domain seems to have an important functional role in Reelin signalling, since it has been shown to bind to phosphorylated Dab1 (Howell et al., 1997). We therefore hypothesise that the SH2 domain of Fyn might have different affinity for individual phospho-tyrosyl residues in Dab1. Furthermore, the kinetic properties of Fyn tyrosine kinase for phosphorylation of the four Dab1 sites might be varying.

Therefore, in preparation for further structural and biochemical experiments the specific interactions between Fyn tyrosine-kinase and Dab1 have been investigated to determine whether certain tyrosine residues are preferred binding partners for the SH2 domain and whether there are differences in the K_m-value of the kinase for different Dab1 phosphotyrosines.

The aim of this work was to establish purification protocols for both a Fyn SH2-kinase construct and Dab1 tail variants that contain different phenylalanine mutations of the four tyrosine-phosphorylation sites. The requirements for the purification strategies were to yield high concentrations of active SH2-kinase with a high degree of purity.

Furthermore, the purified proteins were subsequently used to biochemically characterise the interactions between Fyn and Dab1 *in vitro*. In this context, isothermal titration calorimetry (ITC) was used to determine the binding affinities of the SH2 domain of the Fyn SH2-kinase construct to different synthetic peptides that resembled the Dab1 tail and contained single phosphorylated tyrosine residues. Additionally, a radioactive kinase assay was established to allow for the determination of the kinetic properties of the SH2-kinase construct towards the different Dab1 tail mutants. The kinetic parameters in comparison to the kinase domain alone (data of the latter not shown here) will provide information about the influence of Dab1 targeting by the SH2 domain. In addition, the suitability of the SH2-kinase construct for crystallisation trials was evaluated by using the Stargazer instrument (Senisterra et al., 2006) to define stabilising buffer conditions for the SH2-kinase construct in order to facilitate crystallisation. The protein was tested in different buffer systems and with a number of additives and the stability was evaluated by determining the melting temperature (T_m) at which the protein aggregates under different conditions.

A difference in the binding affinity of the SH2 domain to phosphorylated tyrosines of the Dab1 tail is expected in the ITC studies. Additionally, differences in k_m-values are expected in the *in vitro* radioactive kinase assay. In combination with future structural studies and additional cell-based experiments using an artificial system to induced clustering of Dab1 molecules, these experiments hopefully will provide deeper insight into the interaction mechanism between Fyn and the Dab1 adapter protein.

4 Materials and Methods

4.1 List of Materials

All chemical compounds were purchased, either from Fluka or Sigma-Aldrich unless otherwise noted. Enzymes, protein ladders and DNA ladders were mainly obtained from Fermentas.

4.1.1 Media

To avoid microbial contamination media and compound stock solutions were autoclaved before use. Antibiotic stock solutions and buffers were filtered with 0.2 µm filters for sterility.

Luria-Bertani medium (LB)	10 g tryptone, 5 g yeast extract, 10 g NaCl in 1 L dH_2O, pH 7
Super-Optimal broth (SOB)	20 g tryptone, 5 g yeast extract, 0.5 g NaCl, 2.5 mM Kcl in 1 L dH_2O
Super-Optimal Catabolite repression (SOC)	SOB containing 2 % glucose
SOC-salt	SOC containing additionally 12.5 mM $MgCl_2$ and 12.5 mM $MgSO_4$

4.1.2 Antibiotics

The antibiotics were sterile filtered and generally used as 1: 1000 dilutions of the here listed stock solutions if not otherwise stated.

Ampicillin	100 mg/ml stock solution in dH_2O, stored at -20°C
Chloramphenicol	34 mg/ml stock solution in 70% ethanol, stored at -20°C
Kanamycin	50 mg/ml stock solution in dH_2O, stored at -20°C
Streptomycin	50 mg/ml stock solution in dH_2O, stored at -20°C

4.1.3 Buffers

3x SDS loading buffer	15% glycerol, 7.5% β-mercaptoethanol, 4.5% SDS, 150 mM Tris, bromphenol blue
1x SDS running buffer	25 mM Tris/Hcl pH 8.3, 200 mM glycine, 0,1% (w/v) SDS, prepared as 5x stock and stored at room temperature
10x TAE buffer	0.4 M Tris/HCl pH 8, 0.2 M acetic acid, 10 mM EDTA-Na_2-salt
6x DNA loading dye	0.25% (w/v) bromphenol blue, 50 % (w/v) sucrose in dH_2O, stored at 4°C
1x Western Blot Transfer Buffer	25 mM Tris/Hcl pH 8, 192 mM glycine, 10% methanol prepared as 10x stock without methanol, stored at 4°C
1x Tris buffered saline (TBS)	10 mM Tris/Hcl pH 8, 150 mM NaCl, prepared as 10x stock, sterile filtered, stored at 4°C
1x TBS-T	0.1% Tween-20 added to 1x TBS, stored at 4°C
1x HEPES buffered saline (HBS)	10 mM HEPES, 150 mM NaCl in dH_2O, pH 7.4

4.1.4 Chemical Compounds and Reagents

Stock solutions of prevalently used compounds were prepared, autoclaved and stored at room temperature by the media kitchen facility.

1 M Tris pH 8
5 M NaCl
0.5 M EDTA pH 8

Ammonium persulfate (APS):	10% (w/v) solution in dH_2O, sterile filtered, stored at -20°C
Isopropyl β-D-1-thiogalactopyranoside (IPTG):	0.5 M stock solution in dH_2O, sterile filtered, stored at -20°C

Dithiothreitol (DTT):	1 M sock solution in dH_2O, sterile filtered, stored at -20°C
Imidazole:	4 M and 1 M stock solutions in dH_2O, sterile filtered, stored at room temperature

4.1.5 Enzymes

Restriction enzymes and Pfu polymerase were purchased from Fermentas.

Lysozyme	50 mg/ml stock solution in dH_2O, stored at -20°C, used in a 1:250 dilution for cell lysis
Benzonase	Stratagene, added do cell lysates for DNA degradation
Phusion polymerase	High-Fidelity polymerase (Finnzymes) used for all cloning procedures unless otherwise mentioned.
TEV Protease	Recombinantly expressed and purified in the laboratory.

4.1.6 Bacterial Strains

For molecular cloning purposes and DNA isolation the *E. coli* strains DH5α or XL10-Gold were used. Recombinant proteins were produced with the *E. coli* BL21(DE3) expression system.

Table 4.1: Overview of bacterial strains used in this project.

Bacterial Strain	Provider	Description
DH5α		Used for DNA preparation
XL10-Gold	Stratagene	Enhanced transformation efficiency, therefore used after site-directed mutagenesis
BL21(DE3)	Stratagene	Chromosomal copy of the T7 promoter, high-level protein expression.

4.1.7 Plasmids and Constructs

4.1.7.1 Dab1-tail constructs in pGEX(TEV) vector

A modified version of a pGEX4T vector, with a TEV protease cleavage site introduced to remove the N-terminal GST-fusion tag from the protein of interest, was used for expression of the Dab1-tail constructs (see also 4.2.1.1). This pGEX(TEV) vector carries an ampicillin resistance gene and a multiple cloning site. Gene expression is under the control of the lac promoter. (The pGEX(TEV) vector was provided by Robert Kurzbauer, Clausen lab, IMP).

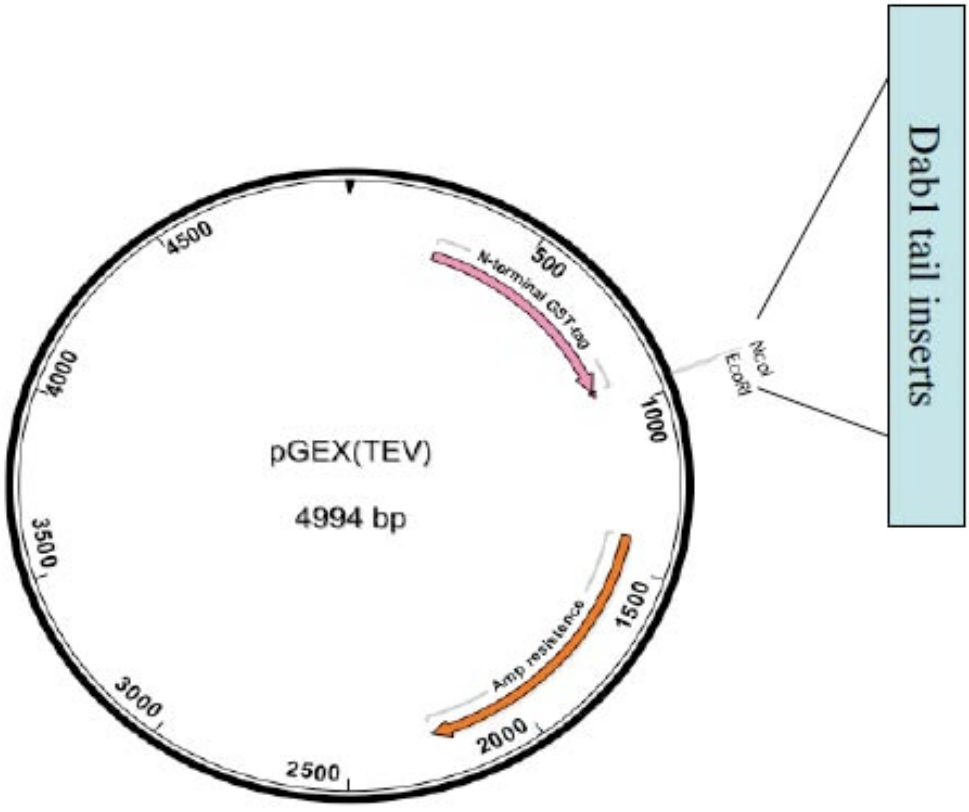

Fig. 4.1: Schematic representation of the pGEX(TEV) plasmid with the Dab1-tail insertion site and an resistance for amicillin.

4.1.7.2 Dab1-tails in pMM vector

Since prior experience had shown that expression of Dab1 without a C-terminal tag was prone to degradation, we were not sure if the fusion of a His-tag to the tails would allow for expression and purification of these proteins. Therefore we additionally cloned the constructs into a pMM-vector that had an N-terminal hydrophobic sequence that would

facilitate the production of inclusion bodies. In this way, the degradation would be retarded, but the proteins would require re-folding during purification. However, these constructs were not used for further experiments, because the His-tag in the pGEX(TEV) expressed Dab1-tails prevents degradation and allows for production of the proteins.

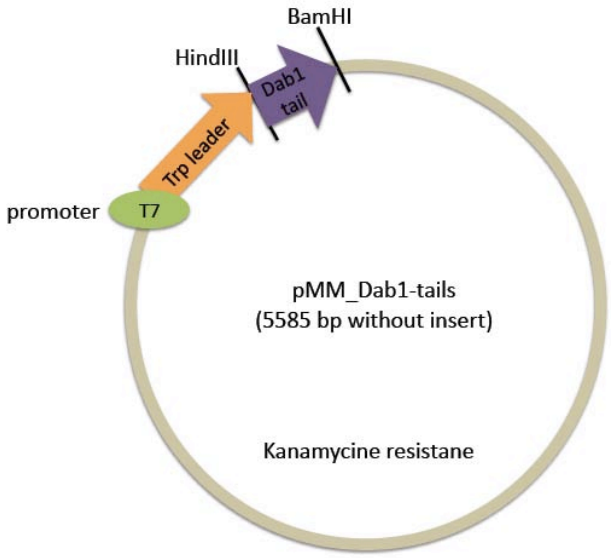

Fig. 4.2: Dab1-tails that were inserted in pGEX(TEV) were additionally cloned into the pMM-vector. The plasmid contains a kanamycine resistance gene, a T7 promoter and a Trp-leader sequence N-terminally fused to the insert. The Trp-leader is a hydrophobic tag that facilitates protein expression in inclusion bodies.

4.1.7.3 Fyn SH2-Kinase in pET21a vector

The 1212 bp construct was designed and cloned by DI Barbara Nussbaumer. Fyn SH2-Kinase domains were inserted into a pET21a expression vector with a C-terminal 6x His-tag. An ampicillin resistance gene allows for positive selection of transformed bacteria. Gene expression is regulated by the T7 promoter.

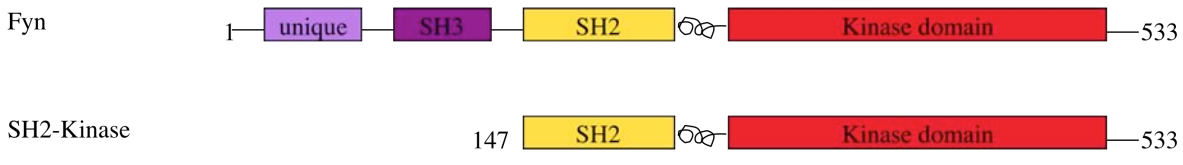

Fig. 4.3: Schematic representation of the domain architecture of the tyrosine kinase Fyn and the SH2-Kinase (SH2K) construct.

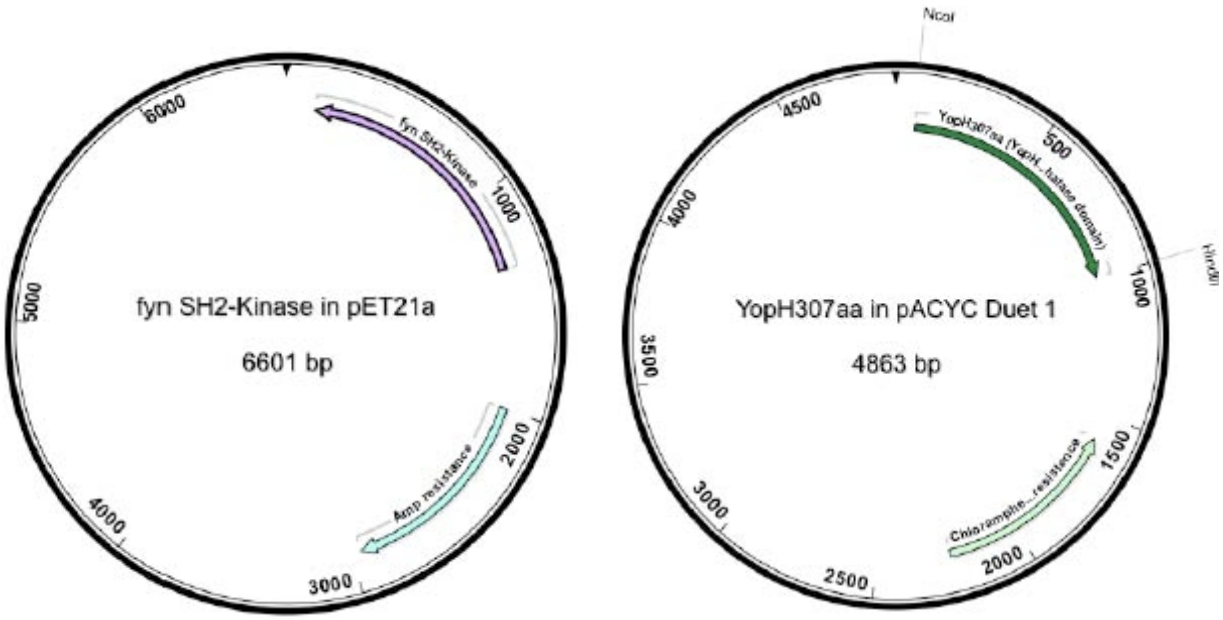

Figure 4.4: Vector maps of SH2-Kinase in pET21a (amoxicillin resistance) and of the YopH phosphatase domain (chloramphenicol resistance) in the pACYC Duet 1 plasmid.

4.1.7.4 YopH Phosphatase domain in pACYC Duet 1 vector

The phosphatase domain (307 amino acids in legth) was inserted into the first multiple cloning site of a pACYC Duret-1 vector which is preceded by the lT7 promoter/lac operator and carries a chloramphenicol resistance gene as a selectable marker (see figure 4.4).

Full-length YopH constructs with or without a N-terminal Strep-tag II were also cloned and tested for co-expression. However, full length YopH was of similar size to SH2K and therefore not appropriate for our purposes. Addition of a N-terminal strep-tag II led to insoluble full length YopH.

Additionally, a strep-tag II was added C-terminally to the phosphatase domain construct (YopH_307aa_strep). The affinity tag did not influence the expression of this construct negatively, however, a frame shift mutation was detected that probably destroyed the tag. Hence, those vectors are not shown here; see section 4.2.1.2 for further information on the different constructs.)

4.2 Methods

4.2.1 Molecular Cloning

4.2.1.1 Cloning of Dab1-tail constructs

Molecular cloning was used to generate three different constructs of the unstructured C-terminal tail of Disabled-1. The variants differ in size and the number of possible phosphorylation sites that are included. The short construct lacks tyrosine 185, which is included in the Dab1-tail long construct. One of the variants additionally includes the phospho-tyrosine binding domain, which binds to a non-phosphorylated tyrosine motif in the Reelin receptors.

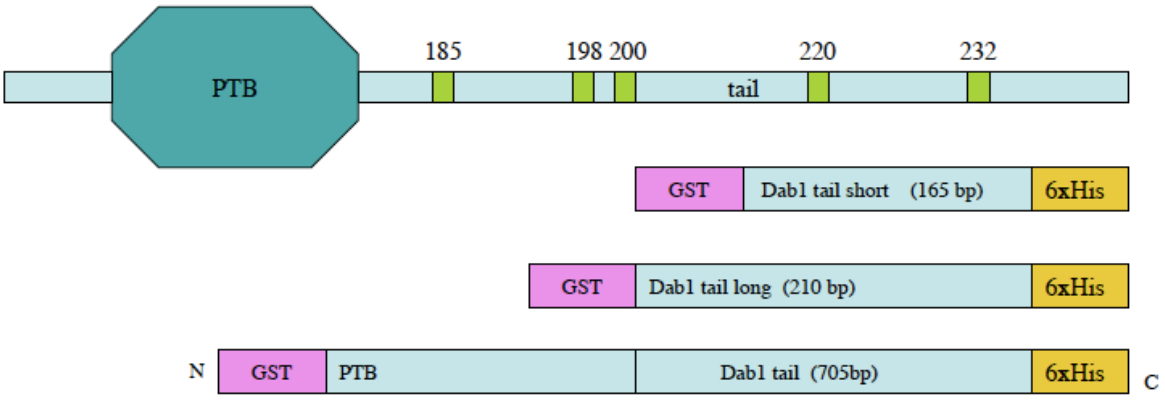

Figure 4.5: Domain architecture of Disabled1 and the designed Dab1-tail constructs that were cloned into the pGEX(TEV) vector. The Dab1-tail constructs contain a TEV protease cleavable N-terminal GST-tag and a non-cleavable 6xHis-tag.

The Dab1-tails were amplified by PCR with Phusion polymerase (Finnzymes) and appropriate primers (see table 4.2 and 4.3). The PCR fragments and pGEX(TEV) vector were digested with NcoI and EcoRI restriction enzymes and subsequently ligated with T4 DNA ligase. *E. coli* DH5α cells were transformed and single colonies were picked for DNA isolation (QIAprep Mini Prep Kit, Qiagen).

Table 4.2: List of primers used for molecular cloning of Dab1 wt constructs and the YopH307aa construct.

Primer Name	Sequence	Annealing Temperature
F_Dab1-tail_long	CATGCCATGGATAAGCAGTGTGAACAAGCT	
R_Dab1-tail	GGAATTCCTAGTGATGGTGATGGTGATG TACAGGTTGACTTTTTGGCACATC	66°C
F_Dab1-tail_short	CATGCCATGGATGTGGAAGATCCCGTGTAC	62°C
fYopH_307aa	CATGCCATGGGCCCGCGTGAACGACCACAC	65°C
rYopH_307aa	GGGAAGCTTCTAGCTATTTAATAATGGTCGCCCTTG	

Table 4.3: Conditions of PRC reactions with Phusion polymerase.

Step	Temperature	Time	Cycles
Initial Denaturation	98°C	30 seconds	1x
Denaturation	98°C	15 seconds	30x
Annealing	Dependent on melting temperature of primers	30 seconds	
Extension	72°C	15 seconds	
Final extension	72°C	5 minutes	1x

4.2.1.2 Cloning of YopH phosphatase domain

Seelinger et al. (2008) demonstrated that co-expression of the YopH phosphatase from *Yersinia* (Bliska et al. 1991) with kinases in prokaryotic expression systems helps to reduce the toxicity that results from uncontrolled kinase activity. Hence, a higher yield of soluble protein can be obtained. Unfortunately, YopH was bnding unspecifically to Ni-NTA beads and eluted at the same volume as the co-expressed Fyn SH2-kinase when applied on gel filtration-based FPLC (fast protein liquid chromatography) due to the similar molecular weight. To overcome these problems, other constructs of YopH were cloned into pACYC Duet 1 vectors and tested for co-expression with SH2K (see figure 4.6).

The phosphatase domain of YopH was amplified by PCR with the Phusion polymerase and after digestion with NcoI and HindIII was ligated into the first multiple cloning site in the pACYC Duet 1 vector. The plasmid derived C-terminal His-tag was deleted by the

insertion. No affinity tag was added to the YopH_307aa construct with a total length of 921 bp (307 amino acids). The construct was cloned according to the phosphatase domain characterised and crystallised by Zhang et al. (1992) and Sun et al. (2003), which comprises aa163-aa468 of full length YopH (926aa).

Full length YopH and the phosphatase domain alone were cloned with the same strategy but with a N-terminal and C-terminal strep tag II, respectively. All of the Yersinia-derived phosphatase constructs were tested in small-scale co-expression experiments with SH2K (see figure 4.6 and table 4.4; also see section 4.2.3.1 and 5.2 for more information). For our aims however, the phosphatase domain alone gave the best results and was used for large-scale co-expression with SH2K.

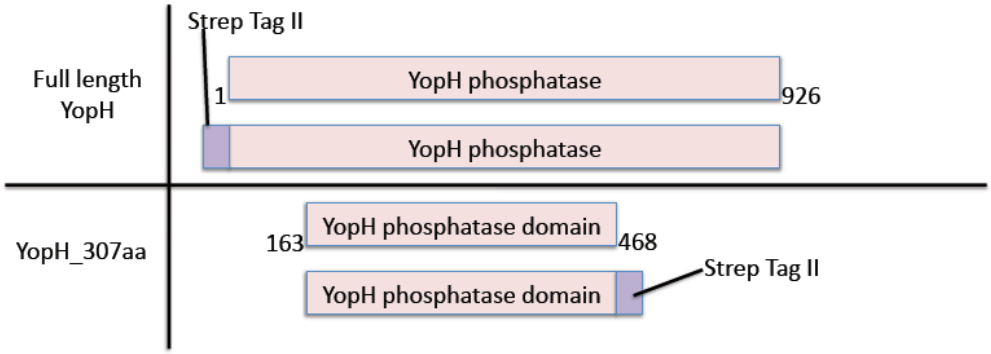

Fig. 4.6: Schematic representation of the YopH constructs tested for SH2K co-expression. Among these constructs YopH_307aa (residues 163-468) proved to be the best for our purposes. It consists of the phosphatase domain of the Yersinia-derived protein without addition of a C-terminal Strep tag II.

Table 4.4: Overview of the YopH variants tested for SH2-Kinase co-expression. YopH307aa (phosphatase domain) was found to be best under the used conditions.

Construct	Vector	Resistance	Troubles
YopH	full length in pCDF Duet	Strep	Binds non-specifically to Ni-NTA and elutes at the same size as SH2K in size exclusion chromatography
YopH_strep	full length in pACYC Duet 1 with C-term. Strep-tag II	Cam	Insoluble and inactive, hence reduces SH2K expression level
YopH307aa	phosphatase domain in pACYC Duet 1	Cam	Different mutations in the different clones led to differences in activity.
YopH307aa_strep	phosphatase domain and strep-tag II in pACYC Duet 1	Cam	Frame shift close to the C-terminus. Hence, probably no strep tag II expression. SH2K co-expression works

4.2.1.3 DNA preparation and purification

DNA was isolated and prepared using the QIAprep® Spin Mini Prep Kit (Quiagen) according to the provided protocol. Purification of DNA samples after gel electrophoresis or after PCR was carried out with the QIAquick gel extraction kit (Quiagen). An Eppendorf microcentrifuge was used for the DNA preparation and purification protocols.

4.2.1.4 Agarose gel electrophoresis

To separate DNA molecules depending on their size agarose gel electrophoresis was performed. For separation of PCR or restriction fragments and purified plasmid DNA, usually 1% agarose in 1x TAE buffer was used. DNA molecules were visualized on the gel by addition of SYBR Safe DNA stain (Invitrogen).

4.2.1.5 Restriction digests and ligation

PCR products and 2-5 µg of the respective vectors were digested in 50 µl reactions over night at 37°C with the two restriction enzymes of choice in 1x reaction buffer according to the requirements of the enzymes (see www.fermentas.com). Alkaline phosphatase was added to the plasmid digest reaction assay to prevent re-ligation of the cut vector.
Ligation of the insert and vector was carried out in 20 µl reactions with T4 DNA ligase with a 5x molar excess of the insert.

4.2.1.6 Transformation of competent *E. coli* cells

50 -100 ng plasmid DNA were used to transform 50 – 100 µl of chemically competent *E. coli* cells by heat shock. The cells were incubated for 10 minutes on ice together with the DNA. To allow for the uptake of the plasmid the cells were incubated at 37°C for 50 seconds and then cooled on ice. 1 ml SOC medium was added and the cells were incubated with shaking at 37°C for 30 minutes. Subsequently the bacteria were plated on LB agar plates with the respective antibiotics for selection of positive clones.

4.2.1.7 Generation of competent *E. coli*

E. coli BL21(DE3) cells were made chemically competent according to the $CaCl_2$-protocol (Sambrook and Russel; Molecular cloning – A laboratory manual, Vol. 2). Cells were streaked out on LB plates and a single colony was picked to inoculate 100 ml of LB medium. The bacteria were grown to an optical density of 0.350 at 37°C and 200 rpm. Then the cells were transferred to 50 ml falcon tubes and cooled on ice before centrifugation at 4°C and 2700 g for 10 minutes. All traces of medium were removed and the cell pellet was then re-suspended in 30 ml of an ice cold and sterile solution of 80 mM $MgCl_2$ and 20 mM $CaCl_2$. Thereafter, the bacteria were centrifuged and each pellet was resuspended in 2 ml of ice-cold 100 mM $CaCl_2$ solution. 140 µl DMSO were added to the *E. coli* suspension and stored on ice for 15 minutes after very gentle mixing. Subsequently, an additional 140 µl of DMSO were added and the competent cells were immediately aliquoted, frozen in liquid nitrogen and stored at -80°C.

4.2.2 Site-directed Mutagenesis

The codons for tyrosine residues that are found in the wild type Dab1-tail construct were substituted for phenylalanine by site-directed mutagenesis. A range of mutants was obtained that vary in the number and location of the possible tyrosine phosphorylation sites exchanged, as shown in figure4.7. The mutants were named according to their non-mutated phosphorylation sites, with Y185 = A, Y198/200 = B, Y220 = C and Y232 = D.

To directly mutate site-specific residues the Pfu polymerase and the respective buffer were used with about 200 ng of DNA template. The conditions used during the PCR run are given in table 6.

2 µl DpnI restriction enzyme was added subsequently to the 50 µl PCR assay and incubated for 2 hours at 37°C. This allows for the specific digestion of the template plasmids that were isolated from *dam+ E. coli* strains and that are therefore positive for dam methylation in contrast to the newly synthesized plasmids.

5 µl of the digestion were then transformed into competent XL10-Gold cells and the cells were plated on LB agar plates that contained ampicillin. Single colonies were picked and grown in 3 ml of LB medium with ampicillin to allow for plasmid DNA preparation. The clones were finally sequenced to determine whether the correct mutations are present.

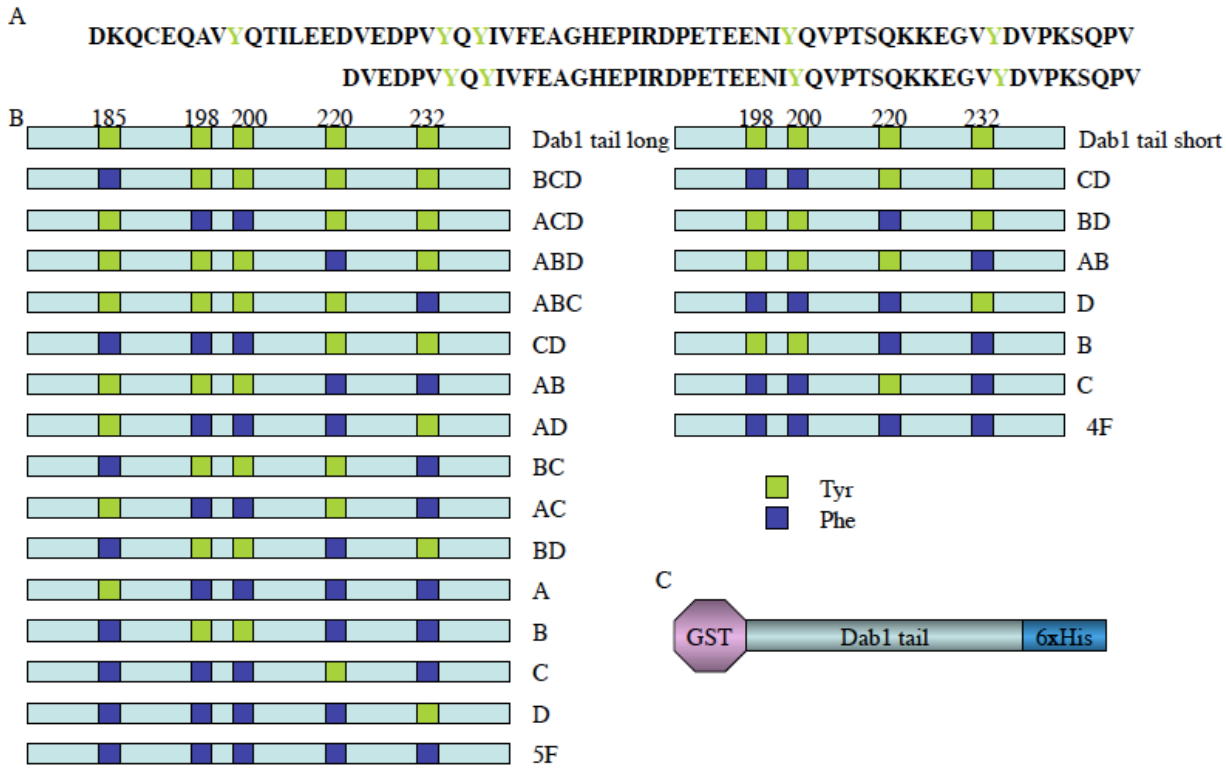

Fig. 4.7: A The amino acid sequence of the short and long Dab1-tail peptide. **B** Schematic representation of different Dab1-tail mutants generated by site-directed mutagenesis. The mutants are named according to the remaining tyrosine residues. **C** All mutants contain an N-terminal GST-tag and are His-tagged at the C-terminus.

Table 4.5: Conditions for site-directed mutagenesis PCR

Step	Temperature	Time	Cycles
Initial Denaturation	95°C	30 seconds	1x
Denaturation	95°C	30 seconds	15X
Annealing	55°C	1 minute	
Extension	72°C	7 minutes	
Final Extension	72°C	10 minutes	1x

4.2.3 Expression of recombinant proteins in *E. coli* BL21(DE3)

All proteins for the experiments described below were expressed in *E. coli* BL21(DE3).

4.2.3.1 Small-scale expression trials

Proteins were expressed in small-scale at different temperatures and over different time periods to define the optimal expression conditions. For that purpose the cultures were grown in 20 ml LB medium with the respective antibiotics. 0.2 mM IPTG were found to be sufficient for induction of protein expression. Either 15 ml of the cultures were then harvested in falcon tubes for cell disruption with glass beads, or 2 ml samples were taken and lysed according to the mini-lysis protocol.

Table 4.6: Conditions tested in small-scale for expression of Dab1-tails and SH2K.

Protein	Temperature	Time	shaking	IPTG
Dab1-tail long	37°C	3 hours	200 rpm	0.1/0.2/0.4 mM
	25°C	6 hours	290 rpm	0.2 mM
Dab1-tail short	37°C	3 hours	200 rpm	0.1/0.2/0.4 mM
	25°C	6 hours	200 rpm	0.2 mM
SH2K/different	37°C	3 hours	200 rpm	0.2 mM
YopH constructs	25°C	6 hours	200 rpm	0.2 mM
	18°C	over night	130 rpm	0.2 mM

4.2.3.2 Large-scale expression

The bacteria were cultivated in 2 L LB medium with the respective antibiotics at 37°C and 200 rpm in 5 L flasks. The medium was inoculated with 15 ml of an overnight starter culture and the bacteria were grown to an optical density between 0.6 and 0.8 prior the induction of protein synthesis with 0.2 mM IPTG, if not stated differently. 30 minutes before induction the temperature was reduced to 18°C and the shaking was slowed to 130 rpm. The protein was expressed overnight under these conditions. Finally the cells were harvested and the pellets were frozen at -20°C.

4.2.3.3 SH2-Kinase co-expression with YopH-phosphatase domain

As mentioned before, SH2K had to be co-expressed with the YopH phosphatase domain to reduce the toxicity caused by uncontrolled protein phosphorylation. Since the constructs

were inserted in two different vectors, a co-transformation of these plasmids had to be performed. For a successful transformation, *E. coli* cells had to be sufficiently competent and the two plasmids had to be added in a similar molar ratio. The induction of synthesis of toxic proteins at higher optical density (between 1.0 and 1.2) was found to yield higher amounts of SH2K (according to Seelinger et al., 2008).

4.2.4 Purification of Recombinant Proteins

4.2.4.1 Purification and analysis of small-scale expression trials

2.2.4.1.1. Mini-lysis protocol:

2 ml of bacterial cell culture (pre and post expression) were centrifuged at 13000 rpm and the cell pellet was re-suspended in 400 µl lysis buffer (50 mM Tris/HCl pH 8, 1 mM $MgCl_2$, 1 mM EDTA). 200 µg/ml lysozyme for lysing the *E. coli* cells and 1 U/ml benzonase for DNA degradation were added to the suspension and incubated for 15 minutes at room temperature. Centrifugation at 13000 rpm in an Eppendorf microcentrifuge allowed for the separation of insoluble protein and cell remnants. Samples were taken from the total cell lysate and the supernatant and prepared for SDS-PAGE for further analysis.

2.2.4.1.1. Cell disruption with glass beads:

The pellet from a 15 ml bacterial culture was re-suspended in 5 ml of buffer and 1 ml aliquots were mixed with 1 ml of 0.1 mm glass beads, unless otherwise stated. Cells were lysed by 3 minutes of vigorous shaking in a cell disruptor. The cell lysate was transferred to a 1.5 ml BioRad column and centrifuged for 2 min at 1000 rpm to remove the glass beads. The flow through was then centrifuged for 20 min at 13 000 rpm to spin down insoluble cell remnants. Samples of the total cell lysate and the supernatant were analysed by SDS-PAGE to determine the solubility of the expressed protein.

4.2.4.2 Large-scale purification of SH2-Kinase

A three step purification strategy that involved Ni-affinity chromatography, cation exchange chromatography and gelfiltration led to the highest degree of purity and

homogeneity, which was the main goal, to possibly allow for successful crystallization in the future.

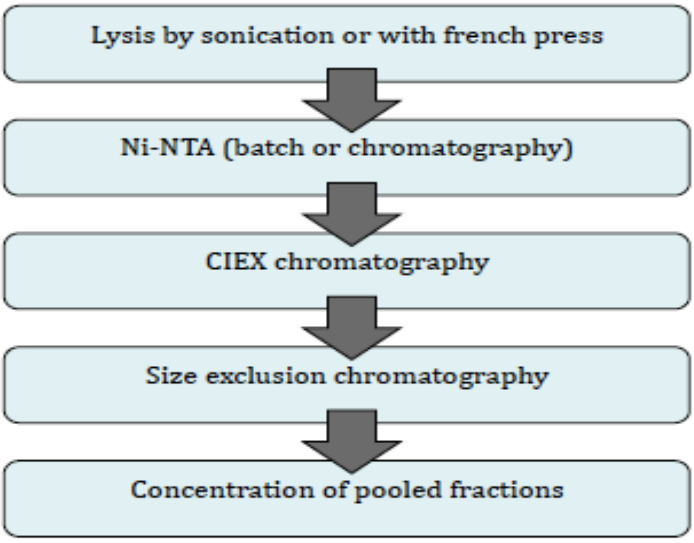

Fig. 4.8: Flow scheme of the different steps and strategies applied for SH2-kinase purification. The combination of affinity chromatography, cation exchange chromatography and a final gel filtration step yielded active enzyme in a high degree of purity.

Cell pellets from 12 L of *E. coli* culture were re-suspended in 100 - 150 ml of SH2K lysis buffer and cells were lysed by three passages at 2 kbar through a cell disruptor. 30 mM imidazole was added to the lysis buffer to reduce nonspecific binding of YopH and other proteins to the Ni-NTA. Because frozen pellets exhibited high levels of viscosity, the amount of buffer added could differ. To avoid blockage of the cell disruptor due to a highly viscous sample sometimes a sonicator was used. In that case, the cells were lysed by 3x sonication for 1 minute at 1-second pulses. The samples were stored on ice throughout the process to avoid damage of the proteins.

Cell remnants were separated from the cell lysate by centrifugation at 20000 rpm for 40 minutes in a Sorvall centrifuge. The supernatant was either applied to a 5 ml Ni-NTA column for affinity chromatography, or incubated in batch with 5 ml of Ni-NTA beads for 4 hours. SH2K that was bound to the beads was eluted with imidazole (linear gradient from 30 to 250 mM in chromatography or with 250 mM in batch experiments). The eluate was directly loaded onto a HiLoad 16/60 Sephadex 75 gelfiltration column to separate aggregated protein from SH2K when a very high degree of purity was not necessary. The protein eluted at a column volume (CV) of 60 ml. In order to improve the purity the eluate was first applied on a HiTrap SP XL 1 column (GE Healthcare) for cation exchange chromatography and eluted with a linear gradient from 5% to 100% buffer B over 15 CV.

The appropriate fractions of the gel filtration run were further analysed by SDS-PAGE, then pooled and concentrated in VivaSpin Concentrator Columns (Vivaspin) with a molecular weight cut-off of 30000 Da. The yield of SH2K was about 8 mg/12 L expression.

Table 4.7: Buffers used for SH2K purification.

SH2K lysis buffer	**SH2K CIEX buffer**		**SH2K GF buffer**
50 mM Tris pH 8	**CIEX A**	**CIEX B**	50 mM Tris pH 8
300 mM NaCl	20 mM phosphate pH6.5	20 mM phosphate pH6.5	300 mM NaCl
5% glycerol	5% glycerol	5% glycerol	5% glycerol
1 mM DTT	1 mM DTT	1 mM DTT	1 mM DTT
30 mM Imidazole		1 M NaCl	
Complete Protease Inhibitor Cocktail (Roche)			

4.2.4.3 Large-scale purification of Dab1-tail variants

Yields from 4 L cultures of Dab1-tail purifications differed depending on the type of mutant, but ranged from 0.3 to 2 mg.

The pellets were re-suspended in 50 ml of Dab1-tail buffer that contained a Complete Protease Inhibitor cocktail (Roche) to prevent proteolytic degradation. After 3x 1 minute sonication at 1 second pulses (Sonicator) under cooled conditions the cell lysate was centrifuged for 40 minutes at 20000 rpm in a Sorval centrifuge. The supernatant was then incubated with 4 ml of glutathione sepharose beads (GE Healthcare) for 4 hours to allow the binding of the GST-tagged protein to the resins. The protein that was bound to the beads was washed 3 times with buffer to remove the remaining lysate. The GST-tag was removed from the protein by incubation with TEV protease overnight at 4°C. The supernatant was incubated for 2 hours with Ni-NTA beads (Qiagen) to achieve higher purity by the second affinity step. The protein was finally eluted from the Ni-beads with 250 mM imidazole in Dab1-tail buffer, and the eluate was loaded onto a HiLoad 16/60

Sephadex 75 gelfiltration column (GE Healthcare) after equilibration of the column with Dab1-tail buffer. Separation of the proteins in the eluate according to the hydrodynamic volume was achieved by size exclusion chromatography (or gel filtration). Dab1-tails eluted from the column at 75 and 80 ml of a column volume for the short and the long construct, respectively. To determine the purity of the protein sample, the respective fractions were analysed by SDS-PAGE, pooled and concentrated in VivaSpin Columns with a molecular weight cut-off of 5000 Da.

Dab1-tail buffer: 150 mM NaCl
50 mM Tris/Hcl pH 8
5% glycerol
1 mM DTT

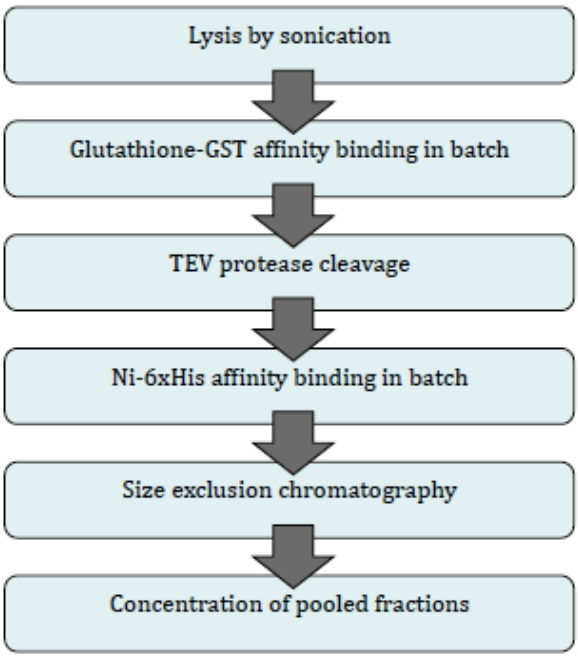

Figure 4.9: Flow-chart of the applied steps Dab1-tail purification. The combination of non-chromatographic affinity binding to Glutathione Sepharose and Ni-NTA beads followed by gel filtration of the eluate yielded protein with a reasonable degree of purity.

SDS-PAGE: SDS-polyacrylamide gel electrophoresis

Unless otherwise mentioned, the SE250 SDS-PAGE system from Amersham/GE Healthcare was used to separate proteins according to their molecular weight on 12%

SDS-polyacrylamide gels. The protein solutions were loaded onto the gel with a 3x sample buffer under reducing conditions (contained β-mercaptoethanol), after the samples had been heated for 5 minutes at 95°C. The gels consisted of two parts, a separating gel (12 % bis/acrylamide) that was topped by a stacking gel (5% bis/acrylamide). Polyacrylamide gels were prepared according to the protocol in „Molecular Cloning: A Laboratory Manual". The proteins were usually separated at 20 mA per gel. As a molecular weight marker an unstained protein ladder from Fermentas was commonly used, except for Western blotting experiments, where the pre-stained protein ladder was more practical.

For Dab1-tails, especially for radioactive kinase assays, 4-20% pre-cast gels from GeneXpress that could be applied in the SE250 system were used. For those gels the electrophoresis was carried out at 140 V for 1 hour and 5 minutes.

After the electrophoresis the gels were stained with a PageBlue protein staining solution (Fermentas) according to the provided protocol. The staining is based on a coomassie blue stain that co-localizes with certain amino acids and hence allows the visualization of proteins on polyacrylamide gels.

4.2.4.4 Western Blotting

Western Blotting is a method to transfer proteins onto a membrane, which allows for further analysis by specific reactions such as interactions with antibodies that recognize certain epitopes on the protein.

SH2K and Dab1-tails were transferred to a PVDF membrane (Millipore Immobilion-P PVDF, 0.45 µm) in a Hoefer TE 22 Mighty Small Transfer Electrophoresis unit (GE Healthcare) at 100 V for 1.5 hour or 45 minutes respectively, depending on the size of the proteins. The membrane had to be activated in methanol and transfer buffer for 5 minutes each to enable the binding of the proteins. The blotting was done under cooled conditions at 4°C in the cold room. The membrane was then blocked in 5% milk in TBS-T for 30 minutes, and finally incubated overnight with anti-penta-His antibody (Qiagen) that was diluted 1:10000 in TBS-T with 5% BSA. Detection of both recombinantly expressed proteins, SH2K and the Dab1-tail mutants, could be detected via their His-tag by this method.

To reduce the background signal the membrane had to be washed 5 times for 7 minutes with TBS-T to remove non-specifically bound antibodies. Antibody binding was visualized using either the PS-3 Western Blot detection kit (Lumigen) or the SuperSignal West Pico Chemiluminescent Substrate (Pierce, ThermoScientific), depending on the strength of the signal on a suitable film (Kodak).

4.2.5 Determination of protein concentration

To determine the concentration of purified protein in solution the absorbance at 280 nm was measured in a NanoDrop spectrophotometer (Thermo Scientific), unless otherwise noted. The extinction coefficient (calculated with the ProtParam tool at http://www.expasy.ch) and the molecular weight of the respective protein were used to calculate the protein concentration from the absorbance measurement.

This method relies primarily on the absorbance of the amino acids tryptophan and tyrosine. Dab1 tail mutants with no, or only one or two tyrosine residues gave a rather weak and inaccurate signal. Therefore, the concentration of the purified Dab1 tails was determined by the BCA Protein Assay (Thermo Scientific). A standard curve of the wild-type long Dab1-tail that contained all 5 tyrosines was used according to the concentration determined with the absorbance at 280 nm. This colorimetric method was used in a micoplate format by following the provided protocol and the absorbance at 562 nm was read in a spectrophotometer. This assay combines the reduction of Cu^{2+} by protein in alkaline conditions with the chelation of the resulting cuprous cation Cu^{1+} by bicinchoninic acid leading to a purple coloured complex. According to the producer, the BCA assay is less affected by the compositional differences of various proteins.

4.2.6 StarGazer – Screening for optimal Buffer Conditions

The melting temperature (T_m) of a protein (the temperature at which 50% of the protein has denatured) correlates with the stability of the respective protein and can be determined among other methods with static light scattering in a high throughput manner using the StarGazer instrument by Harbinger Biotech. The Stargazer uses static light scattering to measure the increase in particle size due to the aggregation of unfolded

protein upon rising temperature. Since the stability of a protein depends on the surrounding conditions, different components such as the buffer, salt and other additives that may stabilize the protein can be screened to determine the optimal buffer conditions for crystallization and protein chemistry in general.

The protein samples (50 µl, final protein concentration 0.1-0.2 mg/ml, overlaid with 50 µl of mineral oil) are prepared in black 384 well plates with a transparent bottom (Nunc) and are heated in the heating block of the Stargazer from 20 to 80°C. (The plates were centrifuged at 3000 g for 5 minutes prior the measurement.) An LED-light source is located under the plate. Images are captured in 0.5°C steps to document the increase in scattered light upon protein aggregation, which is then integrated to plot a melting curve for each of the protein sample (Bioactive program). This allows the calculation of the aggregation temperature (T_{agg}) that is comparable to the T_m. The aggregation temperatures in different conditions can then be compared. The samples were usually tested in duplicates and well A24 was used to measure the temperature with a sensor and contained only buffer and oil.

Two Stargazer screens were done to optimize the buffer conditions for SH2K. In the first experiment basic buffer systems and different salt conditions were screened (conditions not shown here). In the following approach a commercially available screen kit with 96 different compounds (Hampton Research Crystal Screen) was used to test for possible additives that would stabilize SH2K. The protein in different buffers and the buffers without protein were used as controls.

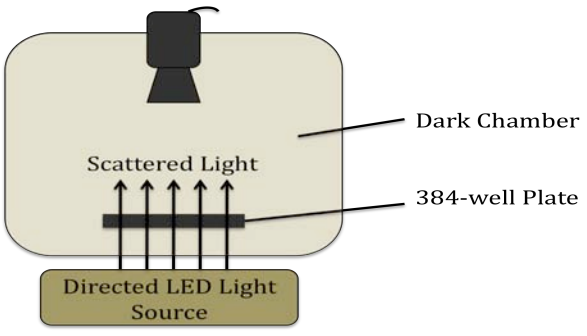

Fig. 4.10: Schematic representation of the Stargazer set up.

4.2.7 Isothermal Titration Calorimetry

Isothermal titration calorimetry (ITC) is a useful and sensitive method to determine the thermodynamic parameters of protein-protein interactions by measuring the heat release upon the binding of two interaction partners. Hence, the changes in Gibbs energy (ΔG) and entropy (ΔS) can be calculated from the parameters determined by ITC, which is binding affinity (K_D), the enthalpy change (ΔH) and the binding stoichiometry (n).

$$\Delta G = -RT\ln K = \Delta H - T\Delta S$$

R = gas constant and T is the absolute temperature.

To analyse the interactions of Dab1 and Fyn tyrosine kinase, the binding affinities of the SH2 domain to synthetic peptides of the Dab1-tail containing a particular phosphorylated tyrosine residue were determined by ITC.

Purified SH2K was added to the reaction cell of the MicroCal ITC instrument at a minimum concentration of 13 µM and phospho-peptides were titrated to the protein in either 29 injections of 10 µl at 25 °C or 42 injections of 7 µl were used, unless otherwise stated. The concentration of the phospho-peptide exceeded the protein concentration in the cell by approximately 15 times and was adapted to the used protein concentration.

Phospho-Y198:	EDVEDPVY(PO)QYIVFEA	(1894,79 Da)
Phospho-Y220:	ETEENIY(PO)QVPTSQKKEGVYDVPK	(2760,28 Da)

4.2.8 Kinase Assays with radiolabeled ATP

To characterize the interactions between Dab1 and Fyn several mutants of the Dab1-tail with the important phophorylation sites (Y185, Y198/Y200, Y220, Y232) substituted with phenylalanin were generated, as mentioned before. These mutants were tested for phosphorylation by Fyn kinase domain and the Fyn SH2-Kinase construct. The interactions were characterized by determination and comparison of the kinase activity and the kinetic parameters. We expect to see differences in the affinity of the kinase domain and SH2-Kinase domains towards the individual phosphorylation sites.

Dab1 tails in varying concentrations were incubated in a 25 µl assay at 30°C with 200 nM SH2K and 0.5 µl γP32-ATP stock solution (5 µCi) in 1x Src Mn/ATP cocktail (Stratagene).

In a preliminary experiment Dab1-tail long wt (0.25/0.5/0.75/1/1.5/3.5/5/10 µM) and the mutants Dab1-tail long AB and Dab1-tail long CD (0.5/0.75/1/1.5/2/2.5/5/10 µM) were used in the kinase assay. The reactions were carried out in 96 well plates to allow simultaneous reaction times for the different substrate concentrations tested.

5 µl samples were taken after 30/60/120/180 seconds; and the reactions were stopped immediately by adding 2.5 µl of 3x sample buffer. The samples were heated to 95°C for 5 minutes before 5 µl were loaded on 4-20% polyacrylamide gels (pre-cast gels from GeneXpress) and separation of the proteins by electrophoresis.

Proteins were fixed on the poyacrylamide gel by incubating the gels for 30 minutes in a 40% methanol and 10% acetic acid solution. The fixed gels were finally dried in a vacuum drier at 80°C for 30 minutes and then exposed on a Storage Phosphor Screen (Kodak) to allow for digital detection of the radioactive bands in a Storm Scanner. The absolute intensities of the bands were quantified with ImageJ (**Rusband W.S.; Abramoff et al., 2004**) and data was further analysed in GraphpadPrism.

4.2.9 Anti phospho-Tyrosine 198 Antibody generation

Antibodies to detect phosphorylated tyrosine residues 220 and 232 of Dab1 were commercially available, however, since it was assumed from former observations by our lab and others, that phospho-tyrosine 198 is a main player in Reelin signalling we wanted to generate an antibody to detect this particular residue.

Three rabbits were immunised with a synthetic peptide of the Dab1-tail, which contained the phosphorylated Tyr198 and was conjugated to KLH (Kpep 2659). Immunisation was performed by Gramsch Laboratories (Germany). Blood was taken 3 times every two weeks and the serum was sent to our lab for further analysis and purification. The sera were frozen in aliquots at -80°C.

Kpep 2659: CEDVEDPVY(PO4)QYIVFEA

Kpep 2667: CEDVEDPVYQYIVFEA

Purification of α pTyr 198 antibody from 5 ml serum by a 2-step affinity chromatography procedure on a HPLC column was carried out by the IMP protein chemistry facility. The

first column contained the unphosphorylated peptide bound via lysine to a carrier to remove non-phosphospecific antibodies (Kpep 2667). In a second step the antibodies specific for the phospho-tyrosine antigen were purified by affinity binding to Kpep 2659.

For a first purification trial 5 ml of serum from each rabbit from the second bleeding were tested. The antibodies were purified by HPLC at a pressure of 15 bar with HBS as the running buffer. The purification was monitored by UV-absorption at 280 nm and the antibodies were eluted in two fractions from the columns, with $MgCl_2$ and glycine respectively.

The fractions of purified antibody had to be dialysed in order to remove the Mg-salt and glycine. The Spectra/Por®3 dialysis tubing with 3500 MWCO had to be soaked in dH_2O for 30 minutes before use. The dialysis was carried out at 4°C in the cold room for 2 hours against HBS, and in a second step over night against HBS and 5% glycerol. After the dialysis the antibodies were slowly and carefully concentrated in VivaSpin Concentrator columns with 50000 MWCO to avoid precipitation.

Finally, the different fractions were analysed by Western Blot for the ability to specifically detect the phosphorylated tyrosine 198 of the unstructured Dab1-tail. Cell lysates from a Hek293 culture expressing different Dab1 variants (prepared by DI Barbara Nussbaumer) were separated by SDS-PAGE on 10 % polyacrylamide gels and blotted on a PVDF membrane as described earlier. 10 ml of a 1 μg/ml dilution of the purified antibodies in TBS-T with 5% BSA were prepared and incubated overnight at 4°C with the membranes. After 3x washing steps with TBS-T 10 ml of a 1:3000 dilution of anti-rabbit HRP-conjugated antibody in TBS-T and 5% BSA were added to each blot and incubated for 2 hours at room temperature. The Western blots were washed 3 times with TBS-T before development.

The cell lysates used for detection of anti phospho-tyrosine 198 antibody from polyimmune sera contained different Dab1 constructs. One of them, Dab1 wt, was phosphorylated *in vivo* by co-expression of Fyn. Dab1 Y198F, however, was unphosphorylated at tyrosine 198 due to a mutation but phosphorylated on the remaining tyrosines. As an additional unphosphorylated control a recombinantly expressed and purified long Dab1-tail was used to exclude nonspecific binding of the purified polyclonal antibody.

5 Results and Discussion

5.1 Expression and purification of Dab1-tail constructs

5.1.1 Cloning and site-directed mutagenesis

Dab1-tails (short, long and PTB-long) were successfully cloned into the pGEX(TEV) and pMM vectors. The short and long Dab1-tails in the pGEX(TEV) expression vector were also used for the generation of a range of mutants by exchange of the four possible tyrosine-phosphorylation sites Y185, Y198, Y220 and Y232 with phenylalanine. The missing hydroxyl group of the phenylalanine eliminates the phosphorylation and hence this enables the investigation and characterization of the phosphorylation of Fyn SH2-Kinase to the different Dab1-tail mutants *in vitro* by Fyn SH2-Kinase.

5.1.2 Expression

Preliminary expression trials of the Dab1-tails nicely showed that expression of the pGEX(TEV)-Dab1-tails leads to soluble proteins that are primarily found in the supernatant of the lysate. On the other hand, the pMM-vector drives the expression of insoluble proteins that are located in inclusion bodies due to the hydrophobic tag added to the Dab1-tails (see figure 5.1).

In both vectors the protein expression is induced with IPTG. Rather low concentrations of IPTG were found to be sufficient to induce the production of Dab1-tails. Hence, for all further expression 0.2 mM IPTG was used.

In a second expression trial, different times and temperatures for expression of the Dab1-tails were tested. The temperature seems to have only minor effects on the production of recombinant Dab1-tails since the expression at 37°C for 3 hours and at 18°C over night was comparable (data not shown). However, for most of the purifications an over night expression at 18°C was preferred.

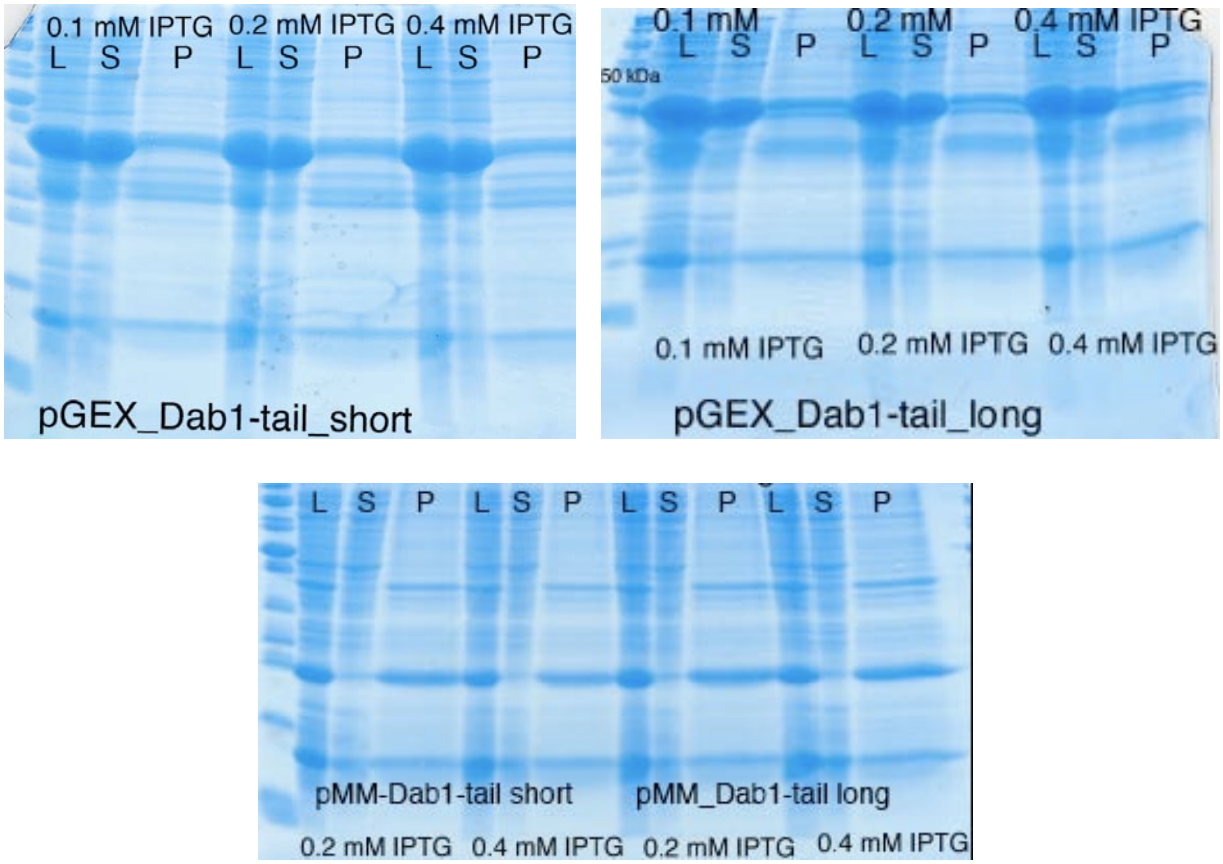

Fig. 5.1: Dab1-tails in pGEX(TEV) are expressed as soluble proteins and are hence predominantly found in the total lysate (L) and supernatant (S) of the lysate, only little insoluble protein is found in the pellet (P). pMM-Dab1-tails are expressed in inclusion bodies and are therefore mainly located in the pellet of the total lysate.

5.1.3 Purification

After the optimal expression conditions were determined, the wild type short and long Dab1-tails were expressed in a larger scale for a first purification experiment. By the combination of two affinity binding steps in batch and a final size exclusion chromatography a reasonably pure short and long wt Dab1-tail could be obtained (see figure 5.2). Therefore, this three-step purification strategy was also applied for the Dab1-tail mutants. First, the lysate was bound to glutathione-sepharose beads followed by cleavage of the N-terminal GST-tag by TEV protease. To increase the purity, and insure recovery of full-length protein, a second affinity binding step to Ni^{2+} ions immobilized on sepharose beads (Ni-NTA) was carried out to capture the C-terminal His-tag of the protein.

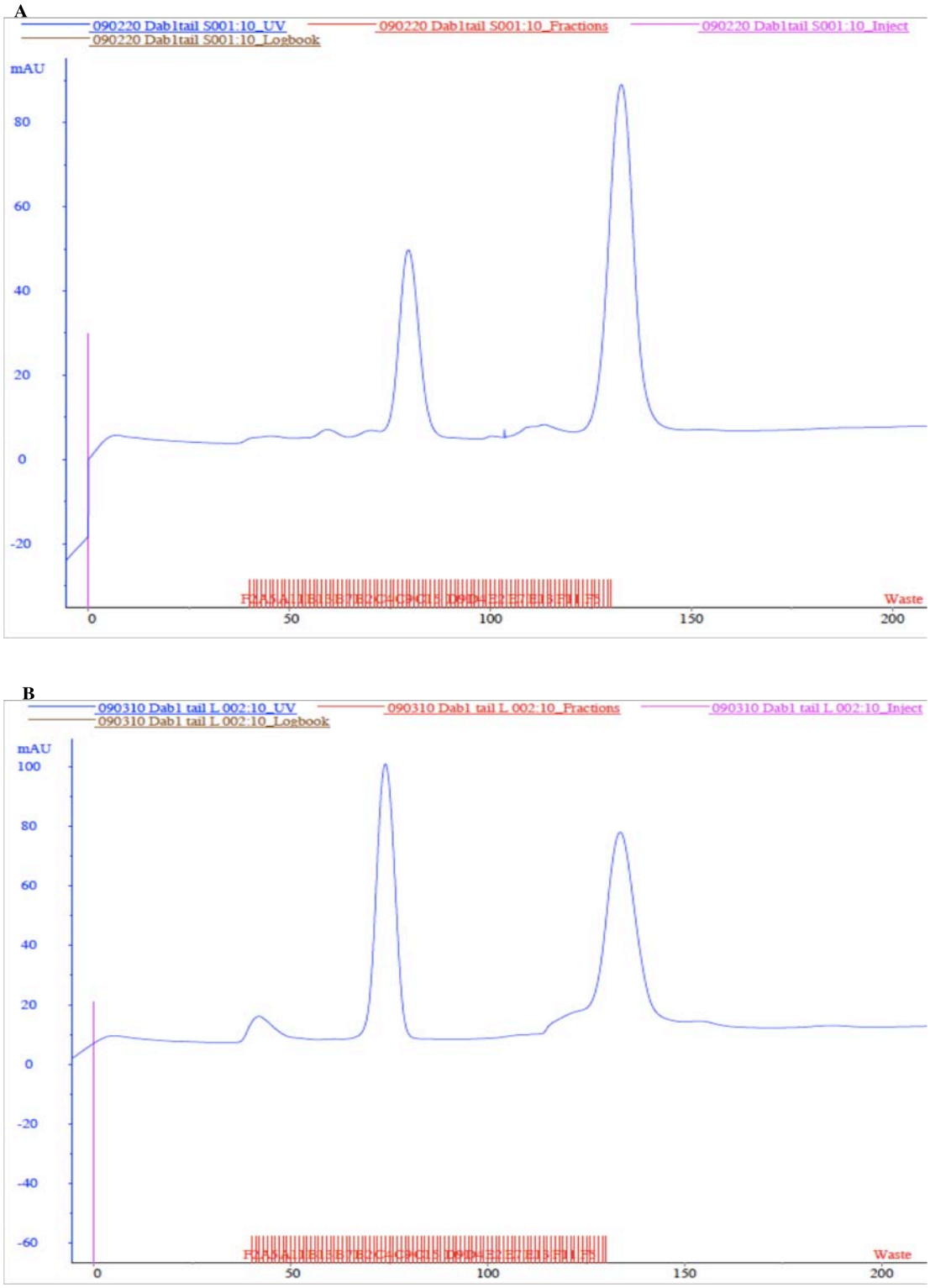

Fig. 5.2: Chromatograms of size exclusion experiments as final steps in purification of Dab1 tail constructs. On the x-axis the volume [ml] is indicated, the column volume was 120 ml. Proteins were detected by UV-absorption and were measured in mAU (milli absorbance unit at 280 nm) as indicated on the y-axis. **A** Gel filtration chromatogram of the Dab1-tail short wt purification from a 2L culture pellet. The protein eluted at about 80 ml. **B** Chromatogram of the Dab1-tail long wt gel filtration from a 4L *E. coli* culture. The protein eluted at about 75 ml.

Dab1-tail short eluted at approximately 80 ml from the gel filtration column and the longer pDab1-tail at 75 ml. The samples of the individual purification steps were analysed on polyacrylamide gels by SDS-PAGE to determine the purity of the sample and to identify the protein. As demonstrated in the respective gels in figure 5.3 that shows the respective gels, a high degree of purity could be reached by the applied purification strategy. Most interesting, the Dab1-tails were running on the gel at slightly higher molecular weight than it would be expected. Dab1 tail short has a molecular weight of 6.5 kDa while the longer peptide has a size of 8.3 kDa, however they run at approximately 14 and 16 kDa, respectively. Because the conditions in the sample buffer are reducing due to the β-ME it contains it is rather unlikely that the proteins are forming dimers. It is possible that the relatively low pI-values of the Dab1-tails (short 5.27, long 4.86 calculated with the ProtParam tool of www.expasy.ch) result from the rather high number of acidic amino acids in the peptide (15 out of 65 amino acids in the longer construct), which can influence the running behaviour (Ye and Sloboda, 1997).

To verify that the purified proteins are indeed the desired Dab1-tails, the C-terminal His-tag was specifically detected with an anti-penta His antibody fused with HRP on a Western blot. In addition, the pooled fractions of the gel filtration peak were analysed by mass spectrometry and exhibited 100% sequence coverage (data not shown).

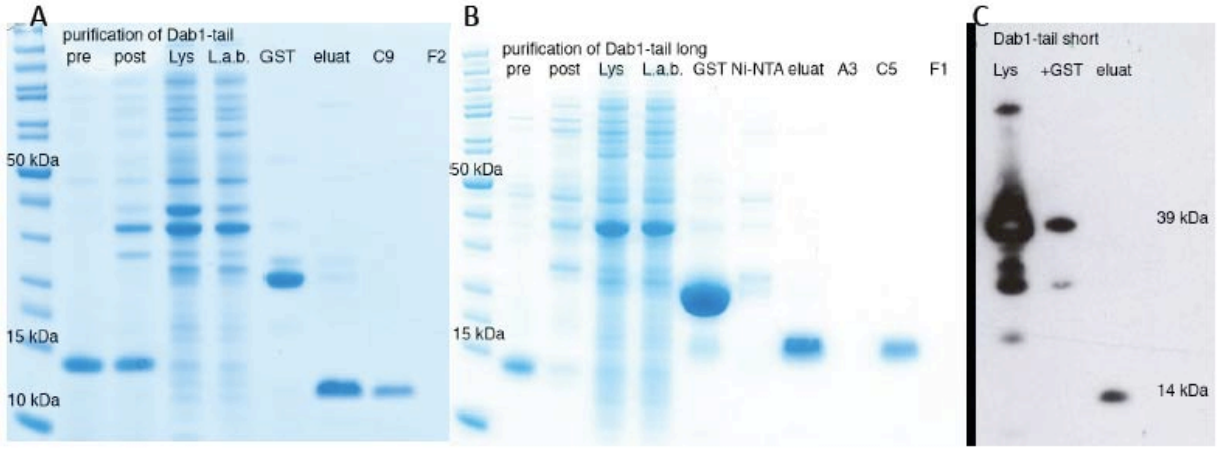

Fig. 5.3: Control of Dab1-tail purification by SDS-page and Western Blot. **A** All steps of the Dab1-tail short purification were analysed on a 12% polyacrylamide gel. The pre and post induction samples and the lysate and lysate after binding to the glutathione beads were diluted 1:10. GST on beads after cleavage with TEV protease was washed before boiling in sample buffer. The eluate was used for further size exclusion chromatography and C9 is the fraction if the peak maximum after gelfiltration. **B** Progress of Dab1-tail long purification analysed on a 12% polyacrylamid gel from pre induction to gel filtration, samples termed like in A, however, with the peak maximum in fraction C5 (tube position in the fractionater) after chromatography.

C Detection of Dab1-tail short by anti penta-His–HRP antibody on Western blot confirmed the presence of the His-taged protein in the eluate.

The purification of the mutant Dab1-tails was carried out according to the protocol established for the wt constructs. Only mutants of the longer Dab1-tail that contained the 4 phosphorylation sites A/B/C/D were purified for further analysis (see figure 5.4). Protein expression was usually done in 2 x 2 L *E. coli* cultures. Similar to the long wt Dab1-tail the mutant variants eluted from the gel filtration column at 75 ml and they behaved similar when applied for SDS-PAGE. Only the 5F mutant, which had all four tyrosines mutated to phenylalanine, was running slightly lower on polyacrylamide gels under equal conditions. Immuno-detection of the His-tagged mutants on Western Blot with a specific anti-penta-His antibody was carried out verified the purification of the Dab1 tail mutants.

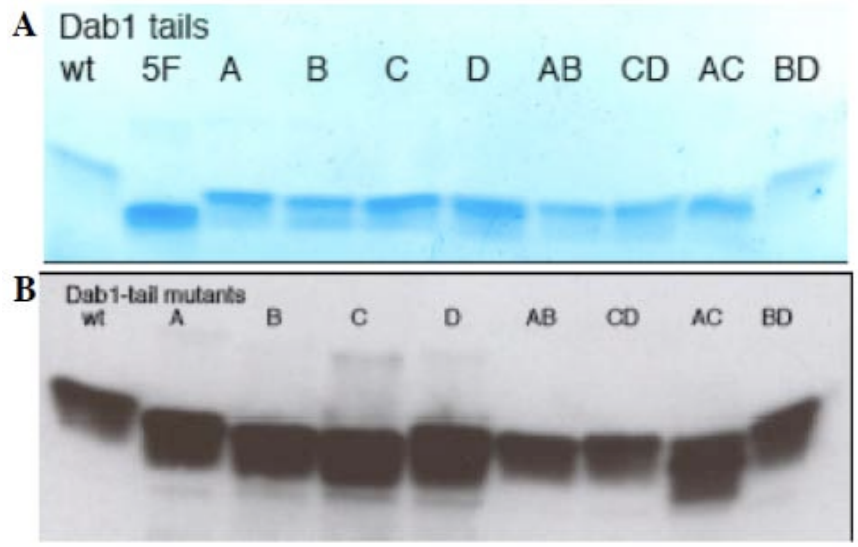

Fig. 5.4: A Purification of the Dab1-tail mutants: Pooled fractions after gel filtration were concentrated and applied on SDS-PAGE to determine the degree of purity of the protein samples. **B** Additional Western Blot analysis was carried out to specifically detect the His-tagged proteins by anti-penta-His antibody.

5.1.4 Secondary structure of the Dab1-tail

X-ray structures of Dab1 (Stolt et al., 2003) only included the PTB domain up to amino acid residue 173, the tail located C-terminally to it is thought to be unstructured. To determine which conformation the Dab1 tail constructs would probably adopt *in vitro* the

secondary structure was predicted with bioinformatic tools. Different programs and tools for secondary structure prediction were tried and the results were quite similar. The N-terminus of the longer Dab1 tail has tendencies to form a α-helix; the shorter construct is missing the first few amino acids, hence these tendencies are less profound.

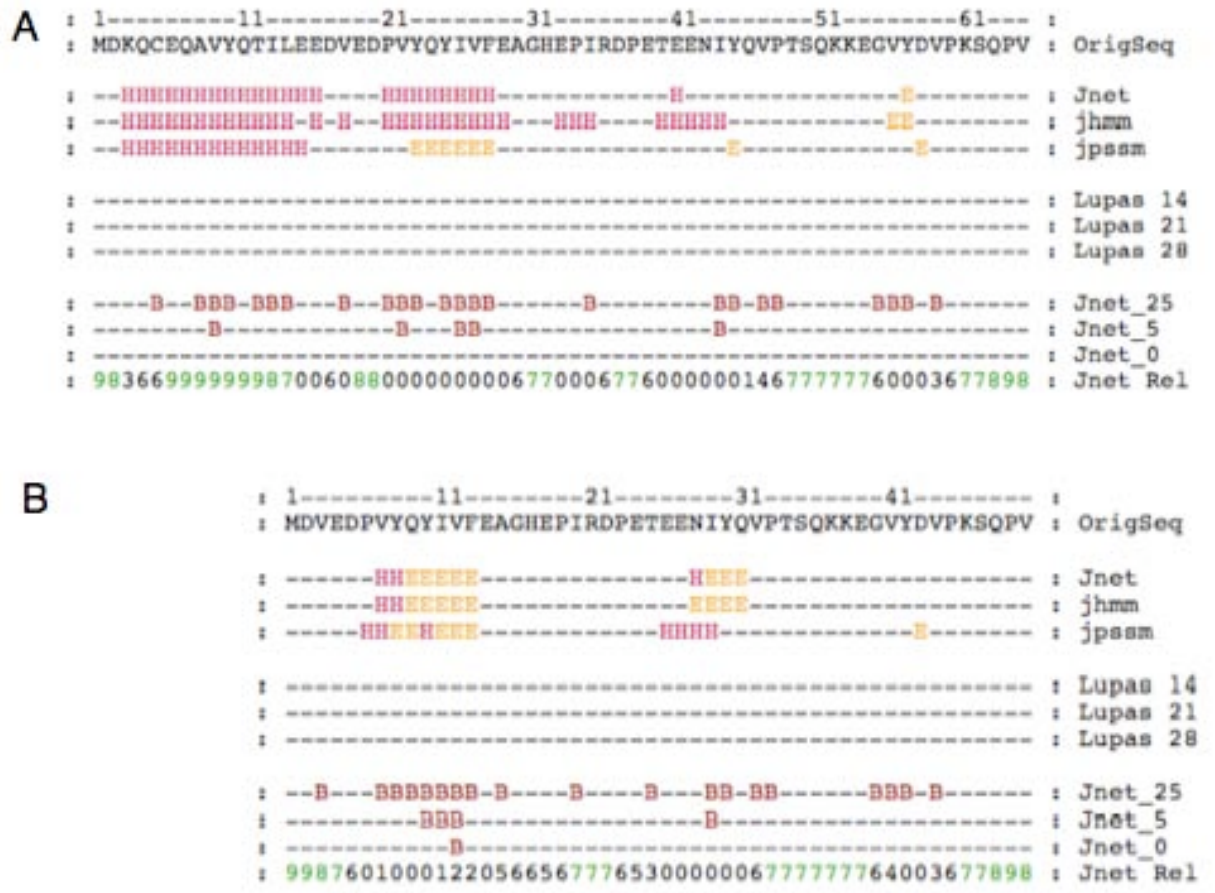

Fig. 5.5: Prediction of secondary structures of the Dab1-tails proposed by the pJpred3 prediction tool (http://www.expasy.ch/tools/) **A** The Dab1-tail long wt secondary structure shows tendencies to form a α-helix at the N-terminus. **B** In the Dab1-tail short wt the first few N-terminal amino acids are missing.

5.2 Optimisation of SH2-Kinase expression and purification strategies

5.2.1 SH2-kinase expression and purification

As mentioned before, the yield in heterologous expression of recombinant src family kinases is increased when the phosphatase YopH from *Yersinia* is co-expressed to reduce the toxicity that results from uncontrolled phosphorylation (Seelinger et al., 2008).

Full length YopH tends to bind to Ni-NTA even without His-tag. Rather large amounts of YopH are co-eluting from Ni-NTA beads with SH2K. Unfortunately, the contaminating phosphatase due to the similar molecular weight full length YopH elutes with SH2K (46 kDa) from the GF column. To overcome this problem we first tried to fuse a C-terminal Strep-tag II to YopH to remove the phosphatase in an additional step by binding to Strep-Tactin resins. However, the strep-tag causes the YopH to be insoluble. Therefore, in a second attempt only the phosphatase domain of YopH (YopH307aa) was used for co-expression with SH2K, with a molecular weight of 35 kDa. Fortunately, YopH307aa is sufficient to generate a reasonable amount of souble SH2K, though the yield is much higher when full length YopH is used as demonstrated in figure 5.6. The crude lysate and the supernatant after centrifugation from small-scale expression trials were separated on agarose gels by electrophoresis to analyse expression of soluble protein. Interestingly, it seems that the phophatase domain of YopH is less able to bind to Ni-NTA beads than the full length YopH.

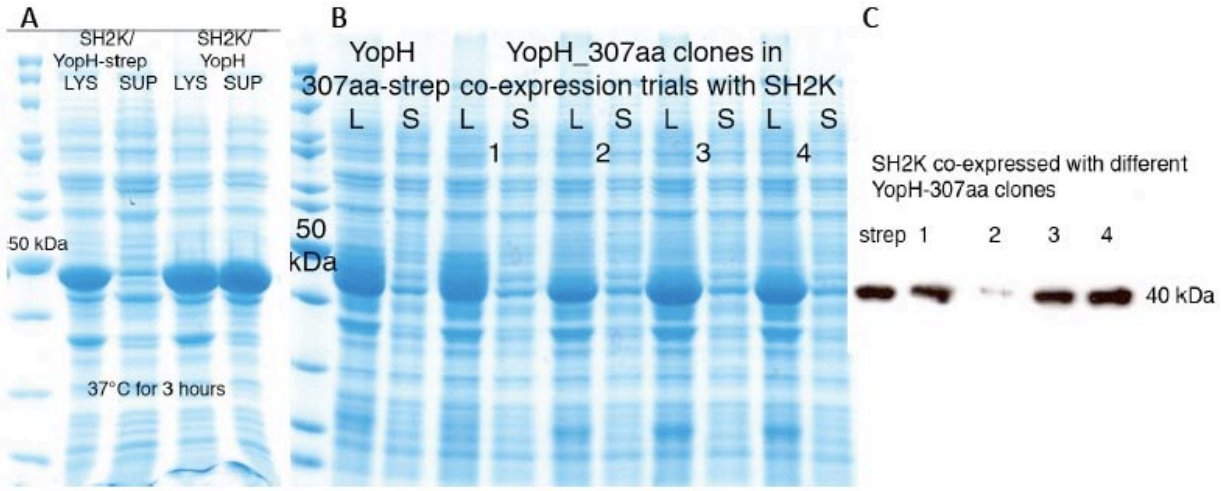

Fig. 5.6: Analysis of small-scale expression trials for SH2K/YopH by SDS-PAGE **A** SH2K co-expressed with full-length YopH with and without an N-terminal Strep tag II. The affinity tag leads to insoluble YopH, hence only la small amount of SH2K is found in the supernatant of the lysate. **B** YopH 307aa also resulted in low amounts of soluble SH2K, however, it resulted in about …mg of protein from …L E. coli culture. **C** Soluble SH2K from co-expression trials with different YopH307aa clones was specifically detected by Western Blot with anti penta-His antibody. The supernatant was diluted 1:5 before applied on the acrylamide gel.

Despite the reduced amount of soluble SH2K from co-expression with YopH307aa compared to co-expression with full-length YopH, a first large-scale purification experiment was carried out from a 4 L culture pellet. SH2K was bound to Ni-NTA beads in

batch and the eluate was applied for size exclusion chromatography as a final purification step.

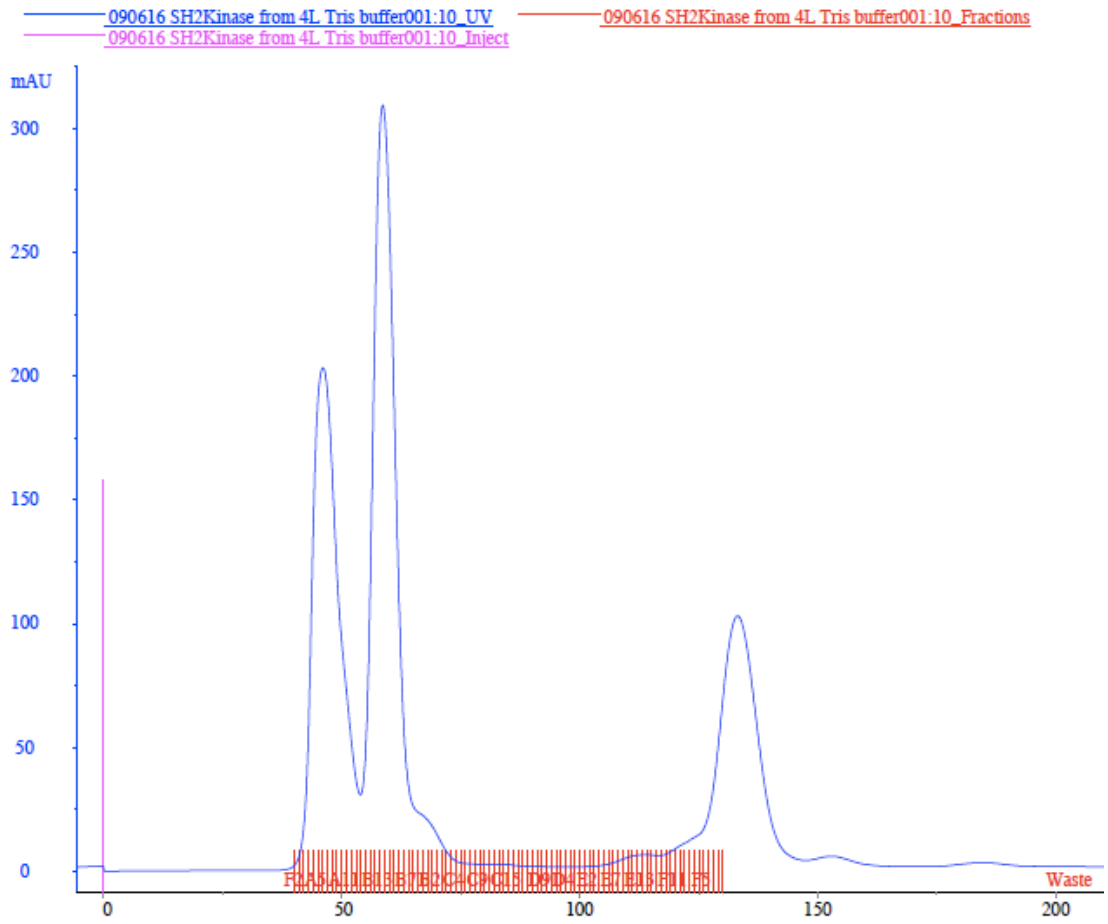

Fig. 5.7: The gel filtration chromatogram of the short SH2K purification protocol with a single affinity binding step in batch prior to chromatography shows an aggregation peak and the elution of SH2K at 60 CV.

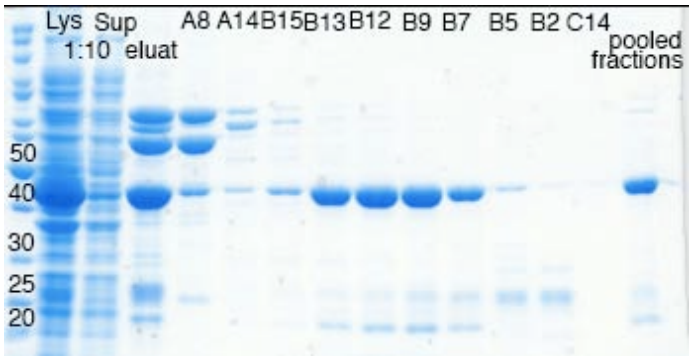

Fig. 5.8: The purification SH2K with the short protocol was analysed by SDS-PAGE on a 12% polyacrylamide gel. In the pooled fractions after size exclusion chromatography some impurities remained that might cause problems in crysallization.

The initial purification showed that SH2K elutes from the GF column at about 60 CV and that impurities are present when this short protocol is applied. The yield in SH2K from the 4 L purification was about 2 mg. To improve the purity and homogeneity of the SH2K sample supplementary purification methods were tested in regard to future crystallization trials.

In addition to the specific detection of SH2K from small-scale expression trials by Western blot, the purified protein from the pooled fractions after gel filtration was analysed by mass spectrometry. It could be identified as SH2K by comparison of the MS data to the Fyn proto-oncogene (figure 5.9).

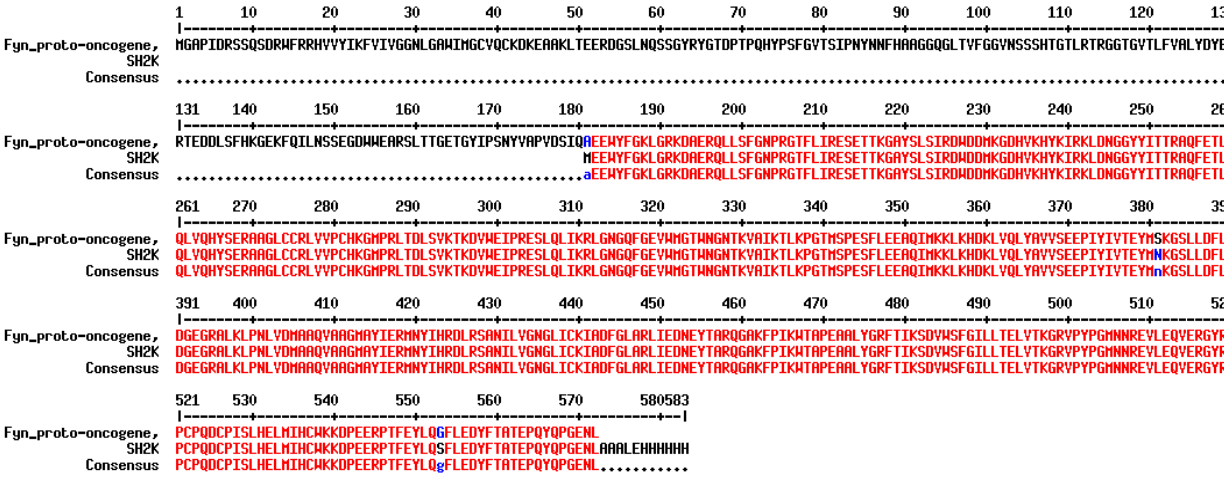

Fig. 5.10: Comparison of the sequence identified by mass spectrometry from the purified SH2K with the mouse Fyn proto-oncogene.

In a first attempt to improve SH2K purity, an additional anion exchange chromatography (AIEX) step. The eluate after binding of SH2K to Ni-NTA beads was applied for AIEX at pH 8.5 on a 1 ml HiTrap Q FF column with a linear gradient from 5% to 50 % NaCl. However, this strategy did not give the expected results. A single peak arises in the AIEX chromatogram (figure 5.11), yet the sample shows high levels of impurities when analysed on a polyacrylamide gel by electrophoresis (lane 5, figure 5.10).

Typically the binding to Ni-NTA beads was carried out in batch under slow shaking, since it is generally thought to be gentler for the protein. Furthermore, the affinity binding step was carried out by FPLC over a 5 ml HisTrap HP column. This strategy was found to lead

to a reduced amount of impurities and contaminations (lane 2, figure 5.10) compared to the eluate from the sample incubated in batch with loose Ni-NTA beads. As a result, also the SH2K fraction after the final gel filtration step becomes more pure (lane 3, figure 5.10).

Finally, cation exchange chromatography (CIEX) was tried for SH2K purification by applying the eluate from Ni-NTA beads on a 1 ml HiTrap SP XL column (figure 5.12). Already after the CIEX purification step a high level of purity can be achieved (lane 4, figure 5.10), but the buffer has to be exchanged afterwards to the normal Tris pH 8 based SH2K buffer.

In conclusion, the highest degree of SH2K purity can be achieved in a three-step purification strategy that involves Ni-affinity chromatography, cation exchange chromatography and a final gel filtration step.

The present impurities are obviously of a smaller size than SH2K, yet they cannot be totally separated from the protein by size exclusion chromatography, suggesting that they might somehow interact with SH2K. From the uncontrolled activity of SH2K it can be reasoned that the phosphorylation of bacterial proteins might result in targets for SH2 domain binding. Otherwise the over-expression of recombinant protein naturally causes stress in the bacterial cell that leads to the activation of chaperones that assist with protein folding. If these impurities are found to disturb crystallization of SH2K the CIEX chromatography could be tried at pH 6 since a lower pH seems to reduce the impurities compared to methods tested at higher pH-values. Additionally, the respective bands can be analysed by mass spectrometry to determine the type of protein that causes the contamination.

In general, the amounts of purified SH2K were rather low and on average about 8 mg from a 12 L culture pellet. This reflects that the toxicity of unregulated kinase activity strongly influences the yield of purified protein.

Furthermore, the yields of purified SH2K varied strongly within different purification attempts, reflecting that the expression level is influenced by the toxicity of the kinase.

Fig. 5.10: Comparison of different SH2K purification strategies. **Lane 1**: molecular weight marker. **Lane 2**: pooled fractions of the second peak from IMAC. **Lane 3**: pooled fractions of GF after Ni-NTA. **Lane 4**: pooled fractions from CIEX chromatography. **Lane 5**: AIEX chromatography results in a very impure sample.

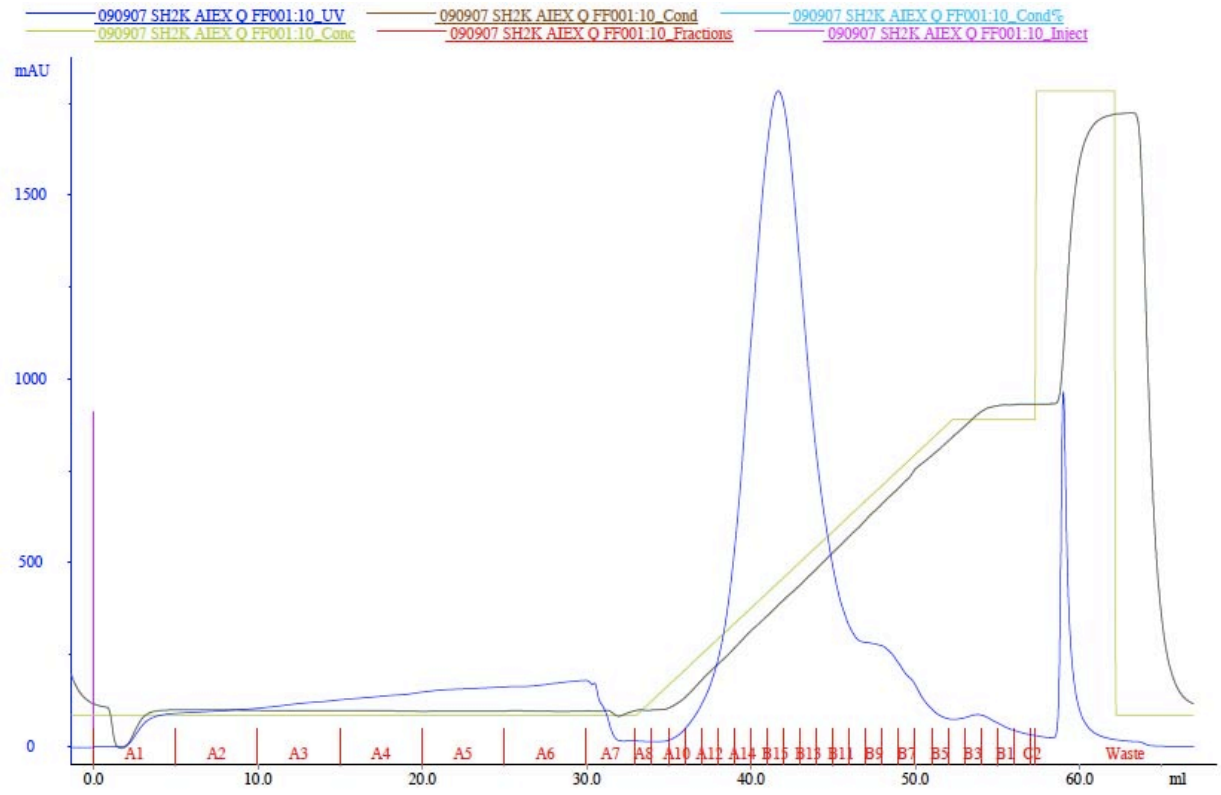

Fig. 5.11: Anion exchange chromatography on a HiTrap Q FF column. Proteins were eluted with a linear gradient from 50 to 500 mM NaCl.

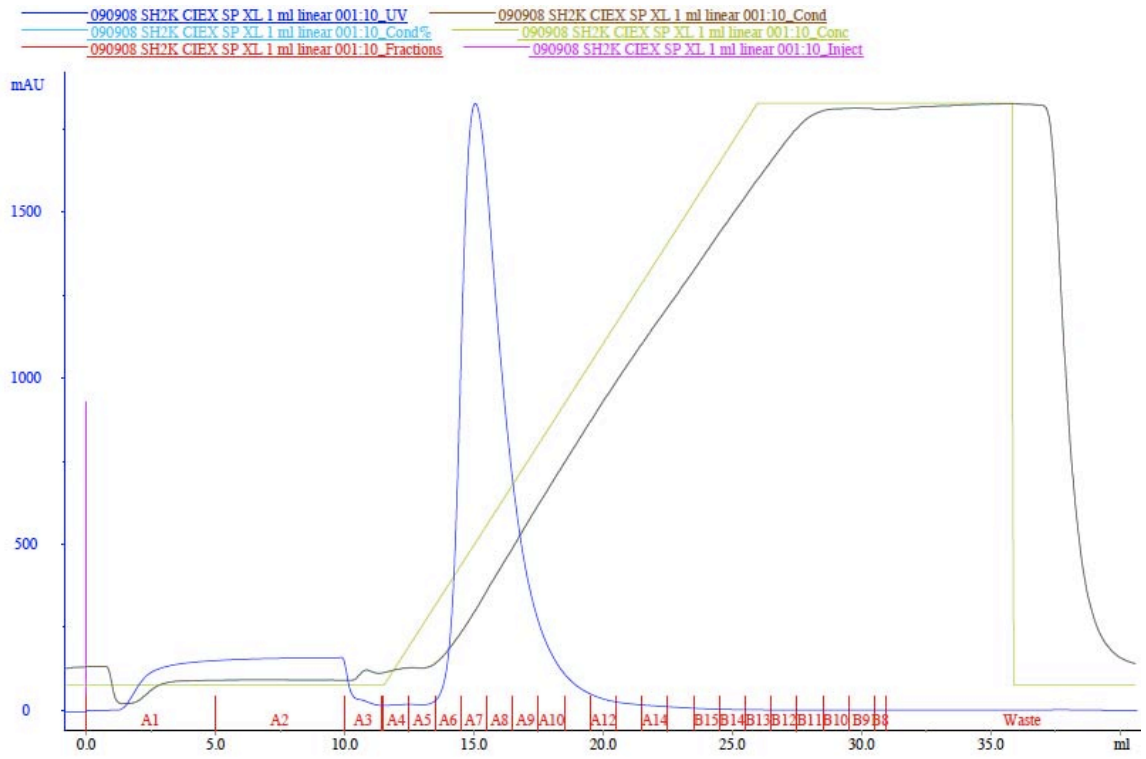

Fig. 5.12: CIEX chromatography on a HiTrap SP XL column with a linear gradient of 50 – 1000 mM NaCl.

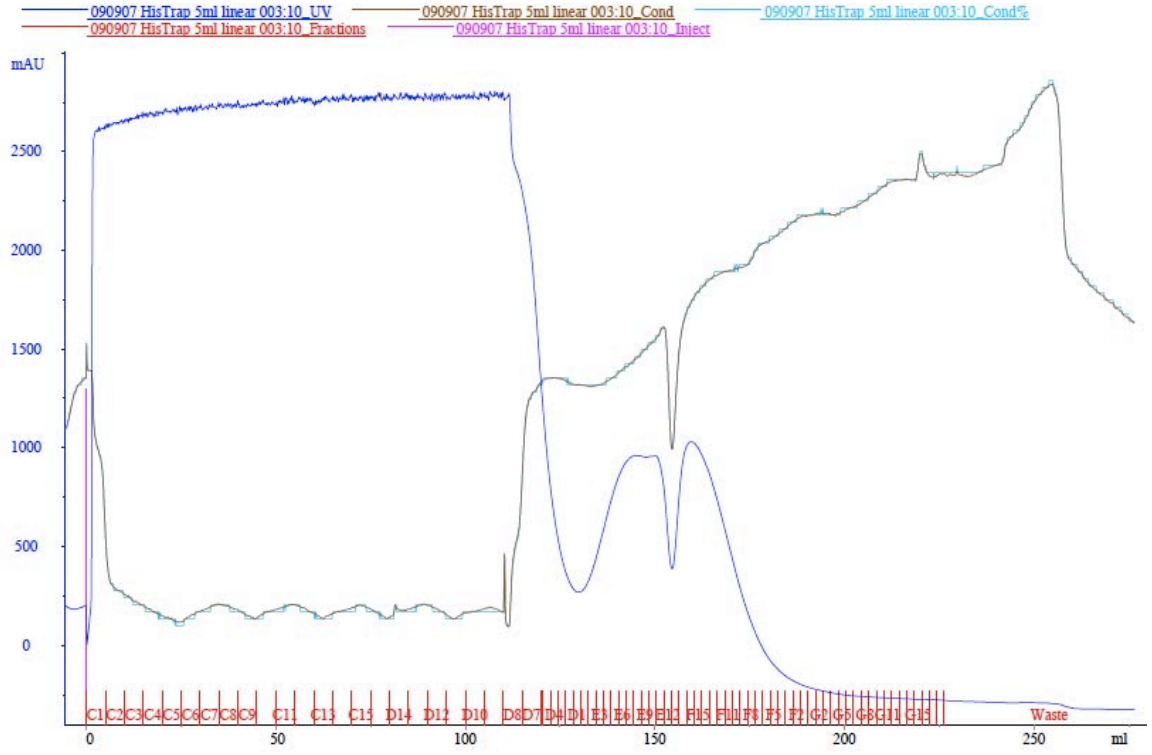

Fig. 5.13: Ni-NTA affinity chromatography on a 5 mL HisTrap HP column and a linear gradient from 30 mM to 250 mM imidazole.

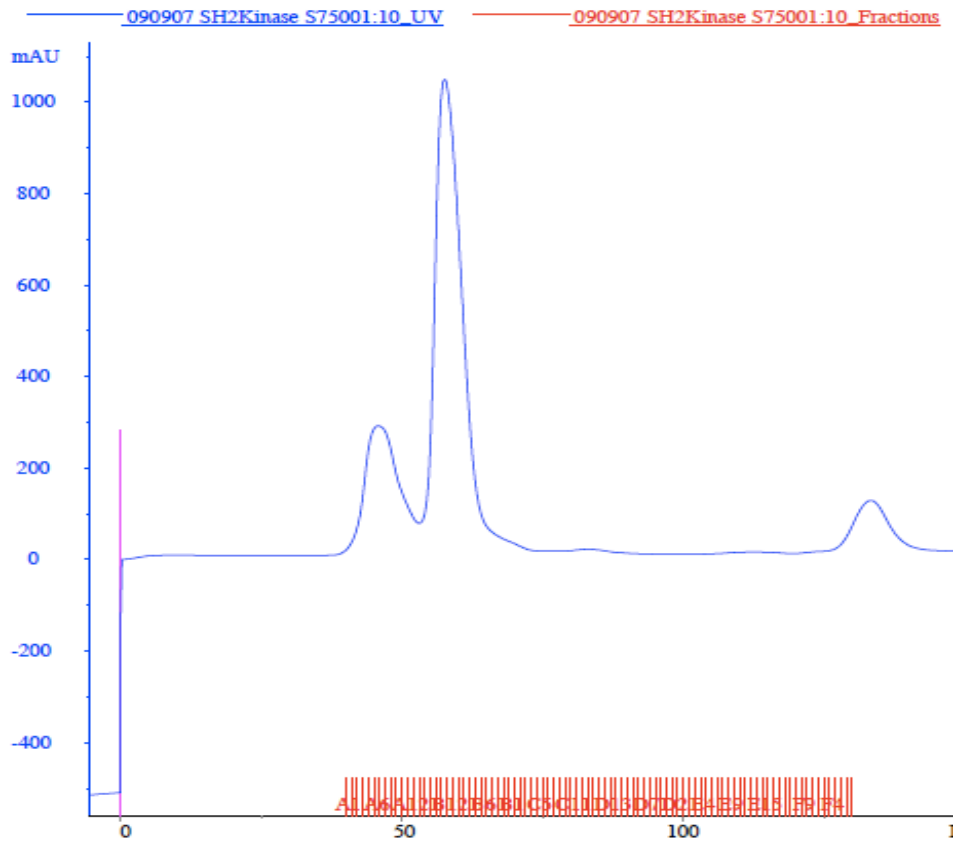

Fig. 5.14: SH2K purification: final size exclusion chromatography step in the long purification protocol.

5.2.2 Stargazer: Optimisation of SH2K buffer conditions by static light scattering

Purification of SH2K was carried out in Tris buffer at pH 8 that contains 300 mM NaCl, 5 % glycerol and 1 mM DTT, as mentioned before. The rather high amount of salt was chosen according to Seelinger et al. (2005), who used even 500 mM salt for purfication of c-Able and c-Src. Although SH2K seemed to be quite stable in this buffer other systems and additives were tested to optimise the conditions for the protein for future crystallisation trials.

Optimisation of the buffer system for improvement of protein stability is necessary to reach high yields of SH2K during the purification and to facilitate crystallization. The StarGazer 384™ from Harbinger Biotech™ is a useful high-throughput screening method that uses static light scattering for determination of the melting temperature of a protein, which correlates with the stability of the respective protein in the given conditions.

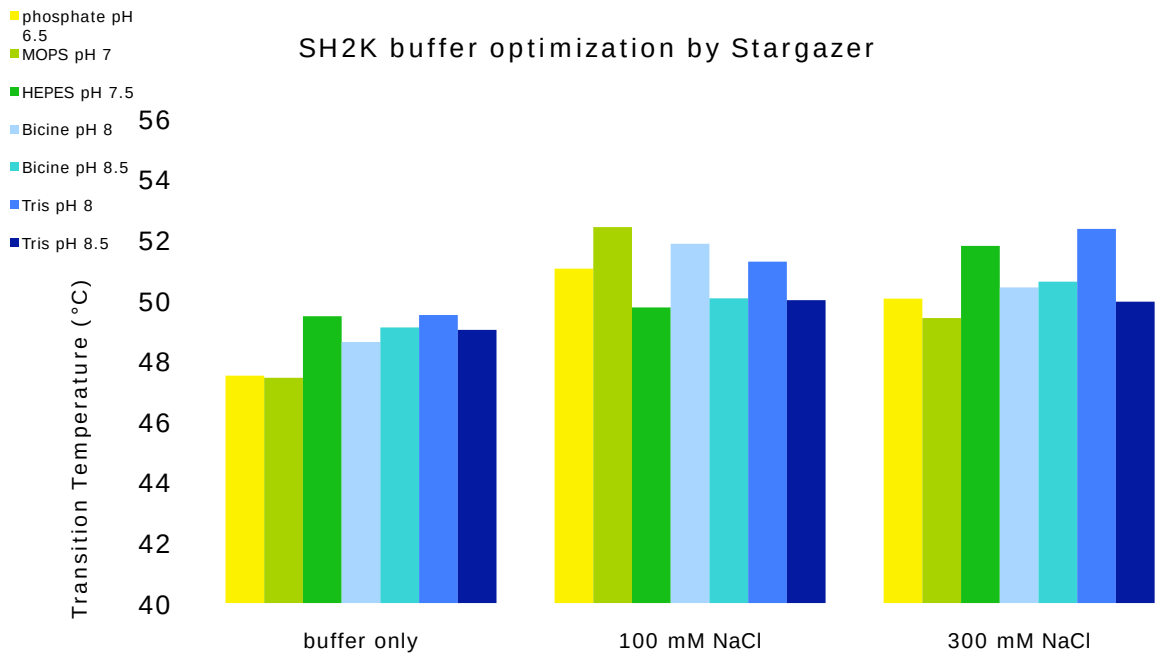

Fig. 5.15: Determination of the transition temperature of SH2K under different buffer conditions by static light scattering. The most interesting results of the 96 different conditions tested are compared.

In the first StarGazer screen several buffer systems at different pH-values and with varying salt concentrations were tested and the transition temperatures were compared (figure 5.15). In the diagram the mean value of the temperatures measured in duplicates is given, however, only the most interesting results are given. The increase of the transition temperature is only about 2°C, but obviously the addition of NaCl is important to improve the stability of SH2K. Especially at low pH-values in phosphate buffer and MOPS the stability increases dramatically. Generally the protein seems to require a pH between 7.5 and 8 with at least 100mM salt. Under the tested conditions the Tris buffer at pH 8 was one of the best. Aside from the conditions described here also lower and higher pHs and the addition of ammonium sulfate instead of NaCl were tested but did not give clear or promising results (data not shown).

For further optimisation of the SH2K buffer 96 different additives from a commercial screen kit (Hampton HR2-428) were tested for improving protein stability. SH2K in the Tris buffer at pH 8 and comparable conditions in other buffer systems were used as controls in order to be able to compare the measured temperatures. The most interesting compounds and the respective mean values of the measured temperatures are given in the diagram in figure 5.16. None of the additives lead to dramatic increase of the

transition temperature, except for the detergent n-dodecyl-β-D-maltoside (DDM) which is however not considered to be added to the SH2K buffer. Detergents are usually not contained in buffers for cytosolic proteins, but they play an important role in crystallization of membrane proteins. Fluoride containing organic compounds in addition to Co^{2+}, Ni^{2+} and other ions were found to destabilize SH2K, sometimes quite significantly. Manganese is a known cofactor for kinases and hence Mn^{2+} and Mg^{2+} ions are ingredients in many respective buffer systems. However, these additives did not influence the transition temperature of SH2K in this measurement. Sugars and sugar derivates like sorbitol, galactose, trehalose and xylositol increased the transition temperature only slightly by 1°C.

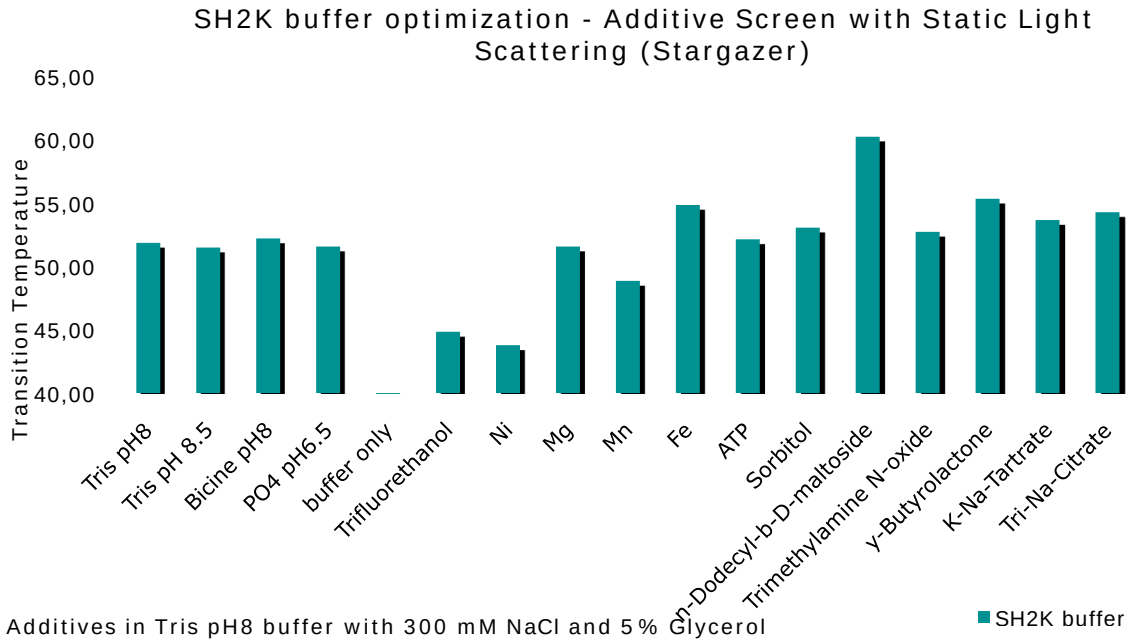

Fig. 5.16: Some of the most interesting compounds tested in the additive screen for improvement of the SH2K buffer are listed here and the respective transition temperatures are given.

In summary, none of the tested compounds had an explicit effect on the transition temperature and it can be assumed that they do not influence the stability of SH2K. These experiments demonstrated that the present conditions seem to be satisfying for SH2K. In fact, the protein is quite stable in the SH2K buffer when it is treated with care. Thus, the composition of the SH2K buffer was not changed, since the StarGazer experiments did not elucidate how to further improve the conditions.

5.3 Biochemical Characterization of Fyn SH2

5.3.1 Determination of the binding affinity of the Fyn SH2 domain to phosphorylated tyrosine residues in the Dab1-tail by ITC

The affinity of a protein to interact with a certain binding motif of an interaction partner can be determined by ITC, a sensitive method that measures the binding energy as heat consumed or released by binding reactions.

The unstructured tail located C-terminally from the PTB domain of Dab1 contains five tyrosine residues, which are phosphorylated by Fyn or Src *in vivo*; both enzymes are members of the Src family kinases (Howell et al., 2000; Bock & Herz, 2003; Arnaud et al., 2003b). There is a basal level of Dab1 phosphorylation present in neurons, which presumably allows the binding of Fyn via its SH2 domain to the adaptor protein and hence the specific phosphorylation of defined tyrosines to transmit the Reelin signal. It is assumed that several SFKs are implicated in these processes. The major sites for Reelin-induced Dab1 phosphorylation in neurons during embryonic development are Y198 and Y220 (Keshvara et al., 2001). It has been shown that the transduction of the Reelin signal is abolished when either the AB (tyrosines 185 and 198) or CD (tyrosines 220 and 232) phosphorylation sites are mutated to phenylalanine. Probably, two tyrosine residues are required to stimulate the SFKs mediated phosphorylation of the other tyrosine residues upon Reelin stimulation (Feng & Cooper 2009). Further, it is assumed that phosphorylation of A or B and C or D is sufficient for transmitting the Reelin signal since these sites seem to be functionally equivalent (Morimura & Ogawa, 2009).

In order to investigate whether the binding affinity of the SH2 domain towards these functionally equivalent phospho-tyrosines (AB and CD) is also different, ITC measurements with the purified SH2K and the SH2 domain were carried out. The dissociation constants ($K_{D)}$ for both, the Fyn SH2 domain and the SH2K, were determined by ITC with short synthetic peptide-fragments of the Dab1-tail that contained one particular phospho-tyrosine as a binding partner (figure 5.17).

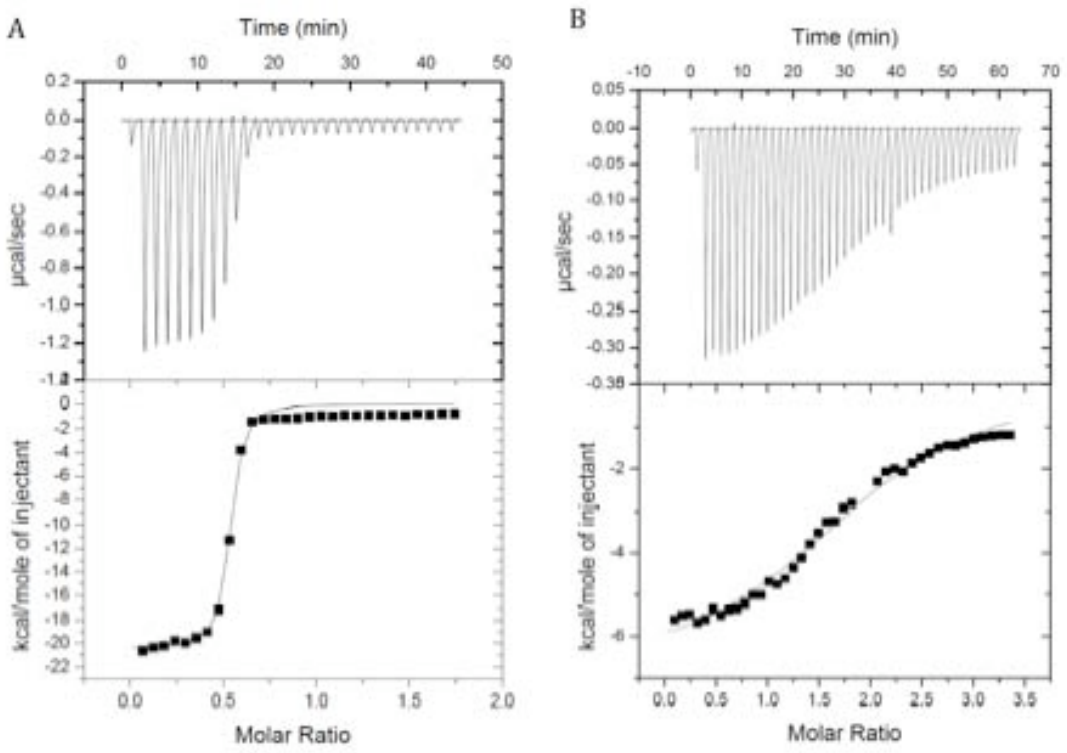

pY198: EDVEDPVY(PO)QYIVFEA
k_D = 50 nM ± 12 nM
ΔH = -14 680 ± 215.1
ΔS = -16.8
n = 0.716
K = 1.24 E7 ± 2,89 E6

pY220: ETEENIY(PO)QVPTSQKKEGVYDVPK
k_D = 4 µM ± 0.4 nM
ΔH = -6812 ± 177.2
ΔS = +1.85
n = 1.98
K = 2.48 E5 ± 2.67 E4

Fig. 5.18: ITC binding isotherms measured at 25°C for SH2K binding to synthetic peptides of the Dab1-tail. The synthetic peptides and the measured thermodynamic parameters are indicated under the figure. **A** Binding to phospho-Y198, K_D was calculated to be 50 nM ± 12 nM **B** For phospho-Y220 the K_D was determined to be 4 µM ± 0.4 µM, hence about 80 times weaker compared to phospho-Y198.

Only two of the four phospho-tyrosine residues were measured with SH2-Kinase (pY198 and pY220), but results are consistent with previous measurements with the purified SH2-domain that included all four phosphorylation sites (data for SH2 not shown). In ITC experiments with both, SH2K and SH2 domain, a significantly higher binding affinity towards the phosphorylated tyrosines 185 and 198 compared to 220 and 232 was measured. This supports the hypothesis that the respective phosphorylation sites are functionally similar (Morimura & Ogawa, 2009). In figure 5.17 the results of the ITC measurement of SH2K binding to phospho-tyrosine 198 and 220 are shown, and K_D-values were calculated to be 50 nM ± 12 nM and 4 µM ± 0.4 µM respectively. Under the given *in vitro* conditions, SH2K was binding 80 times stronger to Y198 than to Y220.

However, it was difficult to precisely determine the concentrations of Dab1 peptides and SH2K to obtain the correct concentration ratio; therefore the resulting ITC curves are not optimal and the errors of the measured K_D-values are quite large. Since the measured values and errors are similar to the results measured for the SH2 domain, it can be reasoned that the phospho-tyrosines 185 and 198 of the Dab1 adaptor protein are the preferred targets of the SH2 domain; they seem to be the main docking sites for Fyn. Generally, the purity of the synthetic peptides is of great importance to allow the exact determination of their concentration, but also the weighing of the peptide can influence the accuracy.

5.3.2 Kinase assays

In general, the binding interactions between an enzyme and its substrate can be characterised by determination of the kinetic parameters of the reaction. The Michaelis constant, k_m (substrate concentration at which the rate of an enzymatic reaction is half of the maximal velocity; under saturating substrate conditions), is considered to be a relative measure of substrate binding affinity. Hence, it is a useful kinetic parameter to compare the affinity of a certain enzyme to different substrates.
Another important kinetic constant is the turnover number k_{cat}, which is defined as the number of turnover events catalysed by the enzyme in a certain time unit [m^{-1} or s^{-1}]. k_{cat} is usually determined by measuring the reaction velocity *v* under conditions [S] >> k_m, so that *v* approaches the maximal velocity v_{max}. This situation of course does not resemble the physiological conditions where typically [S] << k_m. Still, the turnover number allows the comparison of turnover rates of different enzymatic reactions.
The ratio k_{cat}/k_m is generally a valuable measure for defining the catalytic efficiency of an enzyme and it allows the description of effects on interactions between an enzyme and its substrate. By these means, not only the efficiencies of different enzymes can be compared with each other but also the utilisation of different substrates.

The aim of the radioactive kinase assays performed here was to determine kinetic parameters in order to characterise the interaction between Fyn and Dab1 *in vitro* by defining the efficiencies of SH2K for the different phosphorylation sites. A broad range of

mutant Dab1-tail variants with single, double and triple substitutions of tyrosine residues to phenylalanine were generated by site-directed mutagenesis for these experiments, as described earlier. The mutants were used as substrates in kinase activity assays with radiolabeled ATP (γP^{32}-ATP) to determine and compare the kinetic properties, specifically the K_m-value, of SH2K for catalysing the phosphorylation of the different tyrosine residues.

Since such experiments had never been done in our laboratory before, preliminary kinase assays were performed to optimise the experimental conditions, such as substrate and enzyme concentration and reaction time (data not shown). After optimising the experimental procedure, kinase assays for a first estimation of k_m-values were carried out with 200 nM SH2K and varying concentrations of Dab1-tail substrates. The established kinase assay has also been tested with the Fyn kinase domain (carried out by my colleague; data not shown).

By comparing the affinities of both SH2K and the kinase towards the different Dab1 tail mutants it is possible to detect preferences for phosphorylation of certain tyrosines in the Dab1 tail. Additionally, it will provide information on whether the presence of the SH2 domain influences the K_m of the kinase for these tyrosines. We expected to see differences in the affinity, and thus in the k_m, of SH2K to substrates containing the phosphorylation sites A and B (tyrosines 185 and 198, respectively) compared to C and D (tyrosines 220 and 232). Therefore, the Dab1-tail mutants AB and CD were used in the first kinase reactions for comparison with each other and the wt Dab1-tail. In figures 5.18-5.20 the results of these experiments are shown as graphs.

Absolute intensities of radioactive phosphate were determined by quantifiying the measured radioactive signal using ImageJ. By plotting the absolute intensities against the reaction time the velocity of the reaction at each tested substrate concentration was determined. Reaction velocities were then plotted against the increasing substrate concentration and were fitted by nonlinear regression analysis using the program Graphpad Prism.

Table 5.1: Preliminary kinetic properties of SH2K reactions with different Dab1 tail constructs .

Substrate	v_{max} [µmoles/sec]	K_m-value [µM]	R^2
Dab1-tail wt	$9.136e^{-9}$	1.47	**0.9316**
Dab1-tail AB	$4.787e^{-9}$	2.07	**0.7341**
Dab1-tail CD	$6.180e^{-9}$	3.02	**0.9499**

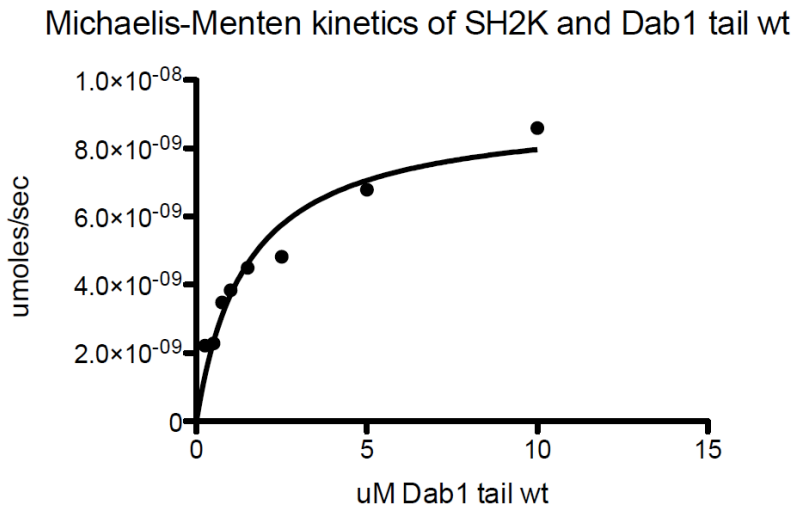

Fig. 5.18: Kinetic measurement for SH2K and Dab1-tail wt.

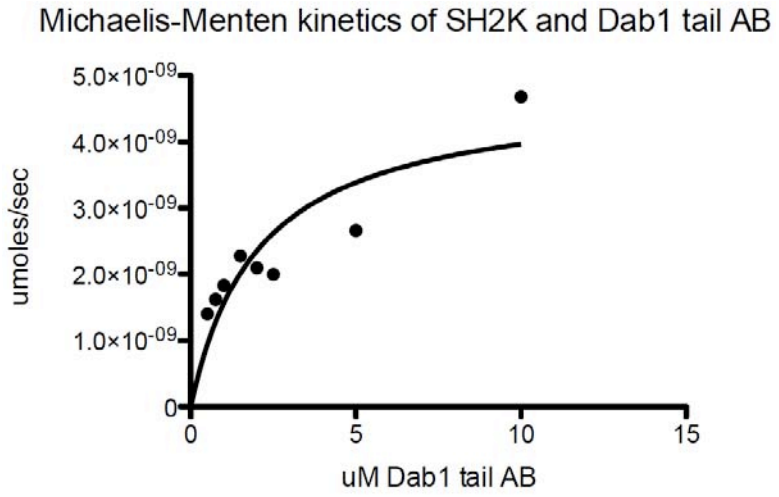

Fig. 5.19: Kinetic measurement for SH2K and Dab1-tail AB.

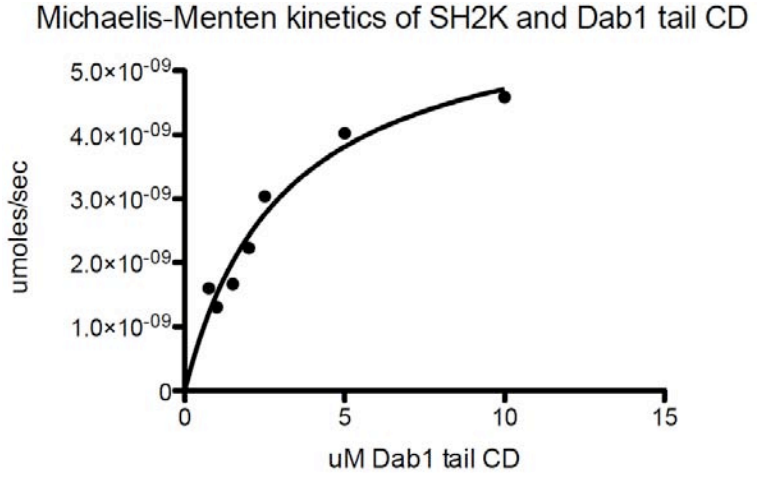

Fig. 5.20: Kinetic measurement for SH2K and Dab1-tail CD.

From the data presented here a difference of about 2-fold in the K_m-value for the AB versus the CD Dab1-tail mutants seems possible. However, additional optimisation of the experimental procedure is required to allow for an accurate determination of the kinetic constants.

These were only initial experiments to set up the experimental assay and determine a first estimation of the k_m-values. Future experiments will also test Dab1 tails containing only a single tyrosine. Additionally, the results of SH2K kinetic studies should be compared to the Fyn kinase domain alone, since the SH2 domain might influence the K_m-values for substrates containing more than one tyrosine by docking to the phosphorylated tyrosine residues. To address the question of whether phosphorylation occurs in a certain order, an additional non-radioactive kinase assay will have to be established. Detection of phosphorylated tyrosines with specific antibodies might be a useful tool in this context. Additionally, the structural basis for a possible in-cis phosphorylation of Dab1-tails by SH2K can be investigated by crystallisation and X-ray crystallography. Crystallographic experiments with SH2K and a Dab1 construct consisting of the PTB domain and the tail containing the phosphorylation sites could further reveal reasons why phosphorylation of Y185 has so far not been detected *in vivo*.

5.4 Anti phospho-tyrosine 198 antibody purification and testing

To have a possibility to specifically detect phosphorylated Y198 of Dab1 in cell lysates after co-expression experiments of Fyn and Dab1 mutants in cell culture, a polyclonal antibody was produced by immunization of three rabbits (2490/2491/2492). The anti-pY198 antibody was purified from the sera by affinity chromatography and eluted with $MgCl_2$ and glycine, as described in the Methods section. The eluates were finally tested as 1 µM dilutions for the ability to detect samples positive and negative for phosphorylated Y198 on a Western blot.

The $MgCl_2$ eluate of the serum from rabbit 2491 gave the expected results; only the phosphorylated wild-type Dab1 was detected but not the pY198-negative samples. The concentration of the antibody that was used is high and therefore several nonspecific

background bands were detected, however, a clear band at about 70 kDa is detected at the lane with the wild-type Dab1. On the other hand, the mutant Dab1 with F198 and the unphosphorylated Dab1-tail do not show a signal at that location. The results for the $MgCl_2$ eluted antibodies of rabbit 2491 are shown in the Western blot in figure 5.21. Unfortunately the antibodies purified from the sera of the other rabbits did not give clear results. For further intended experiments the antibody should be diluted much more to reduce background signals. The purified antibody is stored in a concentration of about 2 µM at -80°C.

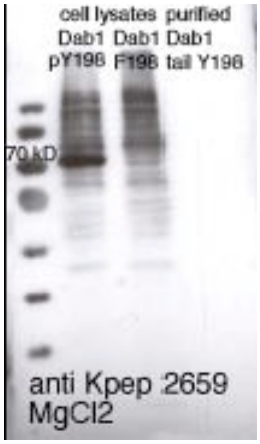

Fig. 5.21: Western blot for testing the polyclonal α-pY198 antibody that was purified from rabbit 2491 serum. The samples (phosphorylated Dab1 wt, phosphorylated mutant Dab1 with F198 and unphosphorylated Dab1-tail long wt) were detected with the polyclonal antibody of the $MgCl_2$ eluate from the second affinity column (Kpep 2659, phospho-Y198).

6 Summary and Conclusions

The aim of this work was to investigate and describe the interactions between Dab1 and Fyn tyrosine kinase biochemically, in preparation for crystallisation trials and further biochemical characterisation. A variety of constructs of Fyn and Dab1 were designed and expressed recombinantly in *E. coli*. The Dab1-tail was expressed as both, the wild-type sequence and with a variety of mutations in the four tyrosine phosphorylation sites. Since the SH2 domain and the kinase domain of Fyn are known to interact with Dab1, the respective construct was designed to include both domains. Additionally, the single domains will be investigated individually in parallel experiments to compare the results with the SH2K, which have already been performed to some extent by my colleagues (data not shown).

Purification protocols for Fyn SH2-Kinase and the different Dab1-tail mutants were successfully established. The combination of several chromatographic steps that mostly involved affinity binding and size exclusion resulted in a high degree of purity, which is necessary for X-ray crystallography. The purified proteins were then used in radioactive kinase assays and ITC measurements to characterise the interactions of the two proteins *in vitro*.

ITC provides insights into the binding behaviour of the Fyn SH2 domain to phosphorylated tyrosine residues of Dab1. Under the given experimental conditions the phospho-tyrosines 185 and 198 have a higher affinity for binding the SH2 domain than the phosphorylated Y220 and Y232 residues (80x for the SH2K construct). This might indicate the importance of the Y185 and Y198 phosphorylation sites as docking units for the SH2 domain of the tyrosine kinase. The respective phosphorylation sites had been found to be functionally similar (Morimura & Ogawa, 2009) and to resemble a SFK consensus sequence (Songyang et al., 1995). The ITC results are further in agreement with data from Feng and Cooper (2008), who found that deletion of the AB sites in mutant mice prevents phosphorylation of the CD sites and hence all downstream signalling events. The authors suggest distinct functions related to phophorylation of AB and CD and

define tyrosines 185 and 198 as sites for binding and stabilising SFKs. These sites seem also to be involved in Akt kinase activation and Dab1 degradation. The CD phosphorylation sites, on the other hand, seem to be important for transmitting the Reelin signal to downstream signalling molecules such as Crk and CrkL. These results also promote the hypothesis of Dab1 phosphorylation occurring in-trans.

In order to determine the affinity of Fyn kinase to phosphorylate Dab1, a kinase assay with radioactive labelled [γ^{32}P]-ATP was established. Preliminary experiments were performed to set up the experimental assay and to estimate the k_m-values for the Dab1-tail mutants AB and CD as compared to the wild-type Dab1 tail. From these initial data a difference of 10-fold in the affinity towards the AB in comparison to the CD Dab1-tail mutants is shown. However, additional optimisation of the experimental procedure is required to allow a more precise determination of K_m-values. Therefore, at this point, no conclusions can be drawn since additional data are required. However, the initial kinetic data support the conclusion from the ITC experiments, as the kinase also phosphorylates the AB sites at a higher rate than the CD sites. This suggests, in agreement with data from Feng and cooper (2008), that *in vivo* probably SFKs need to phosphorylate Dab1 first at the AB sites. Upon Reelin stimulation these phosphotyrosines serve as docking sites to promote phosphorylation of the CD sites, which then transmit the signal to downstream interaction partners of the Dab1 adapter molecule.
In the future, single-tyrosine mutants of Dab1-tails will also be tested with this system and the results of SH2K kinetic studies will be compared to results with the Fyn kinase domain alone, since the SH2 domain might influence the K_m-values.

The Stargazer instrument was used to define stabilising conditions for SH2-kinase in order to facilitate crystallisation. The melting temperature (T_m) of the protein, which correlates with stability, was determined in different buffer systems and with a number of additives. However, none of the tested compounds had an explicit effect on the transition temperature and it can be assumed that they do not influence the stability of SH2K. The protein seems to be quite stable in the present conditions. Of course, also small differences may influence crystallisation.

In conclusion, the experiments performed here support a role for the AB phosphorylation sites in recruiting the Fyn kinase to Dab1. Further experiments will try to answer questions such as whether the SH2 domain influences kinase activity, what is the order of

phosphorylation, and why phosphorylation of the A site (Y185) has never been detected *in vivo*. Additionally, with the purified proteins and assays established here, experiments can now be designed to try to determine whether the tyrosine kinase acts on Dab1 in an "in cis" or "in trans" position relative to the Dab1-tail. Structural studies of Fyn bound to the Dab1 substrate might elucidate the interaction mechanism and provide answers to these questions. In addition to crystallographic data, cell biological and biochemical experiments could provide an even deeper understanding of the function of tyrosine kinases in general, as well as the transduction of the Reelin signal.

7 List of abbreviations

α-pY198 AB	antibody against the phosphorylated tyrosine 198 from Dab1
β-ME	β-mercaptoethanol
[γ^{32}P]-ATP	adenosinetriphosphate labled at γ-position with radioactive phosphor 32
°C	degree Celsius
%	percent
µg	microgram
µl	microliter
µM	micromolar
ADHD	attention deficit hyperactivity disorder
AMPA	α-amino-3-hydroxy-5-methyl-4-isoxazole-propionic acid
ApoER2	apolipoprotein receptor E 2
APS	ammoniumperoxodisulfate
ATP	adenosine triphosphate
BCA	bicinchoninic acid
BSA	bovine serum albumin
$CaCl_2$	calcium chloride
CIEX	cation exchange chromatography
C-terminus	carboxy-terminus of a protein
Cu^{+}	monovalent copper ione
Cu^{2+}	divalent copper ione
CV	column volume
Da	Dalton, mass of molecular weight of proteins
Dab1	Disabled 1
Dab1-tail	construct of the unstructured C-terminal tail of Dab1
dH_2O	deionized water
DMSO	Dimethylsulfoxide
DNA	deoxiribonucleic acid
DTT	dithiothreitol
E. coli	*Escherichia coli*
EDTA	ethylendiaminetetraacetic acid
EGF	Epidermal growth factor

F	single letter code for phenylalanine
FPLC	fast protein liquid chromatography
g	gramm
GABA	γ-aminobutyric acid
GF	gelfiltration/ size exclusion chromatography
GST	Glutathione S-transferase
HCl	hydrochloric acid
HEPES	N-2-hydroxyethylpiperazine-N'-2-ethanesulfonic acid
His-tag	6x histidine tag
IMAC	immobilized metal ion affinity chromatography
IPTG	isopropyl-β-D-1-thiogalactopyranoside
ITC	isothermal titration calorimetry
kb	kilo bases
kbar	kilo bar, unit of pressure
k_{cat}	turnover number
k_{cat}/k_m	ratio of kinetik constants describing the catalytic efficiency of an enzym
kDa	kilo Dalton, unit of protein mass
k_m	Michaelis constant
L	liter
LB	Luria-Bertani medium
mA	milli Ampere, unit of electric current
MCS	multiple cloning site
mg	milligram
$MgCl_2$	magnesium chloride
Mm	milliliter
mM	millimolar, unit of concetration
MS	mass spectroscopy
MWCO	molecular weight cut-off
NaCl	sodium chloride
ng	nanogram
Ni^{2+}	divalent nickel ion
Ni-beads	nickel ions immobilized on agarose or sepharose beads
Ni-NTA	nickel nitriloacetic acid

nm	nanometer
NMDA	N-methyl-D-aspartate
N-terminus	amino terminus of a protein
OD_{600}	optical density, absorbance at 600 nm
PCR	polymerase chain reaction
pDab1	phosphorylated Dab1
PIPES	piperazine-N-N'-bis-2-ethanesulfonic acid
PTB domain	phospho-tyrosine binding domain
PVDF	polyvinylidene difluoride
rpm	rounds per minute
SDS	sodium dodecyl sulfate
SDS-page	SDS-polyacrylamid gel electrophoresis
SH2 domain	Src homology 2 domain
SH3 domain	Src homology 3 domain
SH2K	SH2-Kinase domains of Fyn tyrosine kinase
SOB	super-optimal broth
SOC	super-optimal catabolite repression
TAE	Tris/Acetate/EDTA buffer
TB	Western Blot transfer buffer
TBS	Tris buffered saline
TBS-T	TBS with Tween-20
TEMED	N,N,N',N'-Tetramethylethylendiamine
U	unit
V	Volt, unit of voltage
VLDLR	very low density lipoprotein receptor
v/v	volume to volume
w/v	weight per volume
wt	wildtype
Y	single letter code for tyrosine
YopH	Tyrosine phosphatase derived from *Yersina*
YopH307aa	phosphatase domain of YopH (307 amino acids)

8 List of Tables and Figures

Tables

Figures

9 References

Abramoff M.D., Magelhaes P.J., Ram, S.J. (2004) Image Processing with ImageJ. *Biophotonics International, 11(7): 36-42*

Arnaud L., Ballif B.A., Cooper J.A. (2003a) Regulation of protein tyrosine kinase signalling by substrate degradation during brain development. *Mol. Cell Biol. 23:9293-9302*

Arnaud L., Ballif B.A., Forster E. and Cooper J.A. (2003b) Fyn tyrosine kinase is a critical regulator of disabled-1 during brain development. *Curr. Biol. 13: 9-17*

Assadi A.H., Zhang G., Beffert U., McNeil R.S., Renfro A.L., Niu S., Quattrocchi C.C., Antalffy B.A., Sheldon M., Armstrong D.D., Wynshaw-Boris A., Herz J., D'Arcangelo G., Clark G.D. (2003) Interaction of reelin signaling and Lis1 in brain development. *Nat Genet. 35(3):270-6. Epub 2003 Oct 26.*

Beffert U., Morfini G, Bock H.H. Reyna H., Brandy S.T., Herz J. (2002) Reelin-mediated signalling locally regulates protein kinase b/Akt and glycogen synthase kinase 3beta. J. Biol. Chem. 277: 49958-49964

Beffert U., Weeber E.J., Durudas A., Qiu S., Masiulis I., Sweatt J.D., Li W.P., Adelmann G., Frotscher M., Hammer R.E., Herz J. (2005) Modulation of synaptic plasticity and memory by Reelin involves differential splicing of the lipoprotein receptor Apoer2. Neuron 47(4): 567-79.

Bliska JB, Guan KL, Dixon JE, Falkow S. (1991) Tyrosine phosphate hydrolysis of host proteins by an essential Yersinia virulence determinant. *Proc Natl Acad Sci U S A. 88(4): 1187-91.*

Bock H.H. and Herz J. (2003) Reelin activates SRC family kinases in neurons. *Curr Biol. 13: 18 – 26*

Bock H.H., Jossin Y., Liu P., Förster E., May P., Goffinet A.M., Herz J. (2003) Phosphatidylinositol 3-kinase interacts with the adaptor protein Dab1 in presence to Reelin signaling and is required for normal cortical lamination. *J. Biol. Chem. 278: 38772-38779*

Bock, H. H. Jossin Y., May P., Bergner O. and Herz J. (2004) Apolipoprotein E receptors are required for reelin-induced proteasomal degradation of the neuronal adapter protein Disabled-1. *J. Biol. Chem. 279: 33471-33479*

Boggon T.J. & Eck M.J. (2004) Structure and regulation of Src family kinases. *Oncogene 32: 7918-7927*

Brown M.T. and Cooper J.A. (1996) Regulation, Substrates and functions of src. *Biochem. Biophys. Acta. 1287: 121-149*

Chai X., Förster E., Zhao S., Bock H.H. Frotscher M. (2009) Reelin stabilizes the actin cytoskeleton of neuronal processes by inducing n-cofilin phosphorylation at serine 3. *J. Neurosci 29: 288-299*

Chen W.J., Goldstein J.L., Brown M.S. (1990) NPXY, a sequece often found in cytoplasmic tails, is required for coated pit-mediated internalization of the low density lipoprotein receptor. *J. Biol. Chem. 256: 3116-3123*

Chen K., Ochalski P.G., Tran T.S., Sahir N., Schubert M., Pramatarova A. and Howell B.W. (2004) Interactions between Dab1 and CrkII is promoted by Reelin signalling. *J. Cell Sci. 117: 4527-4536*

Chong Y.P., Mulhern T.D., Cheng H.C. (2005) C-terminal Src Kinase (CSK) and CSK-homologous kinase (CHK)-endogenous negative regulators of Src-family protein kinases. *Growth Factors 23: 233-244*

Cooper J. A. (2008) A mechanism for inside-out lamination in the neocortex. *Trends in Neurosciences 31(3): 113-119*

Cooper J.A. and Qian H. (2008) A mechanism for Src Kinase-dependent signaling by Noncatalytic Receptors. *Biochemistry 47(21): 5681-5687*

D'Arcangelo G. Miao G.G., Chen S.C., Soares H.D., Morgan J.I. & Curran T. (1995) A protein related to extracellular matrix proteins deleted in the mouse mutant reeler. *Nature 374: 719-723*

D'Arcangelo G., Nakajima K., Miyata T., Ogawa M., Mikoshiba K. and Curran T. (1997) Reelin is a secreted glycoprotein recognized by the CR-50 monoclonal antibody. *J. Neurosci. 17: 23-31*

D'Arcangelo G., Homayouni R., Keshvara L., Rice D. S., Sheldon M., Curran T. (1999) Reelin is a ligand for lipoprotein receptors. *Neuron 24: 471-479*

Engen J. R., Wales T. E., Hochrein J. M., Meyn M. A., Banu Ozkan S., Bahar I. and Smithgall T.E. (2008) Structure and dynamic regulation of Src-family kinases. Cell. Mol. Life Sci. 65: 3058-3073

Fatemi, S. H. (2005) Reelin glycoprotein: structure, biology and roles in health and disease. *Mol. Psychiatry 10: 251-257*

Feng L, Cooper JA. (2009) Dual functions of Dab1 during brain development. *Mol Cell Biol. 29(2):324-32*

Förster E., Jossin Y., Zhao S., Chai X., Frotscher M., Goffinet A.M. (2006) Recent progress in understanding the role of Reelin in radial neuronal migration, with specific emphasis on the dentate gyrus. *European Journal of Neuroscience, 23: 901-909*

Förster E., Bock H.H., Herz J., Chal X., Frotscher M. and Zhao S. (2010) Emerging Topics in Reelin Function. *Eur J Neurosci. 31(9): 1511-1518*

Frotscher M. (1998) Cajal-Retzius cells, Reelin, and the formation of layers. *Curr Opin Neurobiol. 8(5): 570-5*

Frotscher M., Chai X., Bock H.H., Haas C.A., Förster E., Zhao S.(2009) Role of Reelin in the development and maintenance of cortical lamination. *J Neural Transm. 116(11): 1451-5*

Frotscher M. (2010) Role for Reelin in stabilizing cortical architecture. *Trends in Neurosciences 33: 407-414*

Gressens P. (2006) Pathogenesis of migration disorders. *Curr Opin Neurol. 19 (2): 135-140*

Gupta A., Tsai L.H. and Wynshaw-Boris A. (2002) Life is a journey: a genetic look at neocortical development. *Nat. Rev. Genet. 3: 342-355*

Harada A., Oguchi K., Okabe S., Kuno J., Terada S., Ohshima T., Sato-Yoshitake R., Takei Y., Noda T., Hirokawa N. (1994) Altered microtubule organization in small-calibre axons of mice lacking tau protein. *Nature 369(6480): 488-91*

Hashimoto-Torii K., Torii M., Sarkisian M.R., Bartley C.M., Shen J., Radke F., Gridley T., Sestan N. and Rakic P. (2008) Interactions between Reelin and Notch signalling regulates neuronal migration in the cerebral cortex. *Neuron. 60: 273-284*

Herz J. & Chen Y. (2006) Reelin, lipoprotein receptors and synaptic plasticity. *Nature Reviews Neuroscience 850: Vol. 7*

Hong S.E., Shugart Y.Y., Huang D.T., Shahwan S.A., Grant P.E., Hourihane J.O., Martin N.D. and Walsh C.A. (2000) Autosomal recessive lissencephaly with cerebral hypoplasia is associated with human RELN mutations. *Nat. Genet. 26: 93-96*

Howell B. W., Gertler F. B. and Cooper J. A. (1997) Mouse disabled (mDab1): a Src binding protein implicated in neuronal development.
EMBO J. 16: 121-132

Howell, B. W., Herrick, T.M., Cooper, J. A. (1999) Reelin-induced tyrosine phosphorylation of disabled 1 during neuronal positioning. *Genes Dev. 13: 643-648*

Howell B.W.; Herrick T.M., Hildebrand J.D., Zhang Y. and Cooper J.A.; (2000) Dab1 tyrosine phosphorylation sites rely positional signals during mouse brain development. *Curr. Biol. 10: 877-885*

Huang Y., Magdaleno S., Hopkins R., Slaughter C., Curran T. and Keshvara L. (2004) Tyrosine phosphorylated Disabled 1 recruits Crk family adaptor proteins. Biochem. *Biophys. Res. Commun. 318: 204-212*

Huang Y., Shah V., Liu T., Keshvara L., (2005) Signaling through Disabled 1 requires phosphoinositide binding. *Biochem. Biophys. Res. Commun. 331:1460*

Huse M, Kuriyan J. (2002) The conformational plasticity of protein kinases. *Cell 109(3): 275-82*

Ingley E. (2008) Src family kinases: Regulation of their activities, levels and identification of new pathways. *Biochemica et Biophysica Acta 1784: 56-65*

Jossin Y, Ignatova N, Hiesberger T, Herz J, Lambert de Rouvroit C, Goffinet AM. (2004) The central fragment of Reelin, generated by proteolytic processing in vivo, is critical to its function during cortical plate development. *J Neurosci. 24(2):514-21.*

Katsuyama Y. & Terashima T. (2009) Developmental anatomy of reeler mutant mouse. *Dev Growth and Differ 51: 271-281*

Katyal S., Gao Z., Monckton E., Glubrecht D., Godbout R. (2007) Hierachical disabled-1 tyrosine phosphorylation in Src family kinase activation and neurite formation. *J Mol Biol. 368: 349-364*

Keshvara L., Benhayon D., Magdaleno S., Curran T. (2001) Identification of Reelin-induced sites of tyrosyl phosphorylation on disabled 1. J*. Biol. Chem. 276: 16008-16004*

Kuo G, Arnaud L, Kronstad-O'Brien P., Cooper J.A. (2005) Absence of Fyn and Src causes a reeler-like phenotype. *J Neurosci. 25(37): 8578-86*

Lambert de Rouvroit C., Goffinet A.M. (2001) Neuronal migration. *Mech Dev 105: 47-56*

May P., Herz J., Bock H. H. (2005) Molecular mechanism of lipoprotein receptor signalling. *Cell. Mol. Life Sci. 62: 2325-2338*

Mayer B.J., Hirai H. and Sakai R. (1995) Evidence that SH2 domans promote processive phosphorylation by protein-tyrosine kinases. *Current Biology 5 (3): 296-305*

Morimura T. and Ogawa M. (2009) Relative importance of tyrosine phosphorylation sites of Disabled-1 to the transmission of Reelin signalling. *Brain Res. 1304: 26-37*

Niu S., Yabut O., D'Arcangelo G. (2008) The Reelin Signalling Pathway Promotes Dentritic Spine Developement in Hippocampal Neurons. *J Neurosci, 28: 10339-10348*

Okawa M. and Nakagawa H. (1989) A protein tyrosine kinase involved in regulation of pp60$^{c\text{-}src}$ function. *J. Biol. Chem. 264: 20886-20893*

Porter M., Schindler T., Kuriyan J., Miller W. T. (2000) Reciprocal regulation of Hck activity by phosphorylation of Tyr(527) and Tyr(416). Effect of introducing a high affinity intramolecular SH2 ligand. *J. Biol. Chem. 275: 2721-2726*

Rasband W.S. ImageJ, U. S. National Institutes of Health, Bethesda, Maryland, USA, http://imagej.nih.gov/ij/, 1997-2011.

Rice D.S., Sheldon M., D'Arcangelo G, Nakajima K, Goldowitz D, Curran T. (1998) Disabled-1 acts downstream of Reelin in a signaling pathway that controls laminar organization in the mammalian brain. *Development 125: 3719-3729*

Rice D.S. and Curran T. (2001) Role of the Reelin Signalling Pathway in central nervous System Development. *Annu. Rev. Neurosci. 24: 1005-039*

Roskoski R. Jr. (2004) Src protein-tyrosine kinase structure and regulation. *Biochemical and Biophysical Research Communications 324: 1155-1164*

Roskoski R. Jr. (2005) Src kinase regulation by phosphorylation and dephosphorylation. *Biochem Biophys Res Commun 331: 1-14*

Schultz A.M., Henderson L.E., Oroszlan S., Garber E.A., Hanafusa H. (1985) Amino terminal myristylation of the protein kinase p60src, a retroviral transforming protein. *Science 227, 427-429*

Seelinger M.A., Young M., Henderson N., Pellicena P., King D.S., Falick A.M. and Kuriyan J. (2008) High yield bacterial expression of active c-Able and c-Src tyrosine kinases. *Protein Sci. 2005 14: 3135-3139*

Senisterra GA, Markin E. Yamazaki K, Hui R, Vedadi M and Awrey D. (2006) Screening for Ligands Using a Generic and High-Throughput Light-Scattering-Based Assay. *Journal of Biomolecular Screening 11(8): 940-948*

Sheldon M., Rice D.S., D'Arcangelo G., Yoneshima H., Nakajima K., Mikoshiba K., Howell B.W., Cooper J.A., Goldowitz D., Curran T. (1997) Scrambler and yotari disrupt the disabled gene and produce a reeler-like phenotype in mice. *Nature 389: 730-733*

Songyang Z., Shoelson S. E., Chaudhuri M., Gish G., Pawson T., Haser W. G., Roberts T., Ratnofsky S., Lechleider R. L., Neel B. G., Birge R. B. Fjardo J. E., Chou M. M., Hanafusa H., Schaffhausen B., Cantley L.C. (1993) SH2 domains recognize specific phosphopeptide sequences. *Cell 72: 767-778*

Songyang Zhou, Carraway K.L. 3rd, Eck M.J., Harrison S.C., Feldman R.A., Mohammadi M., Schlessinger J., Hubbard S.R., Smith D.P., Eng C. et al. (1995) Catalytic specificity of protein-tyrosine kinases is critical for selective signalling. *Nature 373: 536-539*

Stolt P.C. and Bock H.H.; (2006) Modulation of lipoprotein receptor function by intracellular adapter proteins. *Cell Signal 18: 1560 – 1571*

Stolt P.C., Chen Y., Liu P., Bock H.H. Blaclow S.C. and Herz J. (2005) Phosphoinositide binding by the disabled-1 PTB domain is necessary for membrane localization and Reelin signal transduction. *J. Biol. Chem. 280: 9671-9677*

Stolt P.C., Jeon H., Song H.K., Herz J., Eck M.J. and Blacklow S.C. (2003) Origins of peptide selectivity and phosphoinositide binding revealed by structures of disabled-1 PTB domain complexes. *Structure 11: 569-579*

Strasser V, Fasching D, Hauser C, Mayer H, Bock HH, Hiesberger T, Herz J, Weeber EJ, Sweatt JD, Pramatarova A, Howell B, Schneider WJ, Nimpf J. (2004) Receptor clustering is involved in Reelin signaling. *Mol Cell Biol. 24(3):1378-86.*

Sun G., Sharma A. K., Budde R. J. (1998) Autophosphorylation of Src and Yes blocks their inactivation by Csk phosphorylation. *Oncogene 17: 1587-1595*

Sun J.P., Wu L., Fedorov A.A., Almo S.C., Zhang Z.Y. (2003) Crystal structure of the Yersinia protein-tyrosine phosphatase YopH complexed with a specific small molecule inhibitor. *J Biol Chem 29;278(35): 33392-9*

Trommsdorff M., Gotthardt M., Hiesberger T., Shelton J., Stockinger W., Nimpf J., Hammer R.E., Richardson J.A., Herz J. (1999) Reeler/Disabled-like disruption of neuronal migration in knockout mice lacking VLDL receptor and ApoE receptor 2. *Cell 97: 689-701*

Trommsdorff M, Borg JP, Margolis B, Herz J. (1998) Interaction of cytosolic adaptor proteins with neuronal apolipoprotein E receptors and the amyloid precursor protein. *J Biol Chem. 1998 273(50): 33556-60*

Waksman G., Shoelson S. E., Pant N., Cowburn D., Kurlyan J. (1993) Binding of a high affinity phosphotyrosyl peptide to the Src SH2 domain: crystal structures of the complexed and peptide-free forms. *Cell 72: 779-790*

Wang D., Huang X.Y., Cole P.A. (2001) Molecular determinants for Csk-catalyzed tyrosine phosphorylation of the Src tail. *Biochemistry 40: 2004-2010*

Xu W., Harrison S. C., Eck M. J. (1997) Three-dimensional structure of the tyrosine kinase c-Src. *Nature 385: 595-602*

Xu W., Doshi A., Lei M., Eck M. J., Harrison S. C. (1999) Crystal structures of c-Src reveal features of its autoinhibitory mechanism. *Mol. Cell 629-638*

Ye X. and Sloboda R.D. (1997) Characterization of p62, a Mitotic Apparatus Protein Required for Mitotic Progression. *J Biol. Chem. 272 (6): 3606-3614*

Yeatman T. J. (2004) A renaissance for Src. *Nat. Rev. Cancer 4: 470-480*

Zhang Z.Y., Clemens J.C., Schubert H.L., Stuckey J.A., Fischer M.W.F., Hume D.M., Saper M.A. and Dixon J.E. (1992) Expression, purification, and physicochemical characterization of a recombinant Yersinia protein tyrosine phosphatase. *J. Biol. Chem. 267: 23759-23766*

Zhao S., Chai X., Förster E., Frotscher M. (2004) Reelin is a positional signal for the lamination of dentate granule cells. *Development 131(20): 5117-25.*

Zheng X.M., Resnick R.J., Shalloway D. (2000) A Phosphotyrosine displacement mechanism for activation of Src by PTPα. *EMBO J. 19: 964-978*

10 Acknowledgements

The past few years during my studies at BOKU have been difficult and challenging in many ways, still it has been a wonderful time. The year at the IMP was a great experience that I wouldn't want to miss. There are a number of people that I want to thank for their support and friendship, you all mean a lot to me!

Mama. Papa. Ema. Pep. Aunts. Uncles. Cousins. Erni-Tante.
Peggy. Babsi. Bettina. Eli. Stella. Hong-Wen.
Lisa. Beate.
Tobi & the Zarka-Neumann connection. Andrea.
Marie-Theres Hauser. Iain Wilson and Kathi.
Georg. Markus. Jasmin. Dani. Susi. Therese.
Walter.